

**Revisiting species of *Trypanosoma*
(Euglenozoa: Trypanosomatidae)
parasitising amphibians and reptiles
from Southern Africa**

BJ Jordaan

 orcid.org/0000-0001-6800-8007

Dissertation accepted in fulfilment of the requirements for the
degree *Master of Science in Zoology* at the North-West
University

Supervisor: Dr. EC Netherlands

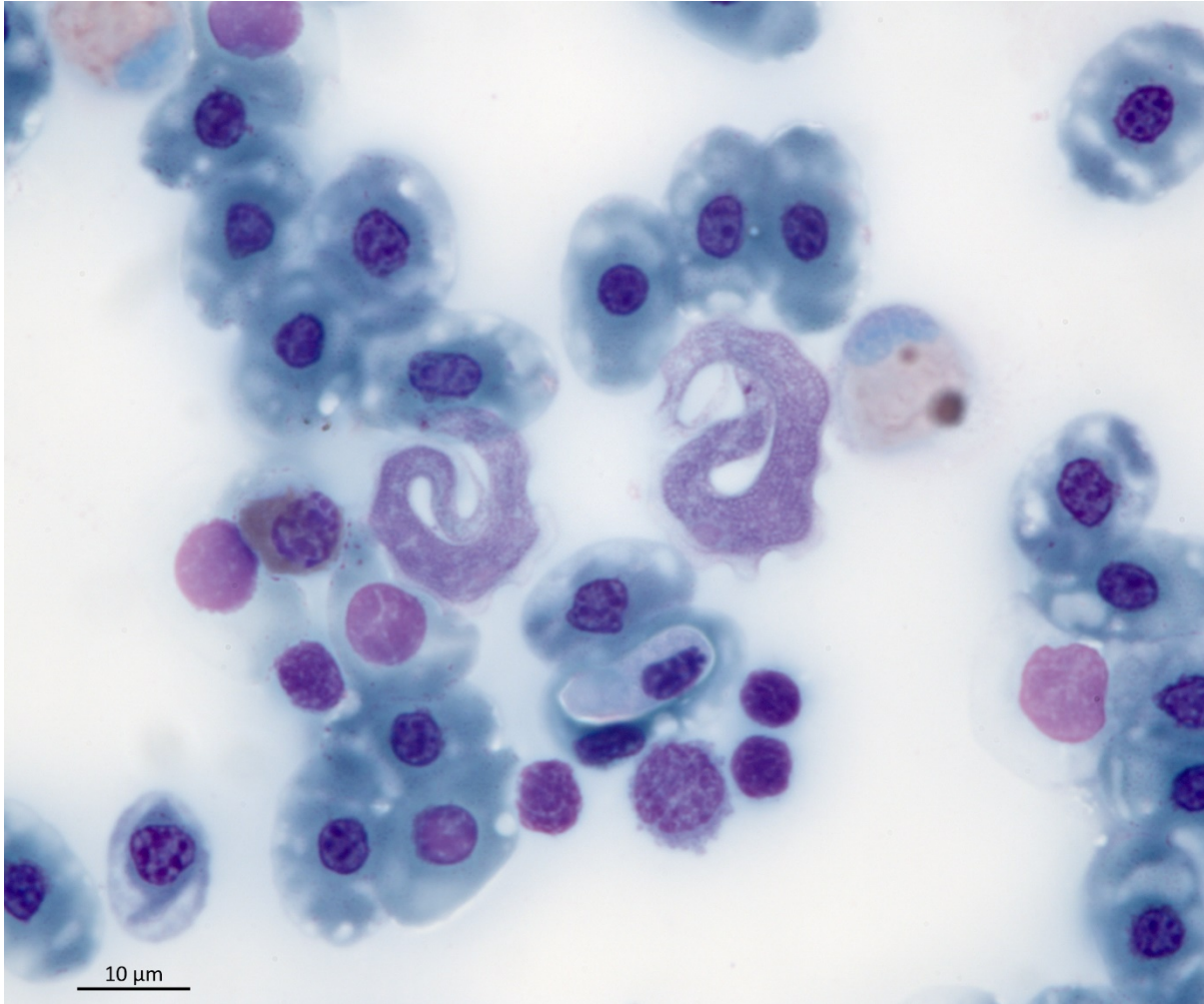
Co-supervisor: Prof. LH du Preez

Graduation May 2023

29706696

DISCLAIMER

No taxonomic changes or new names described herein are considered valid for the purposes of zoological nomenclature according to Article 8.2 of the International Code of Zoological Nomenclature (ICZN, 2012). The work and statements herein are not considered published to the scientific record under Articles 9.9 and 9.12 of the ICZN (2012).



“...there were dark balls between the blood cells, similar to the round pigment cells. They moved very lively, mostly wobbling, but also definitely locomotive. If one watched for some time, a light tail appeared laterally, and later gradually an elongated animal revealed itself, which moved very actively and constantly.”

– **Gabriel G. Valentin, 1841** (translated from German)

“The locomotion of the Trypanosome [*sic*] is very remarkable; first, one must admire the rapidity with which it moves each of its parts to produce the movement around its longitudinal axis, that is to say the movement of the auger, and then the skill that it uses to avoid all the obstacles it encounters in its progress.”

– **David Gruby, 1843** (translated from French)

ACKNOWLEDGEMENTS

I am thankful for the unmatched guidance and leadership from my supervisor, Ed Netherlands, and co-supervisor, Louis du Preez. Thank you both for your patience, input, and support, as well as growing my passion for the fascinating field of and reptile amphibian parasites. It has been extraordinary to be able to explore different parts of Southern Africa and share all the remarkable experiences along the way. I have been privileged enough to learn countless things from you, at the cost of being cursed with a desire for more.

The aid of the members of the African Amphibian Conservation and Research group (AACRG) is much appreciated.

I am grateful to Goro Game Reserve, iSimangaliso Wetland Park, Lajuma Research Centre, Ndumo Game Reserve, Tembe Elephant Park, and Vhembe Biosphere Reserve for their cooperation and for allowing my research activities.

The North-West University and Unit of Environmental Sciences are thanked for use of their facilities.

I am thankful for the company and encouragement of all my friends.

Lastly, thank you to my family for your wholehearted support and motivation. My appreciation and love for nature has been kindled by you for as long as I can remember.

ABSTRACT

Chapter 2.1

The aquatic and terrestrial clades of species of *Trypanosoma* could provide insight into the evolutionary history of the genus, as well as complementary information for biomedical studies of medically and economically important species of *Trypanosoma*. The ecological interactions and phylogeny of aquatic trypanosomes is currently not well-understood, mostly due to their complex life cycles and a deficiency of data. The species of *Trypanosoma* from African anuran hosts are of the least understood taxa in the genus. Trypanosome specimens were collected from South African frogs and subjected to morphological and phylogenetic analyses. This study describes *Trypanosoma* (*Trypanosoma*) cf. *nelspruitense* Laveran, 1904 and *Trypanosoma* (*Haematomonas*) cf. *grandicolor* Pienaar, 1962, with morphological and molecular data. The present study aims to create a platform for further future research on African anuran trypanosomes.

Chapter 2.2

Despite reptile trypanosomes forming a large group, the majority of species descriptions are data deficient, lacking key characteristic data and supporting molecular data. Reptile hosts show potential to facilitate transmission of zoonotic trypanosomiases and offer key information to understanding the genus of *Trypanosoma*. Several species of squamates, from different localities in South Africa, were screened molecularly and microscopically for trypanosomes in the present study. Based on the combination of morphological and molecular analyses, two new species of *Trypanosoma*, *Trypanosoma* (*Squamatrypanum*) sp. 2N and *Trypanosoma* (*Trypanosoma*) sp. 2T, infecting South African cordylid lizards (Cordylidae: Cordylinae) are described in this study. The first molecular data for a South African reptile trypanosome is provided herewith.

Chapter 2.3

Species of *Trypanosoma* infecting reptiles are relatively poorly understood and understudied. The study of trypanosomes infecting turtles could lead to a greater understanding of the genus and its evolutionary history. A supplementary description is provided for two species of *Trypanosoma* infecting freshwater pelomedusid (Pelomedusidae) turtles, *T. (Haematomonas) cf. neitzi* and *T. (Haematomonas) cf. sheppardi*, with molecular data in the present study. Additionally, an undescribed species of *Trypanosoma* is characterised using morphological and molecular data. This study provides the first morphological descriptions and molecular data of South African turtle trypanosomes, setting a base for future research of the reptile trypanosomes of Africa.

Key words: Trypanosoma, blood parasite, Anura, Squamata, Testudines, molecular characterisation.

TABLE OF CONTENTS

ABSTRACT	1
PREFACE	9
CHAPTER 1 GENERAL INTRODUCTION	10
CHAPTER 2.1 RESULTS	
Taxonomic re-evaluation of African anuran trypanosomes with the supplementary description and molecular diagnosis of <i>Trypanosoma (Trypanosoma) cf. nelspruitense</i> Laveran, 1904 and <i>Trypanosoma (Haematomonas) cf. grandicolor</i> Pienaar, 1962	14
CHAPTER 2.2 RESULTS	
Morphological and molecular diagnosis of two undescribed species of <i>Trypanosoma</i> Gruby, 1843 infecting South African cordylid lizards (Squamata: Cordylidae: Cordylinae), <i>Trypanosoma (Squamatrypanum) sp. 2N</i> and <i>Trypanosoma (Trypanosoma) sp. 2T</i>	47
CHAPTER 2.3 RESULTS	
Investigating the trypanosomes infecting pelomedusid (Pelomedusidae) freshwater turtles in Southern Africa with the supplementary description and molecular diagnosis of <i>Trypanosoma (Haematomonas) cf. neitzi</i> Dias, 1951 and <i>Trypanosoma (Haematomonas) cf. sheppardi</i> Dias, 1951, alongside the morphological and molecular characterisation of an undescribed species.....	74
CHAPTER 3 GENERAL DISCUSSION	104
REFERENCE LIST	108
APPENDIX	123

TABLE & FIGURE LIST

Chapter 2.1

Table 2.1.1 – African anuran *Trypanosoma* index. Type hosts, localities, and original description authorities in bold.21

Table 2.1.2 – Morphometric measurements of *Trypanosoma* species infecting South African anurans. Measurement range shown in μm (mean \pm standard deviation). Body length (BL), body width (BW), nucleus length (NL), Nucleus width (NW), mid-nucleus to anterior (MA), mid-nucleus to posterior (MP), undulating membrane width (UMW), number of undulations (NU), kinetoplast length (KL), kinetoplast width (KW), length of free flagellum (F). Body shape index (BI), nuclear index (NI) and nucleus position as a percent (NP). Species from the present study are in bold.27

Table 2.1.3 – Model-corrected pair-wise distances (p-distances) of *Trypanosoma* species. Sequences from the present study in bold. Distance shown as percentage (%).
.....28

Figure 2.1.1 – *Trypanosoma* cf. *nelspruitense* plate. (A-H) Normal trypomastigote forms in the blood. (I-J) Round forms. (K) Stumpy form. (L) Larger normal form. Arrowheads show kinetoplasts (A-L); arrows show flagella (B and C) and undulating membranes (I and L); nuclei are indicated by “n” (A, H, I, J, and L). Internal flagella indicated by “f” (I and J). Host cell indicated by “H”. Scale bar is 20 μm31

Figure 2.1.2 – *Trypanosoma* cf. *grandicolor* plate. (A-K) Normal trypomastigote forms in the blood. (L) Larger normal form. Arrowheads show kinetoplasts (A-L); arrows show

flagellum (F) and undulating membranes (H and L); nuclei are indicated by “n” (B, I, and L). Scale bars are 20 μm36

Figure 2.1.3 – Consensus phylogram of the aquatic trypanosome clade based on 18S rDNA sequences. Tree topologies of Maximum Likelihood (ML) and Bayesian Inference (BI) analyses were similar (represented on the BI tree). Nodal support values of BI posterior probability and ML bootstrap shown as BI/ML. Sequences from the present study are in bold. Subgenera are indicated by an asterisk (*). Scale shown is nucleotide substitutions per site.40

Chapter 2.2

Table 2.2.1: African squamate trypanosome index. Asterisk (*) indicates type host.52

Table 2.2.2: Morphometric measurements of *Trypanosoma* sp. 2N and *Trypanosoma* sp. 2T from the present study. Measurement range shown in μm (mean \pm standard deviation). Measurement range shown in μm (mean \pm standard deviation). Body length (BL), body width (BW), nucleus length (NL), Nucleus width (NW), mid-nucleus to anterior (MA), mid-nucleus to posterior (MP), undulating membrane width (UMW), number of undulations (NU), kinetoplast length (KL), kinetoplast width (KW), mid-kinetoplast to anterior body end distance (KA), mid-kinetoplast to posterior body end distance (KP), mid-kinetoplast to mid-nucleus distance (KN), length of free flagellum (F). Body shape index (BI), nuclear index (NI), nucleus position (PN), kinetoplast position (PK).57

Table 2.2.3: Model-corrected pair-wise distances (p-distances) of *Trypanosoma* species. Sequences from the present study in bold. Distance shown as percentage (%).

.....57

Figure 2.2.1: *Trypanosoma* sp. 2N plate. (A-L) Normal trypomastigote forms in the blood. Arrowheads show kinetoplast (A, D, and L); arrows show flagellum (A, B, and H) and undulating membranes (F, I, and K); nuclei are indicated by “n” (B, D, and L). Scale bar is 20 μ m.61

Figure 2.2.2: *Trypanosoma* sp. 2T plate. (A-L) Normal trypomastigote forms in the blood. Arrowheads show kinetoplast (A, B, and K); arrows show flagellum (A, B, and F) and undulating membranes (C, K, and L); nuclei are indicated by “n” (B, J, and K). Scale bar is 10 μ m.65

Figure 2.2.3: Consensus phylogram of the reptile trypanosome clade based on 18S rDNA sequences. Tree topologies of Maximum Likelihood (ML) and Bayesian Inference (BI) analyses were similar (represented on the BI tree). Nodal support values of BI posterior probability and ML bootstrap shown as BI/ML. Sequences from the present study are in bold. Subgenera are indicated by an asterisk (*). Scale shown is nucleotide substitutions per site.68

Chapter 2.3

Table 2.3.1: Morphometric measurements of turtle trypanosomes Southern Africa.

Species from present study shown in bold. Asterisk (*) indicates values calculated from original descriptions. Measurement range in μ m, with mean \pm standard deviation shown in parentheses. Body length (BL), body width (BW), nucleus length (NL), Nucleus width

(NW), mid-nucleus to anterior (MA), mid-nucleus to posterior (MP), undulating membrane width (UMW), number of undulations (NU), kinetoplast length (KL), kinetoplast width (KW), mid-kinetoplast to anterior body end distance (KA), mid-kinetoplast to posterior body end distance (KP), mid-kinetoplast to mid-nucleus distance (KN), length of free flagellum (F). Body shape index (BI), nuclear index (NI), nucleus position (PN), kinetoplast position (PK).83

Table 2.3.2: Model-corrected p-distance values. Sequences from present study shown in bold. Distance shown as percentage (%).84

Figure 2.3.1: *Trypanosoma cf. neitzi* plate. Normal trypomastigote forms A-E. Slender *Trypanosoma* sp. form F. Scale shown is 10 µm. Arrowheads show kinetoplast (A, D, and F); arrows show flagellum (C and D) and undulating membrane (A and E); nuclei are indicated by “n” (A and B).90

Figure 2.3.2: *Trypanosoma cf. sheppardi* plate. Normal trypomastigote forms A-F. Scale shown is 10 µm. Arrowheads show kinetoplast (A and B); arrows show flagellum (D and E) and undulating membrane (C and F); nuclei are indicated by “n” (B and D).93

Figure 2.3.3: *Trypanosoma* sp. 1A plate. Normal trypomastigote forms A-F. Scale shown is 10 µm. Arrowheads show kinetoplast (C and F); arrows show flagellum (A, B, and F) and undulating membrane (D and E); nuclei are indicated by “n” (D and E).96

Figure 2.3.4: Consensus phylogram of the aquatic trypanosome clade based off the 18S rRNA gene. (Represented on BI tree). Nodal support values shown as posterior

probability over bootstrap values. Values below 0.7 and 70, respectively, were omitted. Sequences from the present study are in bold. Subgenera are indicated by an asterisk (*). Scale shown is number of nucleotide substitutions per site.99

PREFACE

Article format of the journal *Parasitology* (Cambridge) has been selected for the submission of this thesis.

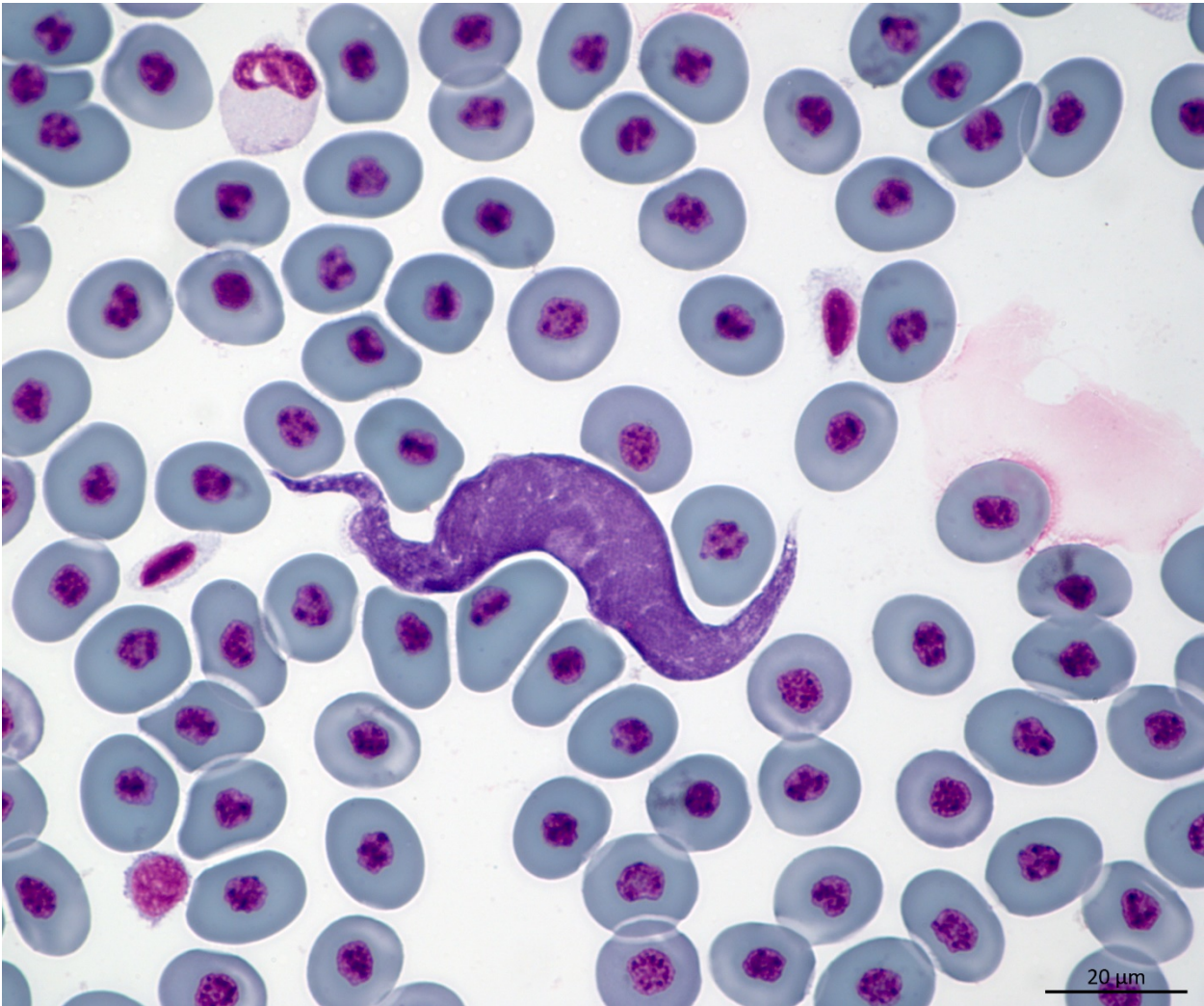
Articles within this thesis are as follows:

- **Chapter 2.1: *Parasitology* (In press)** – Taxonomic re-evaluation of African anuran trypanosomes with the supplementary description and molecular diagnosis of *Trypanosoma* (*Trypanosoma*) cf. *nelspruitense* Laveran, 1904 and *Trypanosoma* (*Haematomonas*) cf. *grandicolor* Pienaar, 1962.
- **Chapter 2.2: *Journal for Eukaryotic Microbiology* (In press)** – Morphological and molecular diagnosis of two undescribed species of *Trypanosoma* Gruby, 1843 infecting South African cordylid lizards (Squamata: Cordylidae: Cordylinae), *Trypanosoma* (*Squamatrypanum*) sp. 2N and *Trypanosoma* (*Trypanosoma*) sp. 2T.
- **Chapter 2.3: (Submission in progress)** – Investigating the trypanosomes infecting pelomedusid (Pelomedusidae) freshwater turtles in Southern Africa with the supplementary description and molecular diagnosis of *Trypanosoma* (*Haematomonas*) cf. *neitzi* Dias, 1951 and *Trypanosoma* (*Haematomonas*) cf. *sheppardi* Dias, 1951, alongside the morphological and molecular characterisation of an undescribed species.

This student was first author, wrote, designed and conceived, was responsible for the data collection and analysis for all the above articles. The co-authors are aware of and have given permission for the articles to be submitted for degree purposes. Note ICZN disclaimer — no new names or nomenclatural changes herein are considered valid.

CHAPTER 1

GENERAL INTRODUCTION



Trypanosoma cf. grandicolor ex. Xenopus laevis

CHAPTER 1

Introduction

Trypanosomes (Euglenozoa: Kinetoplastea: Trypanosomatida: Trypanosomatidae) are a remarkable, large group of unicellular flagellates, which are obligate extracellular haemoparasites. They are known to infect all classes of vertebrates and have a global distribution. Some species of *Trypanosoma* are pathogenic and cause severe, sometimes fatal, diseases in humans and livestock. These pathogenic species have a significant social and economic impact and were a key factor historically in shaping the anthropogeography of sub-Saharan Africa (Steverding, 2008; Headrick, 2014).

Human African Trypanosomiasis (HAT), also known as sleeping sickness, is transmitted by the blood-sucking Tsetse flies. Most species of *Trypanosoma* have a life cycle alternating between vertebrate hosts and invertebrate vectors. As a result of the wide range of trypanosome hosts species, these parasites have developed complex and diverse modes of transmission (Magez *et al.*, 2021). For example, in contrast with HAT, transmission of *Trypanosoma grayi* can occur when the crocodile host ingests the infected tsetse fly vector (Hoare, 1929; Hoare, 1931; Kelly *et al.*, 2014). Some species are transmitted independently of an invertebrate vector, such as *T. equiperdum*, which is spread by sexual contact between equids (Hamilton *et al.*, 2004).

Within the genus of *Trypanosoma*, the most significant division of the phylogeny occurs between the clades of terrestrial and aquatic vertebrates. However, the evolutionary history of trypanosomes and what the ancestral lineage was that all other groups diverged from remains unclear, due to a lack of molecular data and the intricate life cycles of trypanosomes (Spodareva *et al.*, 2018). Data of trypanosomes infecting vertebrate hosts which are exposed to both terrestrial and aquatic vectors, such as amphibian or turtle trypanosomes, could aid in resolving the phylogenetic clades and provide key insight into other species of *Trypanosoma* (Bernal and Pinto, 2016).

CHAPTER 1

Turtles and amphibians are among the most threatened vertebrate classes globally (Lovich *et al.*, 2018; Rhodin *et al.*, 2021; IUCN, 2022), and have had a steady increase in research of recent years. Unfortunately, however, the study of their trypanosomes has not followed the same pace, despite their potential to present valuable information about the host's health, ecological interactions, and environmental intactness (Vanhove *et al.*, 2021). Accordingly, due to their evolutionary significance and possibility to provide information relating to pathogenic trypanosomes of mammals, amphibian trypanosomes show promise to serve as excellent research models (Diamond, 1965).

Problem Statement

South Africa is a global biodiversity hotspot and has among the highest species diversity and richness globally, much of which is endemic. Due to the higher frequency of interspecies interactions in such a species-rich environment allowing the completion of parasitic life cycles (Vanhove *et al.*, 2021), one would expect the trypanosome species richness to be similarly high. Currently, however, only four recognised species of *Trypanosoma* have been described from anuran and reptile hosts in South Africa (Laveran, 1904; Fantham and Porter, 1950; Pienaar, 1962). Furthermore, these species descriptions are severely data deficient, lacking detailed illustrations, morphological measurements, and molecular data, and have not been reported since their original descriptions.

Main Aims of the Study

This study aims to set a basis for future research of the amphibian and reptile trypanosomes of Southern African by revisiting the small number of described species and describe new species, in addition to providing the first molecular data for any reptile or anuran trypanosome from South Africa.

Main Objectives of the Present Study

The aims of this study will be achieved by accomplishing the following objectives:

1). Sampling various potential host species from several localities within South Africa.

1.1). The type host species of the only two recognised species of anuran (Amphibia: Anura) trypanosomes described from South Africa, *T. nelspruitense* Laveran, 1904 and *T. grandicolor* Pienaar, 1962, were targeted from their respective type localities in South Africa.

1.2). Currently, only two recognised species of *Trypanosoma*, *T. psammophis* and *T. sebae*, have been described from South African reptiles, which were both from snake host species (Fantham and Porter, 1950). Accordingly, various squamate (Reptilia: Squamata) species, including the type host of *T. sebae*, were sampled from several sites within South Africa.

1.3). No recognised species have currently been described from South African turtles (Reptilia: Testudines), however three species, *T. neitzi* Dias, 1951, *T. sheppardi* Dias, 1951, and *T. mocambicum* Pienaar, 1962, have been described from infections in pelomedusid (Pelomedusidae) turtles from southern Mozambique (Dias, 1951; Pienaar, 1962) — which borders north-eastern South Africa and shares the same river basin. Hence, several species of pelomedusid turtles were sampled from multiple sites in north-eastern South Africa.

2). A combination of molecular and microscopic screening methods were implemented for the detection trypanosome infections.

3). Species of *Trypanosoma* were characterised with morphological and molecular-based analyses.

CHAPTER 2.1 RESULTS



Common river frog (*Amietia delalandii*)



African clawed frog (*Xenopus laevis*)

CHAPTER 2.1

Taxonomic re-evaluation of African anuran trypanosomes with the supplementary description and molecular diagnosis of *Trypanosoma* (*Trypanosoma*) cf. *nelspruitense* Laveran, 1904 and *Trypanosoma* (*Haematomonas*) cf. *grandicolor* Pienaar, 1962

Bernard J. Jordaan¹, Louis H. du Preez^{1,2}, and Edward C. Netherlands^{1,3}

¹ African Amphibian Conservation Research Group, Unit for Environmental Sciences and Management, North-West University, Potchefstroom, South Africa

² South African Institute for Aquatic Biodiversity, Somerset Street, Makhanda 6140, South Africa

³ Department of Zoology and Entomology, University of the Free State, PO Box 339, Bloemfontein, 9300, South Africa.

CHAPTER 2.1

2.1.1. Abstract

The aquatic and terrestrial clades of species of *Trypanosoma* could provide insight into the evolutionary history of the genus, as well as complementary information for biomedical studies of medically and economically important species of *Trypanosoma*. The ecological interactions and phylogeny of aquatic trypanosomes is currently not well-understood, mostly due to their complex life cycles and a deficiency of data. The species of *Trypanosoma* from African anuran hosts are of the least understood taxa in the genus. Trypanosome specimens were collected from South African frogs and subjected to morphological and phylogenetic analyses. This study describes *Trypanosoma* (*Trypanosoma*) cf. *nelspruitense* Laveran, 1904 and *Trypanosoma* (*Haematomonas*) cf. *grandicolor* Pienaar, 1962, with morphological and molecular data. The present study aims to create a platform for further future research on African anuran trypanosomes.

Key words: *Amietia delalandii*, *Xenopus laevis*, blood parasite, frog, molecular characterisation, morphometrics, phylogeny.

CHAPTER 2.1

2.1.2. Introduction

The genus *Trypanosoma* Gruby, 1843, (Euglenozoa: Kinetoplastea: Trypanosomatidae) is a globally occurring group of unicellular obligate haemoparasites (Netherlands *et al.*, 2014). Trypanosomes are typically recognised by the presence of an undulating membrane and kinetoplast, however, they vary morphologically from elongated to round body shapes, even within a single species (d'Avila-Levy *et al.*, 2015; Attias *et al.*, 2016). Trypanosomes are known to parasitise all the vertebrate classes (i.e. fishes, amphibians, reptiles, birds, and mammals) and are an ancient group of parasites. Fossil records of trypanosomes have been found trapped within amber in triatomine faeces from approximately 15-45 mya (Poinar Jr, 2005), as well as a sister-genus, *Paleoleishmania* Poinar and Poinar, 2004, being reported from the abdominal midgut of a fossilised sand fly dating at least 100 mya (Poinar Jr and Poinar, 2004). The invertebrate vectors of trypanosomes include dipterans (e.g. mosquitoes, biting midges and hippoboscids louse flies), triatomine bugs, and leeches (Ramos and Urdaneta-Morales, 1977), in which the trypomastigotes typically undergo complex development, transforming into several different stages before infecting a new host (Magez *et al.*, 2021; Vanhove *et al.*, 2022). Generally, trypanosomes alternate between infecting a vertebrate and invertebrate host during their lifecycles (Hamilton *et al.*, 2007).

Trypanosomes are of considerable scientific importance, as this group is known to cause several diseases, such as African trypanosomiasis and Chagas disease, in humans and livestock. The majority of scientific research concentrated on trypanosomes that are pathogenic to humans and livestock, however, relatively little is known about the species of *Trypanosoma* parasitising other host animals (Hughes and Piontkivska, 2003; Dvořáková *et al.*, 2015; Attias *et al.*, 2016; Bernal and Pinto, 2016). The availability of data specifically for trypanosomes infecting anurans is lacking (Leal *et al.*, 2009;

CHAPTER 2.1

Netherlands *et al.*, 2014; Dvořáková *et al.*, 2015; Attias *et al.*, 2016; Bernal and Pinto, 2016).

The study of anuran trypanosomes played an important historical role in developing an understanding of the genus of *Trypanosoma*. Trypanosomes were first discovered by Gluge (1842) in a frog host species but were not named. The first description of trypanosomes was provided by Mayer (1843) from the blood of the European frog, *Pelophylax esculentus* Linnaeus, 1758 (syn. *Rana esculenta*), although he initially incorrectly identified the parasites, describing the organisms as *Trypanosoma loricatum* (Mayer, 1843) Dutton, Todd, and Tobey, 1907 (syn. *Paramaecium loricatum*) and *Trypanosoma rotatorium* (Mayer, 1843) Laveran and Mesnil, 1901 (syn. *Amoeba rotatoria*). From an infection in the blood of an unidentified European frog host species, the genus of *Trypanosoma* was created by Gruby (1843) with the description of the type species, *Trypanosoma sanguinis* Gruby 1843. However, it has since been proposed by others that Gruby (1843) described a mixed infection of multiple trypanosome species and that *T. sanguinis* is a junior synonym of *T. rotatorium* (Laveran and Mesnil, 1901; Laveran and Mesnil, 1907; Diamond, 1965; Spodareva *et al.*, 2018).

In Africa, most of the species of *Trypanosoma* from anurans were recorded early in the 20th century. Only 14 recognised species of *Trypanosoma* have been reported from anurans in Africa, shown in Table 2.1.1 (Laveran, 1904; Bardsley and Harmsen, 1973; Dvořáková *et al.*, 2015; Fermino *et al.*, 2019). This is surprising considering the geographical scale and rich biodiversity of the African continent. Furthermore, only two species, *Trypanosoma nelspruitense* Laveran, 1904 and *Trypanosoma grandicolor* Pienaar, 1962, have been described from South African anurans, infecting the common river frog (*Amietia delalandii* Duméril and Bibron, 1841) and the African clawed frog (*Xenopus laevis* Daudin, 1802), respectively. These species descriptions severely lack morphological metrics, with no molecular data available. No records of *T. nelspruitense*

CHAPTER 2.1

nor *T. grandicolor* have been reported since their original descriptions. Fantham *et al.* (1942) briefly mention having observed rounded *T. rotatorium* infections in *Xenopus laevis* and *Amietia fuscigula* (syn. *Rana fuscigula*) from South Africa. Several unnamed trypanosomes were also reported from South African anurans in the study of Netherlands (2019), from grass frogs (*Ptychadena anchietae*), leaf-folding frogs (*Afrivalus delicatus* and *A. fornasini*), reed frogs (*Hyperolius argus*, *H. marmoratus*, *H. tuberilinguis*), shovel-nosed frogs (*Hemisus marmoratus*), tree frogs (*Leptopelis natalensis* and *L. mossambicus*), puddle frogs (*Phrynobatrachus mababiensis*), and toads (*Sclerophrys garmani* and *S. gutturalis*).

Leal *et al.* (2009) proposed that the dissonance in the characterisation of species of *Trypanosoma* is due to the extreme polymorphism that may be found in a single species, as well as individual species being able to infect numerous vertebrate and invertebrate host species. Furthermore, they believe that the absence of molecular and life cycle ecological data in species descriptions, up until recent years, has led to numerous taxonomic errors, thus, species described separately in different hosts or geographical areas could be synonymous (Leal *et al.*, 2009; Hayes *et al.*, 2014). Accordingly, the widespread inclusion of molecular data in non-human trypanosome research, as well as revisiting existing described species, would be of great scientific importance in order to achieve better taxonomic organisation in the genus and a better ecological understanding of all the involved host species.

The most significant division in the phylogenetic relationships of non-human trypanosomes is between the species infecting terrestrial and aquatic vertebrates (Hamilton *et al.*, 2007; Fermino *et al.*, 2019). Based on phylogenetic analyses, amphibian and fish trypanosomes are the origin from which all other trypanosomes evolved, according to Hamilton *et al.* (2007). Because anurans are exposed to both aerial and aquatic trypanosome vectors, they could be a link between the two trypanosome clades

CHAPTER 2.1

(Spodareva *et al.*, 2018), providing insight into other species of *Trypanosoma* (Bernal and Pinto, 2016). Thus, anuran trypanosomes are possibly the key to understanding the evolutionary history of the entire genus. Due to a lack in molecular data for this group in general and no molecular data for any species of anuran trypanosomes from South Africa, it is important to research the trypanosomes infecting frogs. The present study followed the taxonomic classification system of the designated *Trypanosoma* subgenera proposed by Kostygov *et al.* (2021).

The aim of this chapter was to provide a basis for future taxonomic work on amphibian trypanosomes from Africa. Thus, the objectives of this chapter were to: 1) revise the original descriptions as well as provide supplementary descriptions of the only two currently recognised species of anuran trypanosomes described from South Africa, *T. nelspruitense* and *T. grandicolor*; 2) provide the first molecular data for these species; 3) conduct a phylogenetic analysis on these two species of *Trypanosoma* from South Africa. This would provide a platform for future research on trypanosomes within South Africa and would contribute to a better understanding of the genus *Trypanosoma*, as this species is part of the aquatic trypanosome clade, from which all other trypanosome species potentially originated. Herein, we describe *T. cf. nelspruitense* and *T. cf. grandicolor*, with morphological and molecular data. These two species are placed within monophyletic subclades of the aquatic trypanosome clade.

CHAPTER 2.1

Table 2.1.1: African anuran *Trypanosoma* index. Type hosts, localities, and original description authorities in bold.

Species of <i>Trypanosoma</i>	African Record	Reference	Known host species	Known vector species
<i>T. bocagei</i>	Guinea-Bissau Tunisia	França, 1911 Lebailly and Caillon, 1919	<i>Sclerophrys regularis</i> (syn. <i>Bufo</i> <i>Sclerophrys mauritanica</i> (syn. <i>Bufo</i> <i>mauritanicus</i>) <i>Sclerophrys regularis</i> (syn. <i>Bufo regularis</i>)	
<i>T. elegans</i>	Congo	Martin <i>et al.</i> , 1909		
<i>T. grandicolor</i>	South Africa: Potchefstroom	Pienaar, 1962	<i>Xenopus laevis</i>	
<i>T. inopinatum</i>	Algeria: Dra-el-Mizan (Kabylie) Algeria	Sergent and Sergent, 1904, 1905 Billet, 1904	<i>Pelophylax esculentus</i> (syn. <i>Rana</i> <i>esculenta</i>)	<i>Helobdella algira</i> (Desser <i>et al.</i> , 1973)
<i>T. karyozeukton</i>	Gambia: Cape St. Mary	Dutton and Todd, 1903	Frog (unknown species)	
<i>T. loricatum</i>	Gambia	Dutton <i>et al.</i> , 1907	<i>Amnirana galamensis</i> (syn. <i>Rana</i> <i>galamensis</i>) <i>Ptychadena mascareniensis</i> (syn. <i>Rana</i> <i>mascariensis</i>) <i>Ptychadena oxyrhynchus</i> (syn. <i>Rana</i> <i>oxyrhynchus</i>) <i>Ptychadena oxyrhynchus</i> (syn. <i>Rana</i> <i>oxyrhynchus</i>) <i>Sclerophrys regularis</i> (syn. <i>Bufo regularis</i>) <i>Tomopterna tuberculosa</i> (syn. <i>Rana</i> <i>tuberculosa</i>)	
<i>T. mega</i>	Angola Congo	França, 1925 Brodén, 1905 Rodhain, 1907 Kerandel, 1909 Martin <i>et al.</i> , 1909 Schwetz, 1944	Frog (unknown species)	
	Gambia: MacCarthy Island	Dutton and Todd, 1903		
	Nigeria	MacFie, 1914		
	Africa (unspecified)	Walton 1947		
<i>T. nelspruitense</i>	South Africa: Mbombela (formerly Nelspruit)	Laveran, 1904	<i>Amietia delalandii</i> (syn. <i>Rana angolensis</i> and <i>Rana theileri</i>)	
<i>T. parroti</i>	Algeria	Brumpt, 1923	<i>Discoglossus pictus</i>	
<i>T. rotatorium</i>	Congo	Rodhain, 1907 Martin <i>et al.</i> , 1909 Schwetz, 1930, 1944 Pérez-Reyez, 1967	<i>Alytes obstetricans</i> (syn. <i>Bufo obstetricans</i>) <i>Amietia fuscigula</i> (syn. <i>Rana fuscigula</i>) <i>Hoplobatrachus occipitalis</i> (syn. <i>Rana</i> <i>occipitalis</i>) <i>Hyperolius</i> sp.	<i>Culex territans</i> (Desser <i>et al.</i> , 1973) <i>Aedes aegypti</i> (Ramos and Urdaneta-Morales, 1978) <i>Helobdella algira</i> (Desser <i>et al.</i> , 1973)
	Egypt	Mohammed and Mansour, 1959, 1966	<i>Leptodactylus albilabris</i> (syn. <i>Rana</i> <i>albilabris</i>) <i>Leptopelis</i> sp.	
	Guinea-Bissau	Holberton, 1966	<i>Ptychadena mascareniensis</i> (syn. <i>Rana</i> <i>mascariensis</i>)	
	Nigeria	MacFie, 1914 Lloyd <i>et al.</i> , 1924	<i>Ptychadena oxyrhynchus</i> (syn. <i>Rana</i> <i>oxyrhynchus</i>) <i>Ptychadena perreti</i>	
	South Africa	Fantham <i>et al.</i> , 1942	<i>Sclerophrys regularis</i> (syn. <i>Bufo regularis</i>)	
	Sudan	Balfour, 1908 Stevenson, 1911	<i>Xenopus laevis</i>	
	Uganda: Bugala Island	Hoare, 1932	Frog (unknown species)	
	Africa (unspecified)	Rousselot, 1953	Toad (unknown species) <i>Ptychadena trinodis</i> (syn. <i>Rana trinodis</i>) <i>Discoglossus pictus</i>	
<i>T. sanguinis</i>	Gambia	Dutton and Todd, 1903	<i>Sclerophrys regularis</i> (syn. <i>Bufo</i> <i>regularis</i>)	
<i>T. sergenti</i>	Algeria	Brumpt, 1923		
<i>T. somalense</i>	Somalia	Brumpt, 1906		
<i>T. tumida</i>	Burundi: Bujumbura (formerly Usumbura), Tanganyika	Avérinzev, 1916	<i>Amietia nutti</i> (syn. <i>Rana nutti</i>)	

2.1.3. Materials and methods

2.1.3.1. Collection of research specimens

Amietia delalandii, the type host of *T. nelspruitense*, was one of two host species targeted for the present study. The second host targeted was *Xenopus laevis*, the type host of *T. grandicolor*. In June 2020, *A. delalandii* were sampled by hand from two sites in Mbombela (formerly Nelspruit), Mpumalanga, South Africa, the type locality of *T. nelspruitense* (Laveran, 1904). One adult *A. delalandii* specimen was collected from site

CHAPTER 2.1

1 (25°27'43" S, 30°57'55" E), along the bank of the Crocodile River. Six adult *A. delalandii* were collected from site 2 (25°29'16" S, 30°59'32" E), a small stream flowing through a residential area. In 2018, a total of 25 *X. laevis*, were collected from artificial ponds at the North-West University Botanical Gardens, Potchefstroom, South Africa (26°40'56" S, 27°05'43" E).

Blood was drawn from the femoral artery and smears were made onto microscope slides. Blood was also placed into a sterile 2 ml screw cap cryovial with 100% ethanol. The smears were fixed with 100% methanol and stained with a 10% Giemsa solution for approximately 20 minutes. Material from *A. delalandii* specimens in Potchefstroom was acquired from stored blood samples which had been collected during previous studies of Netherlands *et al.* (2014) and Conradie *et al.* (2017).

2.1.3.2 *Morphological characterisation*

Stained blood smears were screened and images taken using a Zeiss Axiocam 208 color with a Nikon Eclipse Ni microscope and Zeiss Axiocam 305 color with a Zeiss AX10 microscope at 1000x magnification. Images were measured using ImageJ version 1.52a (Schneider *et al.*, 2012) according to a morphometric system adapted from Ferreira (2010) and Shannon (2016). Measurements include body length (BL); body width (BW) (measured at point of maximum width, excluding the undulating membrane); nucleus length (NL); nucleus width (NW); undulating membrane width (UMW); number of undulations (NU); kinetoplast length (KL); kinetoplast width (KW); mid-nucleus to anterior body end distance (MA); mid nucleus to posterior body end distance (MP); free flagellum length (F). The body length (BL) for round forms was measured between the two furthest apart points of the body. Body width (BW) of the round forms was measured at 90° to the BL. Derived measurements were: body shape index (BI) = BL/BW; nuclear index (NI) =

CHAPTER 2.1

NL/NW; nucleus position from the anterior end relative to body length, expressed as a percentage (NP) = MA/BL.

2.1.3.3 *DNA extraction, amplification, and sequencing*

DNA was then extracted from infected blood samples using a *Quick-DNA*TM Miniprep Plus Kit, according to the nucleated blood sample protocol (Zymo Research, California, USA). The extracted DNA samples were then transferred to a sterile 1.5 ml microcentrifuge tube and used in polymerase chain reaction (PCR) amplifications or stored when not in use at -20 °C.

The 18S rRNA gene was targeted because it is currently the most commonly used gene for classifying anuran trypanosomes and hence has the most reference sequences available. Amplification of the gGAPDH (Glyceraldehyde-3-Phosphate Dehydrogenase) gene was also attempted, however, was unsuccessful. Two overlapping fragments of the 18S rRNA gene were targeted for amplification using a nested PCR strategy adapted from McInnes *et al.* (2009) and Egan *et al.* (2020). The primary PCR was performed with the primers SLF (5'-GCTTGTTTCAAGGACTTAGC-3') and S762.2 (5'-GACTTTTGCTTCCTCTAATG-3'), sourced from Inqaba Biotec. The secondary PCR was performed twice, using two different primer sets, namely B (5'-CGAACAACTGCCCTATCAGC-3') and I (5'-GACTACAATGGTCTCTAATC-3'); and S825 (5'-ACCGTTTCGGCTTTTGTGG-3') and SLIR (5'-ACATTGTAGTGCGCGTGTC-3'), also sourced from Inqaba Biotec. The primary and secondary PCR cycle conditions included an initial denaturation step 95 °C for 5 minutes, annealing step of 50 °C for 2 minutes and extension step of 72 °C for 4 minutes. This was followed by 35 cycles comprising of a denaturation step of 94 °C for 30 seconds, annealing step of 55 °C for 30 seconds and an extension step of 72 °C for 2 minutes and 20 seconds. Lastly, a final denaturation step of 72 °C for 7 minutes was performed. This entire amplification protocol

CHAPTER 2.1

was conducted on samples of *A. delalandii* (n = 7) from Mbombela and samples of *A. delalandii* (n = 10) and *Xenopus laevis* (n = 10) from Potchefstroom. These specific samples were chosen, as they were found to be infected with trypanosomes during microscopic screening of the blood smears.

Electrophoresis with a 1% agarose gel was utilized to determine if the amplicons were of the correct size (± 900 bp) and desired quality for sequencing. The samples that had clear bands and the correct size were sent to be sequenced with the chain-termination method at Inqaba Biotech (a commercial sequencing company). Samples of poor quality were discarded.

2.1.3.4 *Phylogenetic analysis*

The chromatograph sequences (received from the sequencing at Inqaba Biotech) were edited and trimmed using FinchTV version 1.4.0. (Geospiza, 2006). A contig sequence was created for each sample from the forward and reverse primer sequences using the pairwise alignment method on BioEdit version 7.0.5.3 (Hall, 1999). The overlap of approximately 300 bp between B/I and S825/SLIR sequences was used to merge them and create final consensus sequences using BioEdit.

A nBLAST™ multiple alignment (McEntyre and Ostell, 2013) was performed on the final sequences to determine the percent identity matches of the samples. Comparable 18S rDNA sequences, to be used for the construction of a phylogenetic tree, were obtained from NCBI GenBank with nBLAST™, whereas other sequences from the phylogenetic trees by Yazaki *et al.* (2017) and Bernal and Pinto (2016) were retrieved by accession number from NCBI GenBank. The sequence alignments were constructed using the MUSCLE alignment method on MegaX (Kumar *et al.*, 2018) with default settings in FASTA format. The program jModelTest (Guindon and Gascuel, 2003; Darriba *et al.*, 2012) was used to select the most suitable nucleotide substitution model for the sequence

CHAPTER 2.1

alignment with an Akaike information criterion (AIC) calculation. The general time-reversible (GTR) model (Tavaré, 1986) with inverse (+I) and gamma (+G) distribution was selected as the best model, with a proportion of invariable sites 0.3190 and gamma shape of 0.4220. Maximum likelihood (ML) phylogenetic trees were constructed using RAxMLGUI 2.0 (Edler *et al.*, 2021) with thorough bootstrap setting and 1000 bootstrap replicates. A Bayesian inference (BI) analysis was performed within MrBayes (Huelsenbeck and Ronquist, 2001; Ronquist and Huelsenbeck, 2003) using the GTR model with a proportion of invariable sites (+I) and a gamma-distributed rate variation (+G). This analysis used the Markov Chain Monte Carlo (MCMC) algorithm with 10 000 000 generations, where every 100th generation was sampled and the first 25% of trees discarded as burn-in. Due to the similar tree topology of ML and BI analyses, a consensus phylogram of the aquatic trypanosome clade was constructed and is represented on the BI tree. A model-corrected (GTR +I +G) pair-wise distances (p-distances) were calculated in PAUP version 4.0a169 (Swofford, 2003) for the sequences used in the phylogenetic analyses.

CHAPTER 2.1

2.1.4. Results

Of the seven *Amietia delalandii* femoral blood samples collected from Mbombela, one (14%) was found to have trypanosomes conforming morphologically to *T. nelspruitense* infections during microscopic screening of the blood smears (sample AB200704A1). Additionally, trypanosomes with similar morphological characteristics to *T. nelspruitense* were also observed in two archived *A. delalandii* blood samples from Potchefstroom (samples AR150210A48, and AE150225B12). Three of twenty-five (12%) *Xenopus laevis* from Potchefstroom exhibited trypanosomes conforming morphologically to *T. grandicolor* in the blood (samples AE180112A9, AE180112A6, and AE180112A5). Molecular sequencing was performed alongside morphological characterisation for each sample due to the unreliability of only using morphological characteristics to classify trypanosomes.

Table 2.1.2: Morphometric measurements of *Trypanosoma* species infecting South African anurans. Measurement range shown in μm (mean \pm standard deviation). Body length (BL), body width (BW), nucleus length (NL), Nucleus width (NW), mid-nucleus to anterior (MA), mid-nucleus to posterior (MP), undulating membrane width (UMW), number of undulations (NU), kinetoplast length (KL), kinetoplast width (KW), length of free flagellum (F). Body shape index (BI), nuclear index (NI) and nucleus position as a percent (NP). Species from the present study are in bold.

Species of <i>Trypanosoma</i>	BL	BW	NL	NW	MA	MP	UMW	NU	KL	KW	F	BI	NI	NP (%)
<i>T. cf. nelspruitense</i> (Present study)	46.68–55.82 (50.9 \pm 3.28) n=18	4.19–10.69 (6.45 \pm 1.67) n=18	12–20.98 (14.9 \pm 2.67) n=9	1.03–2.2 (1.44 \pm 0.36) n=10	33.64–42.15 (37.73 \pm 2.64) n=11	10.27–16.09 (13.28 \pm 1.8) n=11	2.24–5.68 (3.43 \pm 0.94) n=18	6–12 (8.78 \pm 1.8) n=18	0.8–1.72 (1.06 \pm 0.2) n=18	0.38–0.74 (0.52 \pm 0.1) n=18	17.33–32.83 (24.29 \pm 6.61) n=6	4.37–12.15 (8.41 \pm 2.24) n=18	6.38–12.95 (10.53 \pm 2.15) n=9	66.75–79.75 (73.17 \pm 3.57) n=11
<i>T. nelspruitense</i> (Laveran, 1904)	24–35	2.5–3.5									20–35			
<i>T. cf. grandicolor</i> (Present study)	84.39–151.38 (111.73 \pm 13.13) n=30	9.57–26.19 (16.49 \pm 4.41) n=33	4.99–15.13 (9.1 \pm 2.4) n=32	3.05–7.18 (5.34 \pm 1) n=32	51.17–79.12 (61.68 \pm 6.33) n=30	34.56–69.73 (49.81 \pm 8.45) n=32	1.22–4.47 (2.18 \pm 0.76) n=15	12–19 (15.69 \pm 2.09) n=16	1.01–1.74 (1.37 \pm 0.18) n=31	0.69–1.22 (0.94 \pm 0.13) n=31	1.8–5.93 (3.68 \pm 1.44) n=6	3.1–12.51 (7.26 \pm 2.14) n=31	1.13–3.38 (1.76 \pm 0.47) n=32	51.05–66.04 (55.56 \pm 3.91) n=31
<i>T. grandicolor</i> (Pienaar, 1962)	120–150	13–16												60

CHAPTER 2.1

2.1.4.1. *Diagnosis*

Phylum: Euglenozoa Cavalier-Smith, 1981

Class: Kinetoplastea Honigberg, 1963, emend. Vickerman, 1976

Subclass: Metakinetoplastina Vickerman, 2004

Order: Trypanosomatida Kent, 1880

Family: Trypanosomatidae Doflein, 1951

Genus: *Trypanosoma* Gruby, 1843

Subgenus: *Trypanosoma* Gruby, 1843 emend. Votýpka and Kostygov, 2021

Supplementary description of *Trypanosoma cf. nelspruitense* Laveran, 1904

Type host: *Amietia delalandii* Duméril and Bibron, 1841 (Anura: Pyxicephalidae) (syns. *Amietia quecketti*, *Rana theileri* and *Rana angolensis*).

Voucher material: Pending formal peer-review publication.

Type locality: Mbombela (formerly Nelspruit), Mpumalanga province, South Africa (Laveran, 1904; Laveran and Mesnil, 1907).

Localities in this study: Stream in residential area (25°29'16" S, 30°59'32" E) Mbombela, Mpumalanga province, South Africa; Botanical Gardens (26°40'56" S, 27°05'43" E), North-West University campus, Potchefstroom, North West Province, South Africa.

Site of infection: Peripheral blood.

Vector: Unknown.

Stages in vector: Unknown.

Representative DNA sequences: The sequence data specifically associated with *T. cf. nelspruitense* (upon which the present biological description is based) have been submitted to GenBank and are as follows: Nuclear 18S rDNA (nu 18S) partial sequence

CHAPTER 2.1

AB200704A1, AE150225B12, and AR150210A48 (GenBank accession numbers OP502085, OP502084, and OP502083, respectively).

Description: Measurement range shown in μm (mean \pm standard deviation). Body length 46.68–55.82 (50.9 ± 3.28) and body width 4.19–10.69 (6.45 ± 1.67) ($n = 18$). Nucleus length 12.00–20.98 (14.9 ± 2.67) ($n = 9$); nucleus width 1.03–2.20 (1.44 ± 0.36) ($n = 10$); undulating membrane width 2.24–5.68 (3.43 ± 0.94); number of undulations 6–12 (8.78 ± 1.8); kinetoplast length 0.80–1.72 (1.06 ± 0.2) and kinetoplast width 0.38–0.74 (0.52 ± 0.1) ($n = 18$). Mid-nucleus-to-anterior-body-end distance 33.64–42.15 (37.73 ± 2.64) and mid-nucleus-to-posterior-body-end distance 10.27–16.09 (13.28 ± 1.8) ($n = 11$). Free flagellum length 17.33–32.83 (24.29 ± 6.61) ($n = 6$). Body index 4.37–12.15 (8.41 ± 2.24), nuclear index 6.38–12.95 (10.53 ± 2.15) and nuclear position as a percentage 66.75–79.75% (73.17 ± 3.57). The body stains purple in colour with uniform density (Figure 2.1.1 A-H). The undulating membrane stains lighter purple with a colourless and transparent outer edge. The nucleus stains light pink and is thin and elongated. It is positioned parallel to the body and present in the posterior half. The kinetoplast is distinct, stains deep pink in colour and is typically positioned close to the posterior end. The flagellum is faint and not always visible.

CHAPTER 2.1

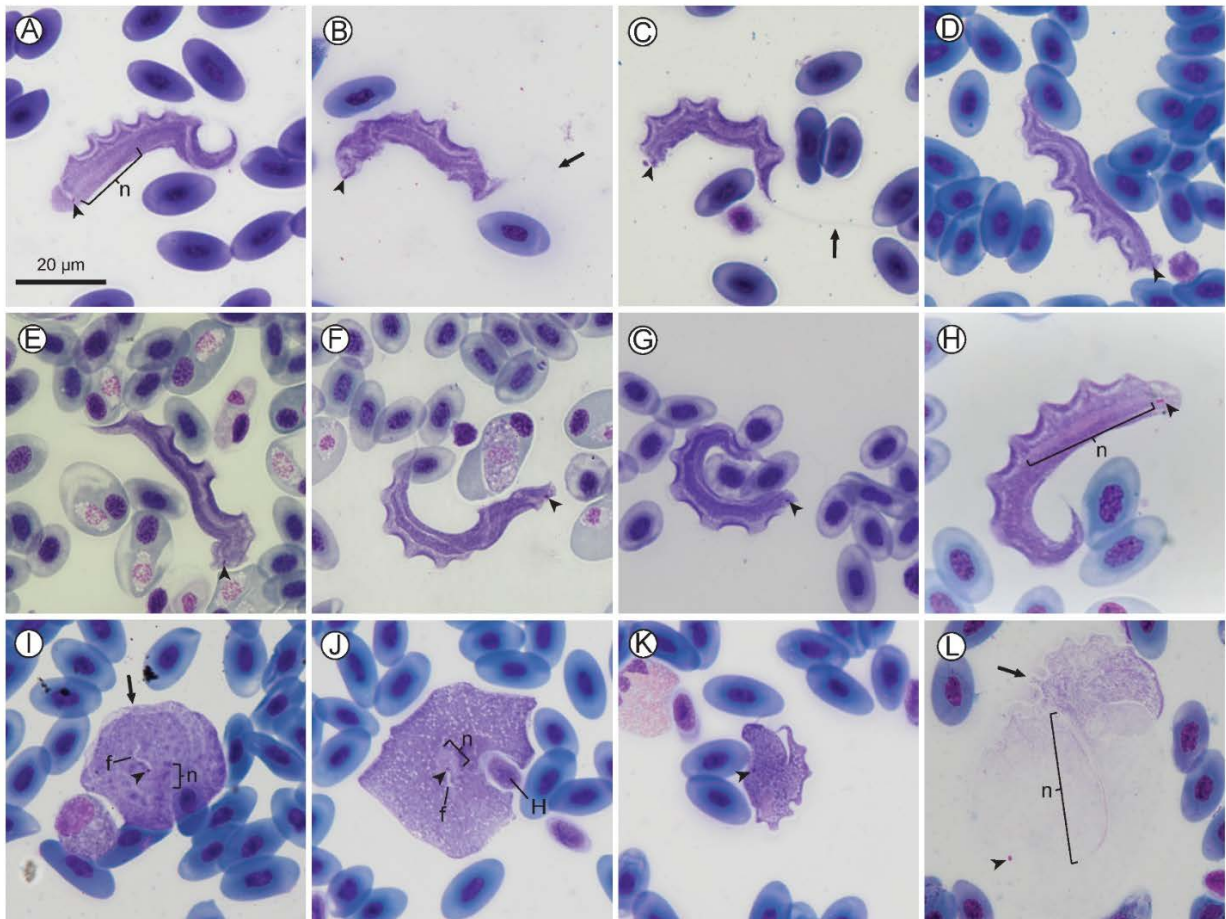


Figure 2.1.1: *Trypanosoma cf. nelspruitense* plate. (A-H) Normal trypomastigote forms in the blood. (I-J) Round forms. (K) Stumpy form. (L) Larger normal form. Arrowheads show kinetoplasts (A-L); arrows show flagella (B and C) and undulating membranes (I and L); nuclei are indicated by “n” (A, H, I, J, and L). Internal flagella indicated by “f” (I and J). Host cell indicated by “H”. Scale bar is 20 µm.

Remarks: The mean morphometric measurements of this species from Mbombela and Potchefstroom were all within 2 µm of each other, which was less than the standard deviation. Therefore, and because the nucleotide sequences of both localities were identical, both localities' specimen morphometrics were combined in Table 2.1.2, as it is evident that they are the same species based on morphometric and molecular data. A small number of round and stumpy forms were observed alongside the normal morphotype for this species, as seen in Figure 2.1.1 (I, J, and K).

This trypanosome, described in the present study infecting *Amietia delalandii* from Mbombela, morphologically resembles the description of *T. nelspruitense* by Laveran (1904) from the same type host and type locality. It shared the characteristic long, slender

CHAPTER 2.1

body, long free flagellum and pronounced undulations. The body size of *T. cf. nelspruitense* was larger yet remained proportionate to the dimensions in Laveran's (1904) description (50.9×6.45 vs. $24\text{--}35 \times 2.5\text{--}3.5$ μm). *Trypanosoma cf. nelspruitense* has a distinctly free flagellum (24.29 μm), which is in accordance with the size ($20\text{--}35$ μm) described by Laveran (1904), where he also notes it as being 'unusually long'. However, Laveran (1904) estimates its length to be generally the same length as the body, a 1:1 ratio, whereas the body length to free flagellum ratio in the present study was observed to be more than twice as long, at 2.1:1. There is no observed difference in stained colour or density between the posterior and anterior, in contrast to Laveran's (1904) description. This is possibly due to the visible colour or apparent density changing, depending on the staining method, although Giemsa solution (containing Azure, Methylene blue and Eosin) and Methylene blue with Eosin staining compounds were used in the present study and Laveran (1904), respectively.

The kinetoplast, which Laveran (1904) refers to as the centrosome, is stated as consistently being positioned slightly away from the posterior end, which is also true in the present description. Furthermore, the body posterior ends do not taper and are rounded, unlike the description of Laveran (1904). The variance in morphological measurements between the two parasites could also be due to the difference in techniques and microscopy equipment used between 1904 and 2022. Laveran (1904) states the parasite's dimensions are fairly consistent and the standard deviation is, indeed, shown to be low by this study. Only the SD of the free flagellum length of this species varied significantly, which is likely due to the difficulty of accurately measuring it, as the full flagellum of the majority of specimens was obscured and often folded. *Trypanosoma cf. nelspruitense* had a pronounced undulating membrane with a rounded up average NU of 9. The average NU is not stated by Laveran (1904), only that many of the specimens he encountered had 12 undulations, which is also true for *T. cf.*

CHAPTER 2.1

nelspruitense in the present study. The nucleus of normal trypomastigote forms of *T. cf. nelspruitense* is not rounded or oval as described by Laveran (1904), instead it is observed to be thin and elongated. Rounded nuclei were observed in the round and stumpy forms of *T. cf. nelspruitense* (Figure 2.1.1 I, J, and K). This difference could be due to the parasites being in different stages of division, as Ivanic (1936) reported an elongated nucleus in a 'giant' trypomastigote form and round nucleus in a round form of apparently the same species, *Trypanosoma rotatorium*, stating that the protoplasmic body influences the nucleus shape. Diamond (1965) believes the situation described by Ivanic (1936) could be a mixed infection of two species of *Trypanosoma* and that the different nucleus forms could be due to different stages of nucleic division, although this is unproven.

Because of the advancements in technology and the addition of molecular profiles in species descriptions of protozoans since 1904, the original description of *T. nelspruitense* by Laveran (1904) may be considered incomplete by modern standards. Compounding matters further there is no type material available for comparison. However, based on the data provided in the original description and for the reasons stated above, we propose the supplementary description and designation of *Trypanosoma (Trypanosoma) cf. nelspruitense* Laveran, 1904 voucher material from the same type locality and type host as the original description.

In comparison with other trypanosomes from anuran hosts, normal trypomastigote forms of *T. cf. nelspruitense* in the present study morphologically resemble those of the 'larger' form of *T. karyozeukton*, described by Dutton and Todd (1903) infecting west African anurans. *Trypanosoma karyozeukton* is, however, longer (67.2 μm), has a shorter free flagellum (15.2 μm) and has a characteristic chain of granules which is absent in *T. cf. nelspruitense*, furthermore, there is a great geographic distance between these two species' localities and the host species are different. *Trypanosoma cf. nelspruitense*,

CHAPTER 2.1

from the present study, also shares morphological similarities with experimentally infected ‘adult’ forms of the anuran trypanosome *T. pipientis* (see Fig. 5 and 6, Diamond, 1965). However, *T. pipientis* was shorter and narrower (43.4 × 3.4 µm) than *T. cf. nelspruitense* and is geographically restricted to North America, infecting different host species. Furthermore, these experimentally infected forms of *T. pipientis* might not be morphologically representative of a natural infection.

Variation in the normal trypomastigote form was observed for *T. cf. nelspruitense* (Figure 2.1.1 L). A small number of specimens were noticeably larger and stained faintly with a light pink colour, in contrast to the typical deep purple. Many of these larger specimens had damaged or poorly defined outer body membranes making their measurement imprecise. These larger specimens were not different enough to be distinguished as a separate morphotype from the normal form and were, thus, included in the morphometric measurements, when not damaged. Stumpy (Figure 2.1.1 K) and round forms (Figure 2.1.1 I and J) were sometimes observed alongside the *T. cf. nelspruitense* infections which are believed to be a different morphotype of *T. cf. nelspruitense* and not a different species. A single round form of *T. cf. nelspruitense* in this study (Figure 2.1.1 J) had similar features to *T. chattoni* reported by Diamond (1965) and Shannon (2016), where the kinetoplast appears to be intranuclear, and an internal flagellum is observed. The other rounded form observed (Figure 2.1.1 I) also has an internal flagellum visible starting at the kinetoplast, however, the nucleus is positioned separately and the formation of an undulating membrane is visible.

Subgenus: *Haematomonas* Mitrophanow, 1883 emend. Votýpka and Kostygov, 2021

Supplementary description of *Trypanosoma cf. grandicolor* Pienaar, 1962

CHAPTER 2.1

Host: *Xenopus laevis* Daudin, 1802 (Anura: Pipidae).

Voucher material: Pending formal peer-review publication.

Type locality: Stream ("spruit"), Potchefstroom, North West province, South Africa.

Localities in this study: North-West University Botanical Gardens (26°40'56" S; 27°05'43" E), North-West University campus, Potchefstroom, North West province, South Africa.

Site of infection: Peripheral blood.

Vector: Unknown.

Stages in vector: Unknown.

Representative DNA sequences: The sequence data specifically associated with *Trypanosoma cf. grandicolor* (upon which the present biological description is based) have been submitted to GenBank and are as follows: Nuclear 18S rDNA (nu 18S) partial sequence AE180112A9 and AE180112A5 (GenBank accession numbers OP502081 and OP502082, respectively).

Description: Measurement range shown in μm (mean \pm standard deviation). Body length 84.39–151.38 (111.73 ± 13.13) ($n = 30$); body width 9.57–26.19 (16.49 ± 4.41) ($n = 33$); nucleus length 4.99–15.13 (9.1 ± 2.4) ($n = 32$) and nucleus width 3.05–7.18 (5.34 ± 1) ($n = 32$); mid-nucleus-to-anterior-body-end distance 51.17–79.12 (61.68 ± 6.33) ($n = 30$); mid-nucleus-to-posterior-body-end distance 34.56–69.73 (49.81 ± 8.45) ($n = 32$); undulating membrane width 1.22–4.47 (2.18 ± 0.76) ($n = 15$); number of undulations 12–19 (15.69 ± 2.09) ($n = 16$); 1.01–1.74 (1.37 ± 0.18) and kinetoplast width 0.69–1.22 (0.94 ± 0.13) ($n = 31$) ($n = 31$). Free flagellum length 1.80–5.93 (3.68 ± 1.44) ($n = 6$). Body index 3.1–12.51 (7.26 ± 2.14) ($n = 31$); nuclear index 1.13–3.38 (1.76 ± 0.47) ($n = 32$) and nuclear position as a percentage 51.05–66.04% (55.56 ± 3.91) ($n = 31$). Body stains dark purple in colour with uniform density (Figure 2.1.2 A-K). The undulating membrane stains lighter purple when visible with a colourless and transparent outer edge, cutting across the parasites body (see Figure 2.1.2 A-L). The nucleus is ellipsoid in shape, staining light

CHAPTER 2.1

purple and is positioned centrally to the body. The kinetoplast is small, stains deep pink in colour, and is typically positioned in halfway between the nucleus and posterior end. The flagellum is faint and not always visible.

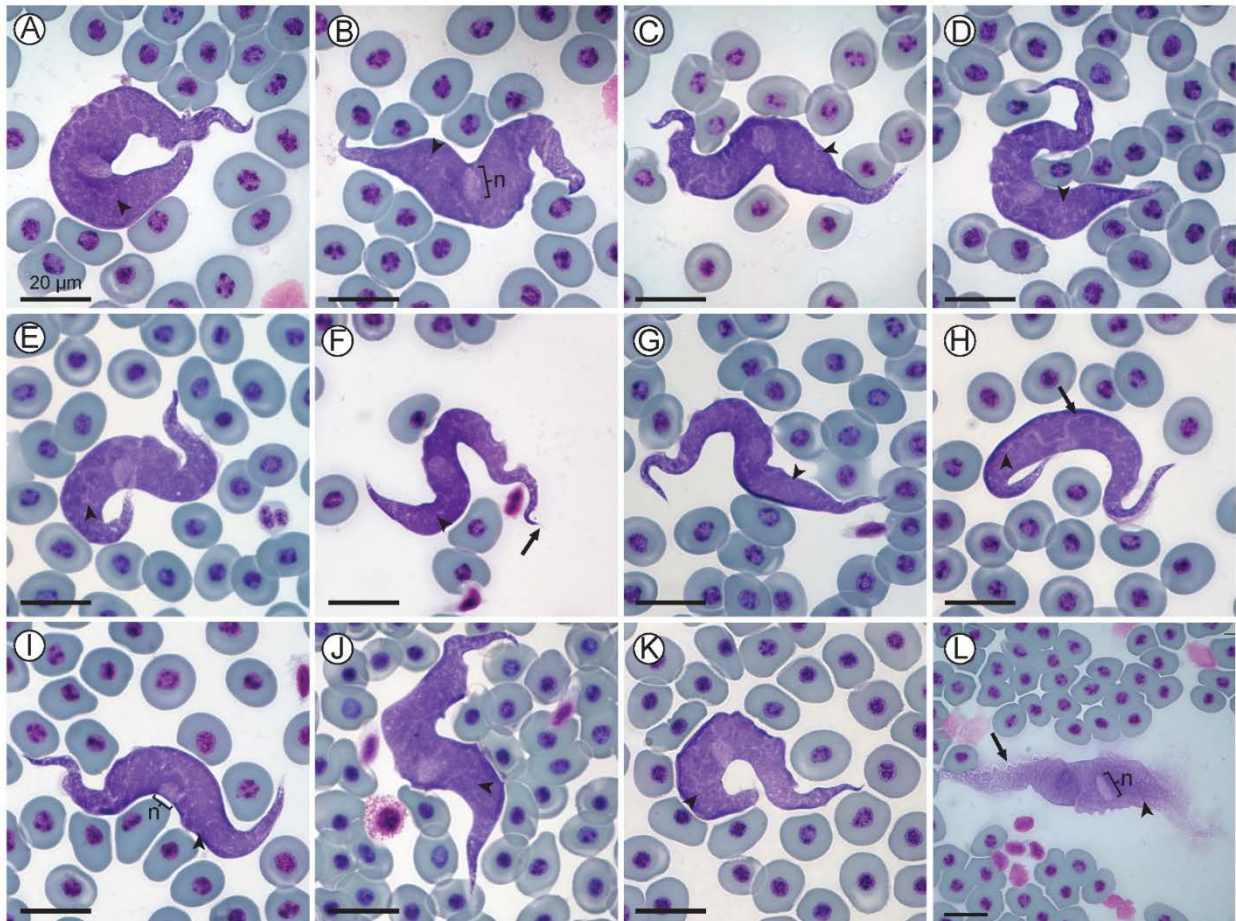


Figure 2.1.2: *Trypanosoma cf. grandicolor* plate. (A-K) Normal trypomastigote forms in the blood. (L) Larger normal form. Arrowheads show kinetoplasts (A-L); arrows show flagellum (F) and undulating membranes (H and L); nuclei are indicated by “n” (B, I, and L). Scale bars are 20 μ m.

Remarks: Morphologically the trypanosome from the present study is large and basophilic in shape, with a prominent undulating membrane and short flagellum visible (Figure 2.1.2 A-L). This species conforms morphologically to *Trypanosoma grandicolor*, a species previously reported from South Africa by Pienaar (1962). However, the species reported by Pienaar (1962) was poorly described without any type material deposited.

Only one trypomastigote form was observed in this study as well as by Pienaar (1962). One especially large specimen was observed (Figure 2.1.2 L); however, it

CHAPTER 2.1

appears as if this form is partially damaged, as also seen with the large form of *T. cf. nelspruitense* (Figure 2.1.1 L). The measurement ranges for the body length and width of the species of *Trypanosoma* given by Pienaar (1962) are 120–150 × 13–16 µm, respectively. In the present study, morphometric ranges of the species of *Trypanosoma* are 84.39–151.38 × 9.57–26.19 µm, conforming with the species of *Trypanosoma* from Pienaar (1962) and falling within the ranges of a giant anuran trypanosome, as it is larger than 50 µm in length. The nucleus is indeed observed to be stained lighter with an average nuclear position of 55.56%, similar to the position of approximately 3/5^{ths} from the anterior body end as described by Pienaar (1962). In contrast to Pienaar (1962), the kinetoplast is clearly visible in the present study and is positioned approximately one third of the body length from the posterior end. The kinetoplast is positioned towards the posterior at the base of the undulating membrane. The nucleus is oval with an average nuclear index (NL:NW) ratio of 1.7:1. Some granules are observed throughout the body, not just the anterior end as with Pienaar (1962) and the body stains evenly, with longitudinal striations observed that run its entire length. Based on the above, we propose the supplementary description of *Trypanosoma (Haematomonas) cf. grandicolor* Pienaar, 1962, for the species from the present study found parasitising the host *Xenopus laevis* (note — ICZN disclaimer). Additionally, we designate voucher material from the same type host and type locality as the original description of *T. grandicolor*.

Trypanosoma cf. grandicolor is classified as belonging to the giant anuran trypanosome complex (≥ 50 µm in length) (Martin *et al.*, 2002). This species is morphologically similar to the reptilian trypanosome, *T. superciliosae*, although the former can be differentiated by its larger body size, circular nucleus and shorter flagellum. Furthermore, the infection of *T. superciliosae* (Walliker, 1965) is reported in a different class of host from a separate continent. Trypomastigotes of *T. schmidtii* (see Fig 55 and 56, Diamond 1965) bear a morphological resemblance to *Trypanosoma cf. grandicolor*,

CHAPTER 2.1

however, the former species is both shorter and narrower, with a longer flagellum. Although similar, *T. superciliosae* has a shorter BL and BW (96.2 and 14.2 μm) than *Trypanosoma* cf. *grandicolor* and has an elongated nucleus instead of the elliptical nucleus found in the latter species. Additionally, the flagellum of *T. superciliosae* is over four times longer on average (16.1 μm) and the posterior was reported to stain paler than the rest of the body, which is in contrast to *Trypanosoma* cf. *grandicolor* from the present study. *Trypanosoma superciliosae* is also geographically isolated from *Trypanosoma* cf. *grandicolor*, as it was described from the iguanomorph lizard *Uranoscodon superciliosus* (syn. *U. superciliosae*) from Brazil. *Trypanosoma schmidti*, an anuran trypanosome from Florida, U.S.A., also shares morphological similarities with *Trypanosoma* cf. *grandicolor*, however, it only has a BL of 85.9 and BW of 9.3 μm , which are roughly 30% and 77% smaller than the latter species, respectively (Diamond, 1965). The flagellum of *T. schmidti* reportedly measures 13.6 μm long which is 3.7 times longer than that of *Trypanosoma* cf. *grandicolor*. The host species and geographic locality of *T. schmidti* are also distinct from *Trypanosoma* cf. *grandicolor*. Notably, *T. schmidti* was described from experimentally infected frogs, and might not represent the wild phenotype occurring in natural infections.

2.1.4.2. Molecular characterisation

A multiple alignment BLAST™ was performed to determine the percent identity matches of the samples' sequences. All three samples of *T. cf. nelspruitense*, OP502083, OP502084 and OP502085, were shown to be a single genotype, due to their close sequence matches. The sequences OP502083 and OP502084 had 100% identity matches for the query cover of 1356 bp (aligned using ClustalW), with a p-distance of 0.00 (Table 2.1.3). Whereas the sequences OP502083 and OP502085 had 99.91% identity matches (differing by a single base pair) for their (ClustalW) alignment with a query cover of 1223 bp, with a p-distance of 0.08. No matches above 96% were observed

CHAPTER 2.1

using BLAST™ for the 18S rDNA of *T. cf. nelspruitense* and the closest sequence matches were from unnamed trypanosome species from South America with an interspecific divergence (model-corrected genetic distance) of 4.60.

One *Trypanosoma cf. grandicolor* sequence, OP502082, was only a half fragment and was thus a shorter sequence (882 bp) than the other, OP502081 (1502 bp), however the sequences shared 100% identity match, thus confirming they are the same species. The closest relatives to *Trypanosoma cf. grandicolor* are trypanosomes isolated from turtle, fish, and platypus samples, with no matches above 98.1%, utilising BLAST™. Although the closest percent identity match was shown by BLAST™ to be 98.06% with the freshwater fish trypanosome, *Trypanosoma cobitis*, with an interspecific divergence (model-corrected genetic distance) of 1.80, *Trypanosoma grandicolor* was well-nested between species of freshwater turtle, platypus, and marine fish hosts in the subgeneric clade *Haematomonas* of the phylogram in Figure 2.1.3, with a BLAST™ identity match of 97.33% and interspecific divergence of 3.25 with *Trypanosoma sp. 5184*.

CHAPTER 2.1

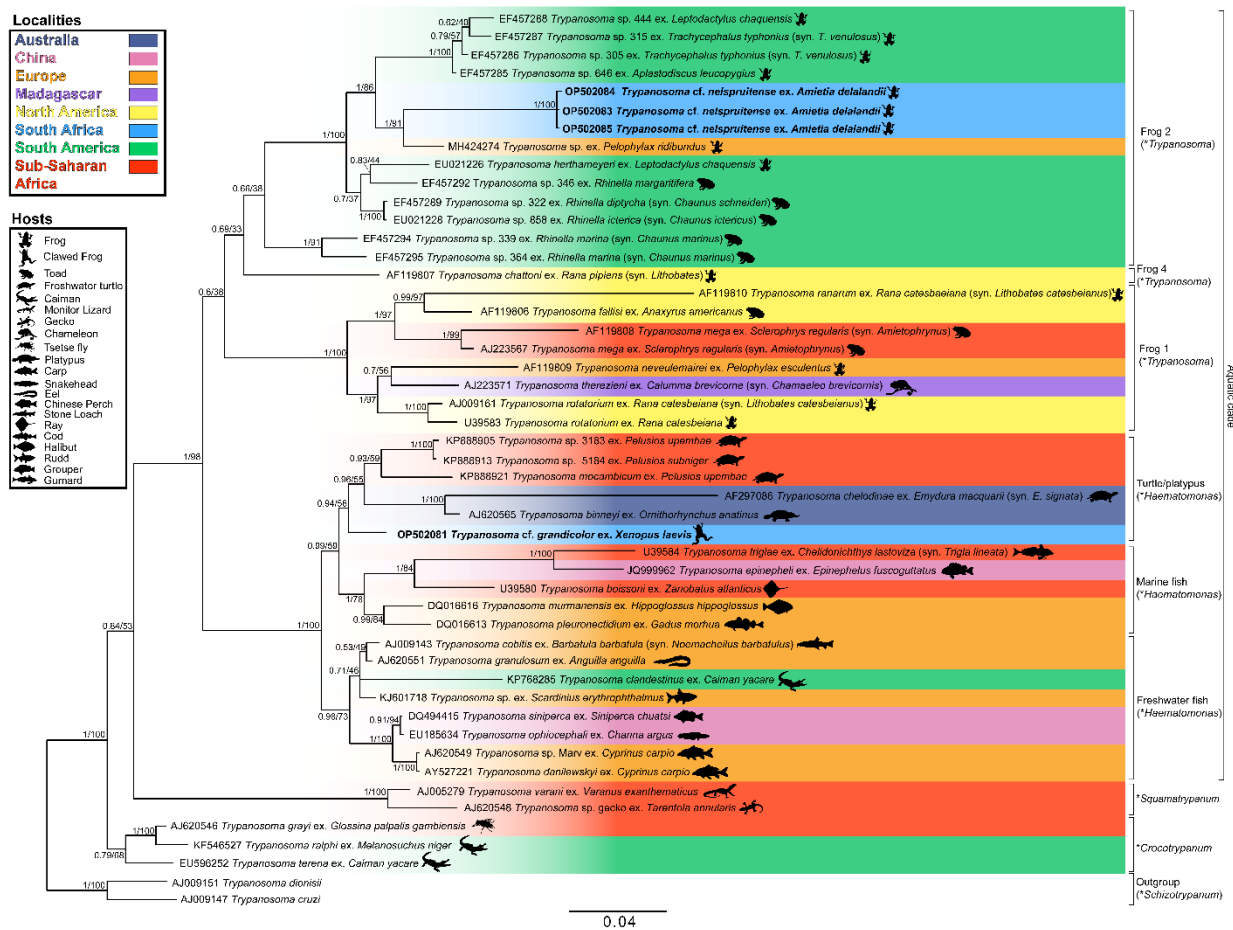


Figure 2.1.3: Consensus phylogram of the aquatic trypanosome clade based on 18S rDNA sequences. Tree topologies of Maximum Likelihood (ML) and Bayesian Inference (BI) analyses were similar (represented on the ML tree). Nodal support values of BI posterior probability and ML bootstrap shown as BI/ML. Sequences from the present study are in bold. Subgenera are indicated by an asterisk (*). Scale shown is nucleotide substitutions per site.

2.1.4.3. Phylogenetic analysis

The consensus phylogram in Figure 2.1.3 represents the aquatic trypanosome clade and is shown with few bootstraps below 75% and posterior probability below 0.80, indicating a high level of confidence. The clades with lower bootstrap values are likely caused by a deficiency of aquatic trypanosome sequences, making it difficult to position the clade precisely. The relationship of the clades in this study's phylogram is consistent with that of other studies' phylogenies and is believed to be an accurate representation of part of the larger trypanosome phylogeny (Lima *et al.*, 2012; Dvořáková *et al.*, 2015; Attias *et al.*, 2016; Bernal and Pinto, 2016; Spodareva *et al.*, 2018; Kostygov *et al.*, 2021). The *Crocotrypanum* and *Squamatypanum* clades are shown to be separate from the aquatic

CHAPTER 2.1

clade as expected, the turtle/platypus clade is positioned with a close relation to the fish clades, and there is a split between the anuran (clade Frog 2 and 4) and anuran/chameleon (clade Frog 1) trypanosomes. This division appears to be geographically related, as there appears to be a dichotomy between North American and South American species. However, trypanosomes of other geographic localities are interspersed between the two anuran clades.

The present study focused on the aquatic clade. The trypanosome species from this study, *T. cf. nelspruitense* [GenBank Accession OP502083, OP502804, and OP502085] and *T. cf. grandicolor* [GenBank Accession OP502081 and OP502082], are placed in two separate novel monophyletic subclades, confirming their identity as two distinct species. The two South African trypanosomes from this study also do not cluster with any of the other African anuran species. There is a significant estimated evolutionary distance between the *T. cf. nelspruitense* clade and its nearest hypothesised clade, the unnamed South American anuran trypanosomes. It possibly indicates that the common ancestral lineage of these two groups could have existed during the period of Gondwanaland and diverged evolutionarily with the break-up of this land mass into the continents of South America and Africa. *Trypanosoma cf. grandicolor* is grouped within a clade of the platypus, turtle, and marine fish trypanosomes. It clades closely with African turtle trypanosomes, *T. mocambicum* and sequences of unnamed trypanosome species from terrapins in Mozambique. This relatedness is likely due to the neighbouring distribution of South Africa and Mozambique, their aquatic hosts and potential leech vector transmission.

2.1.5. Discussion

2.1.5.1. *Morphological characterisation*

CHAPTER 2.1

Morphological analysis is notoriously unreliable with anuran species of *Trypanosoma* due to their lack of rigid structures and extreme pleomorphism (Shannon, 2016; Spodareva *et al.*, 2018). Some species of *Trypanosoma* are known to have several different morphotypes and have a widespread distribution (Desser, 2001). However, morphology can still aid in distinguishing species by being used in conjunction with molecular analyses. Two distinct species were found in this study by analysing blood smear slides. Different forms for the same species were also observed to be present. There are no morphological measurements available for closely related African anuran trypanosome species from other studies to compare against the measurements of specimens in this study.

Suspected pleomorphism was observed on the same slides as the 'normal' trypomastigote morphotypes for both species. No dividing stages were observed in any of the blood samples. It is believed that these forms are not separate from their associated species, as some species of *Trypanosoma* are known to have multiple morphotypes associated with different stages of their life cycles. Interestingly, most of the polymorphism is seen within the leech and dipteran vectors of anuran trypanosomes (Netherlands, 2019; Vanhove *et al.*, 2022), however, there are several reports of rounded trypanosome forms. Shannon (2016) found round forms of *T. chattoni* in the peripheral blood of North American species of *Lithobates*. Interestingly, *T. chattoni* is only known to occur as rounded forms in the vertebrate host and not the typical trypomastigote form (Diamond, 1965). Fantham *et al.* (1942) also found rounded forms of *T. rotatorium*, mostly in the organs (spleen, heart, liver, and lung) and less frequently in the peripheral blood of two species of anurans (*X. laevis* and *A. fuscigula*) from South Africa, as well as several Canadian and European anurans. Diamond (1965) is of the opinion that these rounded forms of Fantham *et al.* (1942) are not conspecific with *T. rotatorium* and instead belong to *T. chattoni*, although it cannot be determined as no description or figure was provided

CHAPTER 2.1

in the original report. These forms were additionally reported to have different morphological changes such as an absent undulating membrane and flagellum. Laveran and Mesnil (1907) confirmed this morphological variance in several examples with the occurrence of ovoid and rounded forms of several species of *Trypanosoma* in frogs and visually established that it is a normal trypanosome that changed shape, which they believed to be due to the change in conditions when leaving blood vessels (and not a different species as suggested by Mayer (1843) and Grassi (1881) (see Laveran and Mesnil, 1907)). These forms are described by Laveran and Mesnil (1907) and Fantham *et al.* (1942) as sometimes lacking an undulating membrane and/or flagellum, as can be seen with some forms of *T. cf. nelspruitense* in Figure 2.1.1 (I and J). Future studies, focusing on the life cycle and identifying morphotypes in the vector could elucidate the different developmental stages for each species. A culturing method might be useful in studying the different forms; however, trypanosomes from cultures are often known to have extremely variable morphology and are not necessarily representative of the wild type (Ferreira *et al.*, 2007).

2.1.5.2. *Molecular characterisation*

The method used in this study can present problems when sequences are isolated from host blood samples with infections of multiple species of *Trypanosoma*. Having a larger sample size could possibly resolve this dilemma by increasing the potential number of hosts with an infection of only one trypanosomatid species, resulting in a single morphospecies per sequence. Dvořáková *et al.* (2015) used PCR-based screening methods to determine the species of samples with mixed infections. The manner of DNA isolation used in the present study is a 'catch-all' method, isolating the trypanosomal DNA from the frog's but not from other trypanosomes in the sample. In the future, it might be

CHAPTER 2.1

possible to isolate individual trypanosome specimens from the blood sample and extract only their genetic material.

2.1.5.3. *Phylogenetic analysis*

Trypanosomatid phylogenies can often be misleading due to the multi-host life cycle of trypanosomes, which cause overlap and merging of seemingly unrelated clades (Martin *et al.*, 2002). This indistinct separation of trypanosome clades is compounded by the fact that most of these vector-transmission routes are unknown. The dipteran and leech vectors of trypanosomes are typically generalist feeders and can potentially transmit trypanosomes between unrelated animal taxa. Trypanosomes are generally transmitted through dipteran or leech vectors. These vector organisms are usually not host-specific and target many different types of species. Theoretically, the same species of *Trypanosoma* could be found in fish, amphibian and reptilian hosts, with vectors such as mosquitoes and leeches transmitting infections between the various host species. This poses the question: is there an overlap of the trypanosome clades' hosts or a trypanosome species that links two clades (e.g. amphibian and squamate)? Spodareva *et al.* (2018) consider the amphibian trypanosomes to be a potential link between the aquatic and terrestrial clades, as they are transmitted by both leech and dipteran vectors.

In future, it could be beneficial to implement additional statistical methods of constructing phylogenetic trees and compare trees of different DNA barcodes, such as gGAPDH, to see if the hypothesised evolutionary relationships stay consistent across the different comparative methods. However, this would require other studies' co-operation in obtaining enough trypanosome sequences using these DNA barcodes for comparison. Increased sampling of trypanosome sequences would allow us to get closer to a representation of the true trypanosomatid phylogeny and eventually bridge the gaps between the current phylogeny's clades.

CHAPTER 2.1

2.1.6. Conclusion

The morphological analysis proved useful in addition to the molecular analyses within the present study, as two distinct morphological species were supported in the phylogeny with two discrete taxonomic units. Larger sample sizes or improved DNA isolation methods could provide more certainty about the genetic identity of morphological species in future studies. Based on the combination of molecular and morphological data, supplementary descriptions of two species of *Trypanosoma* infecting South African anurans are presented in this study: 1) *Trypanosoma* cf. *nelspruitense* Laveran, 1904, which was recorded from infected *Amietia delalandii* hosts from Mbombela and Potchefstroom; and 2) *Trypanosoma* cf. *grandicolor* Pienaar, 1962, recorded from infected *Xenopus laevis* hosts from Potchefstroom. No discernible difference between the molecular and morphological data of *T.* cf. *nelspruitense* from Potchefstroom and Mbombela was observed, showing it is the same species which occurs in multiple localities. Due to the morphological plasticity of trypanosomes and occurrence of mixed species infections in a single host, additional studies would be helpful in providing further insight and perspective.

Ultimately, this study is just a starting point for the taxonomic resolution of the anuran trypanosome clade and creates a platform for future taxonomic characterisation of trypanosomes. Further research needs to be conducted in order to grasp the true ecology and phylogeny of anuran trypanosomes.

2.1.7. Data

Sequence data is available from NCBI GenBank, under accession numbers OP502081-OP502085.

CHAPTER 2.1

2.1.8. Acknowledgements

The authors are grateful for aid from members of the African Amphibian Conservation Research Group and the Water Research Group for access to their facilities. This paper was submitted as part of BJ Jordaan's master's degree at the North-West University (Supervisor EC Netherlands and co-supervisor LH du Preez).

2.1.9. Author contributions

Authors BJ, ECN, and LdP conceived and designed the study. BJ and ECN conducted data gathering and analyses thereof. BJ, ECN, and LdP wrote the article.

2.1.10. Financial support

The financial assistance of the National Research Foundation (NRF) of South Africa, towards BJ and ECN, is hereby acknowledged. Opinions, findings and conclusions or recommendations expressed in any publication generated by an NRF supported study, is that of the author(s) alone, and the NRF accepts no liability whatsoever in this regard (Grant UID 124174; UID 129669).

2.1.11. Conflicts of interest

The authors declare there are no conflicts of interest.

2.1.12. Ethical standards

This study forms part of an approved NWU's AnimCare ethics committee project: Ecology, systematics and evolutionary biology of ectotherm blood parasites (Ethics Number: NWU-00372-16-A5 and NWU-00427-21-A5; North West Department of Rural, Environmental and Agricultural Development research permit number: HQ 18/05/16-088 NW).

CHAPTER 2.2 RESULTS



Jones' girdled lizard (*Cordylus jonesii*)



Soutpansberg girdled lizard (*Smaug depressus*)

CHAPTER 2.2

Morphological and molecular diagnosis of two undescribed species of *Trypanosoma* Gruby, 1843 infecting South African cordylid lizards (Squamata: Cordylidae: Cordylinae), *Trypanosoma (Squamatrypanum)* sp. 2N and *Trypanosoma (Trypanosoma)* sp. 2T

Bernard J. Jordaan¹, Johann van As², and Edward C. Netherlands^{1,3}

¹ African Amphibian Conservation Research Group, Unit for Environmental Sciences and Management, North-West University, Potchefstroom, North West, South Africa.

² Department of Zoology and Entomology, University of the Free State, Qwaqwa Campus, Phuthaditjhaba, Free State, South Africa.

³ Department of Zoology and Entomology, University of the Free State, P.O. Box 339, Bloemfontein, 9300, Free State, South Africa.

CHAPTER 2.2

2.2.1. Abstract

Despite reptile trypanosomes forming a large group, the majority of species descriptions are data deficient, lacking key characteristic data and supporting molecular data. Reptile hosts show potential to facilitate transmission of zoonotic trypanosomiases and offer key information to understanding the genus of *Trypanosoma*. Several species of squamates, from different localities in South Africa, were screened molecularly and microscopically for trypanosomes in the present study. Based on the combination of morphological and molecular analyses, two new species of *Trypanosoma*, *Trypanosoma (Squamatripanum)* sp. 2N and *Trypanosoma (Trypanosoma)* sp. 2T, infecting South African cordylid lizards (Cordylidae: Cordylinae) are described in this study. The first molecular data for a South African reptile trypanosome is provided herewith.

Key words: Blood parasite; *Cordylus jonesii*; reptile; sleeping sickness; *Smaug depressus*; squamate.

CHAPTER 2.2

2.2.2. Introduction

The genus of *Trypanosoma* is a large group of unicellular, flagellate, extracellular obligate haemoparasites. These parasites have been described from all classes of vertebrates and from every continent. Several species are pathogenic causing severe, sometimes fatal, diseases in people and domestic animals. One such disease caused by these parasites and arguably the most well-known, is the infamous sleeping sickness, or Human African Trypanosomiasis (HAT). Monitor lizards have been shown to be naturally infected with *Trypanosoma brucei*, the pathogen responsible for causing HAT. These hosts were shown to experimentally transmit *T. brucei* to laboratory-bred rats (*Rattus norvegicus*) and tsetse flies (*Glossina morsitans*) (Njagu, 1998), one of the main natural vectors responsible for transmission of HAT to humans. The ability of some reptiles to potentially facilitate the transmission cycle of a human-infecting pathogen highlights the importance of researching reptile trypanosomes and gaining a better understanding of the group and their hosts.

Studying reptilian trypanosomes can be troublesome since infections are uncommon, typically with low parasitaemia and infected hosts lack apparent symptoms. Effective species identification is hindered by a deficiency of non-pathogenic trypanosome molecular data and morphological plasticity. This is exacerbated by the fact that many species are unnamed or have poor descriptions. Subsequently, the validity of many taxonomic species is unclear, and many species have no additional records besides their original descriptions.

Currently, only 26 recognised species of squamate trypanosomes, shown in Table 2.2.1, have been reported from Africa (including Madagascar), generally with poor descriptions lacking characteristic data. Additionally, molecular data is available for only four species of African squamate trypanosomes on the NCBI GenBank (*Trypanosoma varani* (AJ005279), *Trypanosoma* sp. gecko (AJ620548), *T. cf. varani* (AB447493), and *T.*

CHAPTER 2.2

therezieni (AJ223571)). Despite lizard trypanosomes having the most reported species of the reptilian group (Viola *et al.*, 2008), none have been described from South Africa. Of all the Squamata in South Africa, only two species of trypanosomes have been described from snakes, namely *Trypanosoma sebae* Fantham and Porter, 1950 and *Trypanosoma psammophis* Fantham and Porter, 1950.

Cordylids (Cordylidae: Cordylinae) are a group of moderately sized, armoured lizards and are the only lizard family restricted to mainland Africa. Only two species of *Trypanosoma* have been described from cordylid lizards, namely *Trypanosoma cordyli* Telford, 1995, and *Trypanosoma zonuri* Telford, 1995, from *Cordylus tropidosternum* and *Cordylus cordylus sensu lato* in Tanzania (Telford, 1995b). A single species of *Trypanosoma*, *T. betschi* Brygoo, 1966, has been described from Gerrhosauridae, the sister family of Cordylidae, from the host *Zonosaurus madagascariensis* (syn. *Gerrhosaurus madagascariensis*) from Madagascar (Telford, 2009). Currently the trypanosomes of South African cordylid lizards remain unknown. The present study aimed to investigate and explore the diversity of South African squamate trypanosomes using microscopic and molecular screening and provide the first molecular data for South African reptile trypanosomes. The subgeneric classification system for the genus of *Trypanosoma*, proposed by Kostygov *et al.* (2021), was followed in the present study.

CHAPTER 2.2

Table 2.2.1: African squamate trypanosome index. Asterisk (*) indicates type host.

Host suborder	Host Family	Species of Trypanosoma	African Record	Author	Known Host Species	
Sauria	Chamaeleonidae	<i>T. chamaeleonis</i>	South Sudan: Bahr el Ghazal Province	Wenyon 1908	<i>Chamaeleo gracilis</i> (syn. <i>Chamaeleon gracilis</i>)	
		<i>T. petteri</i>	Madagascar: Ankara	Brygoo 1966	<i>Phelsuma madagascariensis</i>	
	Cordylidae	<i>T. therezieni</i>	Madagascar: Perinet	Brygoo 1963	<i>Calumma brevicorne</i> (syn. <i>Chamaeleo brevicornis</i>)	
		<i>T. cordyli</i>	Tanzania: 21 km west of Ngorongoro Crater, Arusha Region	Telford 1995	<i>Cordylus tropidosternum</i>	
	Eublepharidae	<i>T. zonuri</i>	Tanzania: 3.8 km west of Rondo Forestry Station, Rondo Forest, Lindi Region	Telford 1995	<i>Cordylus cordylus</i>	
		<i>T. gallayi</i>	French West Africa	Bouet 1909	<i>Hemithelyx caudicinctus</i> (syn. <i>Psylodactylus caudicinctus</i>)	
	Gekkonidae	<i>T. cnemaspi</i>	Tanzania: Kimboza Forest, south side of Uluguru Mountains, Morogoro Region	Telford 1995	<i>Cnemaspis barbouri</i> *	
		<i>T. garnamhi</i>	Kenya	Grewal 1965	<i>Hemidactylus platycephalus</i>	
		<i>T. kimbozae</i>	Tanzania: Kimboza Forest, south side of Uluguru Mountains, Morogoro Region	Telford 1995	<i>Hemidactylus angulatus</i> (syn. <i>Hemidactylus brookii angulatus</i>)	
		<i>T. lygodactyli</i>	Tanzania: north slope of Uluguru Mountains, Morogoro Region*	Telford 1995	<i>Hemidactylus platycephalus</i>	
			Tanzania: Kimboza Forest, south side of Uluguru Mountains, Morogoro Region		<i>Lygodactylus picturatus</i> (syn. <i>Lygodactylus luteopicturatus</i>)*	
			Tanzania: north slope of Uluguru Mountains, Morogoro Region*		<i>Lygodactylus grotei</i> (syn. <i>Lygodactylus capensis grotei</i>)	
			Tanzania: Kimboza Forest, south side of Uluguru Mountains, Morogoro Region		<i>Hemidactylus platycephalus</i>	
			Tanzania: north slope of Uluguru Mountains, Morogoro Botanical Garden, Morogoro Region*	Telford 1995	<i>Hemidactylus platycephalus</i> *	
			Tanzania: Morogoro		<i>Lygodactylus luteopicturatus</i>	
			Tanzania: "University Campus", Morogoro		<i>Lygodactylus capensis grotei</i>	
			Tanzania: Mindu Mountain, Morogoro region		<i>Lygodactylus williamsi</i>	
			Tanzania: Bahari Beach, 21 km north of Dar-es-Salaam			
		Gerrhosauridae	<i>T. betschi</i>	Madagascar: Ankara	Brygoo 1966	<i>Zonosaurus madagascariensis</i> (<i>Gerrhosaurus madagascariensis</i>)
		Opluridae	<i>T. domerguei</i>	Madagascar: Ampijoroa	Brygoo 1965	<i>Oplurus cuvieri</i> (syn. <i>Oplurus sebae</i>)
		Phyllodactylidae	<i>T. platydactyli</i>	Tunisia	Catouillard 1909	<i>Tarentola mauritanica</i>
	Scincidae		<i>T. boueti</i>	Guinea (French Guinea)*	Martin 1907*	<i>Trachylepis albilabris</i> (syn. <i>Mabuya raddoni</i>)*
				D.R. Congo: Kisangani (Stanleyville)	Schwetz 1931	<i>Trachylepis macullabris</i> (syn. <i>Mabuya macullabris</i>)
			D.R. Congo: Kinshasa	Telford 2009	<i>Trachylepis striata</i> (syn. <i>Mabuya striata</i>)	
			Ethiopia: Sabeta	Ashford et al. 1973		
			Senegal	Leger and Leger 1914		
			Tanzania: Morogoro	Telford 2009		
		<i>T. martini</i> (syn. <i>T. mabuia</i>)	Côte d'Ivoire (French West Africa)*	Bouet 1909*	<i>Trachylepis macullabris</i> (syn. <i>Mabuya macullabris</i>)*	
			South Sudan: Wau, Bahr el Ghazal Province	Wenyon 1908	<i>Trachylepis perroteti</i> (syn. <i>Mabuya perroteti</i>)	
			Guinea-Bissau (Portuguese Guinea)	Franca 1911	<i>Trachylepis quinquetaeniata</i> (syn. <i>Mabuya quinquetaeniata</i>)	
			Kenya: near Lake Victoria	Garnham 1950	<i>Trachylepis albilabris</i> (syn. <i>Mabuya raddoni</i>)	
			Kenya: Pole, West Pokot County	M. Musinga (unpublished, see Telford 2009)		
			D.R. Congo: Kivu Province	van den Berghe et al. 1964	<i>Mochlus fernandi</i>	
	<i>T. mochli</i>	Guinea	Franca 1911	<i>Trachylepis perroteti</i> (syn. <i>Mabuya perroteti</i>)*		
	<i>T. perroteti</i>	Tanzania: Amani, Tanga Province	Telford 2009	<i>Trachylepis striata</i> (syn. <i>Mabuya striata</i>)*		
Varanidae	<i>T. striatae</i>			<i>Trachylepis macullabris</i> (syn. <i>Mabuya macullabris</i>)		
	<i>T. varani</i>	Sudan: Tautikia*	Wenyon 1908*	<i>Varanus niloticus</i> *		
Serpentes	Colubridae		Senegal	Minter-Goedbloed et al. 1993	<i>Varanus exanthematicus</i>	
		<i>T. clozeli</i>	Côte d'Ivoire (West Africa)	Bouet 1909	<i>Afronatrix anoscopus</i> (syn. <i>Tropidonotus ferox</i>)*	
Elapidae		<i>T. psammophis</i>	South Africa	Fantham & Porter 1950	<i>Psammophis mossambicus</i> (syn. <i>P. sibilans</i>)	
		<i>T. najae</i>	South Sudan: Sobat River	Wenyon 1908	<i>Naja nigricollis</i>	
Pseudoxyrhopiidae		<i>T. voltaiae</i>	Ghana	Macfie 1919	<i>Naja nigricollis</i>	
		<i>T. haranti</i>	Madagascar: Perinet	Brygoo 1965	<i>Thamnosophis lateralis</i> (syn. <i>Liopholidophis lateralis</i>)	
Pythonidae		<i>T. sebae</i>	South Africa	Fantham & Porter 1950	<i>Python natalensis</i> (syn. <i>P. sebae</i>)	

2.2.3. Materials and methods

2.2.3.1. Collection of research specimens

Two *Cordylus jonesii* (Jones' girdled lizard) were found basking on tree trunks and collected by hand, in Ndumo Game Reserve (KwaZulu Natal, South Africa) in March 2021. In total, fifteen *Smaug depressus* (Zoutpansberg girdled lizards) were collected from rock crevices by hand and using a noose, from several sites on the Soutpansberg mountain (Lajuma Research Camp, Limpopo, South Africa) over a three-year period. Two *S. depressus* specimens were collected in November 2020, three in September 2021 and ten in September and October 2022. Other squamates, including chameleons, geckoes, monitor lizards, skinks, and snakes, from several localities in South Africa were captured opportunistically by hand or with a noose (see Supplementary Table 2.2.1). Animals were

CHAPTER 2.2

examined externally for parasites.

Blood was collected through a cardiac, femoral, or caudal venipuncture. Glass slide smears and blood samples were prepared using standard methods Netherlands *et al.* (2015). Blood smears were made onto a clean microscope slide, air-dried and fixed with absolute methanol. Once dry, the slides were stained for roughly twenty minutes with a 10% solution of modified Giemsa (Sigma-Aldrich, Steinheim, Germany). Additional blood was stored in sterile 2-ml screw cap cryovials. Wet smears were made in the field of all ten *S. depressus* specimens captured in 2022, using a drop of blood underneath a cover slip on a clean microscope slide of all ten *S. depressus* specimens captured in 2022 and immediately screened using light microscopy. Additional blood samples were collected, and stained blood smear slides made using the aforementioned technique on two occasions after capture from three of these *S. depressus* specimens.

2.2.3.2. *Morphological characterisation*

Stained blood smears were screened for trypanosomes with a Zeiss AX10 microscope and images were captured using a Zeiss Axiocam 305 color at a magnification of 1600x. Morphometrics were measured according to a system adapted from Telford (1995a), Ferreira (2010), and Jordaan *et al.* (Chapter 2.1) using ImageJ version 1.52a (Schneider *et al.*, 2012). Measurements of each morphological character were taken from 30 different specimens, when visible. Measurements include body length (BL); body width (BW) (measured at point of maximum width, excluding the undulating membrane); nucleus length (NL); nucleus width (NW); undulating membrane width (UMW); number of undulations (NU); kinetoplast length (KL); kinetoplast width (KW); mid-nucleus to anterior body end distance (MA); mid nucleus to posterior body end distance (MP); free flagellum length (F); mid-kinetoplast to anterior body end distance (KA); mid-kinetoplast to posterior body end distance (KP); mid-kinetoplast to mid-nucleus distance (KN). Derived measurements were nuclear index, NL/NW (NI); and body shape index, BL/BW (BI), are

CHAPTER 2.2

expressed as ratios. Nucleus position from the anterior end relative to body length, MA/BL (PN); and kinetoplast position from the anterior end relative to body length, KA/BL (PK), expressed as percentages.

2.2.3.3. *DNA extraction, amplification, and sequencing*

DNA extraction, amplification, and sequencing followed the methods of Jordaan *et al.* (Chapter 2.1). DNA was extracted using a NucleoSpin® Tissue DNA, RNA, and protein purification kit (Macharey-Nagel, Düren, Germany).

Samples (see Supplementary Table 2.2.1) were screened molecularly for trypanosomes by targeting two overlapping fragments of the 18S rRNA gene for amplification, using a nested PCR strategy adapted from McInnes *et al.* (2009) and Egan *et al.* (2020), following Jordaan *et al.* (Chapter 2.1). The primary PCR was conducted with the external primers SLF (5'-GCTTGTTTCAAGGACTTAGC-3') and S762.2 (5'-GACTTTTGCTTCCTCTAATG-3'). Two secondary PCR's were performed, using two different internal primer sets, namely B (5'-CGAACAACTGCCCTATCAGC-3') and I (5'-GACTACAATGGTCTCTAATC-3'); and S825 (5'-ACCGTTTCGGCTTTTGTGG-3') and SLIR (5'-ACATTGTAGTGCGCGTGTC-3'). The cycle conditions of the primary PCR included an initial denaturation step 95°C for 5 minutes, annealing step of 50°C for 2 minutes, and extension step of 72°C for 4 minutes. This was followed by 35 cycles containing a denaturation step of 94°C for 30 seconds, annealing step of 60°C for 30 seconds, and an extension step of 72°C for 2 minutes and 20 seconds. Lastly, a final denaturation step of 72°C for 7 minutes was performed. The conditions of both secondary PCR's consisted of an initial denaturation step of 95°C for 5 minutes, followed by 35 cycles of a denaturation step of 95°C for 30 seconds, annealing step of 57°C for 30 seconds, and an extension step of 72°C for 1 minute. Thereafter, a final denaturation step of 72°C for 7 minutes was carried out.

Amplicons were electrophoresed with a 1% agarose gel to determine if they were

CHAPTER 2.2

of the correct size (\pm 900 bp) and desired quality for sequencing. Samples showing clear bands of the correct size were sent to Inqaba Biotech to be sequenced with the chain-termination method in both directions. Poor quality samples were discarded. Cultivation of these trypanosomes was not attempted.

2.2.3.4. *Phylogenetic analysis*

Geneious R9 (Kearse *et al.*, 2012) was used to edit and trim the chromatograph sequences (received from Inqaba Biotech). A consensus sequence was created for each sample from the forward and reverse primer sequences of both B/I and S825/SLIR primer sets using the De Novo assembly method with Geneious R9 (Kearse *et al.*, 2012).

A standard nucleotide BLAST™ (McEntyre & Ostell, 2013) search of the NCBI database was conducted using the final sequences to determine the percent identity matches of the samples. For the construction of a phylogenetic tree, comparable 18S rDNA sequences from the NCBI GenBank database were identified using BLAST™ (McEntyre & Ostell, 2013). Additionally, sequences were also adapted from the phylogenetic trees by Bernal and Pinto (2016) and Jordaan *et al.* (Chapter 2.1). A multiple sequence alignment was constructed using the MUSCLE alignment method in Geneious R9 (Kearse *et al.*, 2012) with default settings in FASTA format. The most appropriate nucleotide substitution model for the multiple sequence alignment was selected using jModelTest (Darriba *et al.*, 2012; Guindon & Gascuel, 2003) with an Akaike information criterion (AIC) calculation. The general time-reversible (GTR) model (Tavaré 1986) with inverse (+I) and gamma (+G) distribution, with a proportion of invariable sites of 0.3113 and gamma shape of 0.4154, was selected as the most suitable model. Phylogenetic trees using Maximum likelihood (ML) analysis were constructed using RAxMLGUI 2.0 (Edler *et al.*, 2021) with thorough bootstrap setting and 1000 bootstrap replicates. To perform a Bayesian Inference (BI) analysis, the Markov Chain Monte Carlo (MCMC) algorithm with 10 000 000 generations was used in the program MrBayes (Huelsenbeck

CHAPTER 2.2

& Ronquist, 2001; Ronquist & Huelsenbeck, 2003), where every 100th generation was sampled. The first 25% of trees were discarded as burn-in. A model-corrected pairwise distance (p-distance) matrix was calculated in PAUP* v.4.0a169 (Swofford, 2003).

2.2.4. Results

Of the 32 reptile specimens captured (see Supplementary Table 2.2.1), ten of fifteen *Smaug depressus* (67%) and one of two *Cordylus jonesii* (50%) were found to be infected with trypanosomes after PCR screening. Microscopic screening of blood smears from an infected *C. jonesii* specimen revealed a positive infection, with a single trypomastigote morphotype and no dividing forms found. A positive infection was only observed in one of the infected *Smaug depressus* specimens (RE221002A1), after microscopic screening of the blood smears revealed only a single trypomastigote in one slide. A single live trypomastigote was observed in the wet smear of the same specimen, but in none of the other specimens. Positive infections of a single trypomastigote morphotype identical to the infection of *S. depressus* RE221002A1 were observed when microscopically screening the blood smear slides of the three resampled *S. depressus* specimens (RE221002A1, RE221001B4, and RE221002C1). An extremely low parasitaemia was noted, with a single trypomastigote being observed only every second or third blood smear slide.

A small number of mites were found feeding externally on the body of the non-infected cordylid specimen, preliminarily identified as Trombiculidae larvae (Castro *et al.*, 2019). Ectoparasitic mites preliminarily identified as Trombiculidae larvae, *Ophyionyssus*-like sp., and Pterygosomidae mites were observed on several of the infected *S. depressus* specimens. It is unknown whether or not these mites are potential vectors for trypanosomes.

CHAPTER 2.3

2.2.4.1. *Diagnosis*

Phylum: Euglenozoa Cavalier-Smith, 1981

Class: Kinetoplastea Honigberg, 1963, emend. Vickerman, 1976

Subclass: Metakinetoplastina Vickerman, 2004

Order: Trypanosomatida Kent, 1880

Family: Trypanosomatidae Doflein, 1951

Genus: *Trypanosoma* Gruby, 1843

Subgenus: *Squamatrypanum* Votýpka and Kostygov, 2021

Description of *Trypanosoma* sp. 2N

Host: *Cordylus jonesii* Boulenger, 1891 (Squamata: Cordylidae: Cordylinae)

Voucher material: Pending formal peer-review publication.

Representative DNA sequence: The sequence data specifically associated with *T.* sp. 2N (upon which the present biological description is based) has been submitted to GenBank and are as follows: Nuclear 18S rDNA (nu 18S) partial sequence OQ297738.

ZooBank registration: Pending formal peer-review publication.

Locality: Ndumo Game Reserve (26°52'02" S; 32°10'08" E), KwaZulu-Natal province, South Africa.

Site of infection: Peripheral blood.

Vector: Unknown.

Stages in vector: Unknown.

Morphology: Measurements in micrometres (μm). Range shown with mean \pm standard deviation in parentheses (Table 2.2.2). Body length 24.17–44.63 (35.40 ± 3.53) ($n = 30$) and body width 7.54–12.27 (9.87 ± 1.18) ($n = 30$). Nucleus length 1.20–2.16 (1.63 ± 0.2) ($n = 30$); nucleus width 0.92–1.82 (1.44 ± 0.25) ($n = 30$); undulating membrane width

CHAPTER 2.3

2.07–3.47 (2.69 ± 0.39) ($n = 29$); number of undulations 6–9 (7.19 ± 0.9) ($n = 26$); kinetoplast length 0.64–1.05 (0.82 ± 0.12) ($n = 31$); and kinetoplast width 0.41–0.77 (0.54 ± 0.09) ($n = 31$). Mid-nucleus to anterior body end distance 14.34–29.35 (23.40 ± 2.95) ($n = 30$) and mid-nucleus to posterior body end distance 9.70–13.75 (11.75 ± 1.06) ($n = 31$). Free flagellum length 5.61–16.33 (10.06 ± 2.43) ($n = 17$). The Nucleus is small and circular, positioned 59.33–74.07% ($66.01 \pm 4.25\%$) ($n = 30$) from the anterior body end. Body shape index 2.75–4.89 (3.63 ± 0.52) ($n = 30$) and nuclear index 0.89–1.60 (1.17 ± 0.21) ($n = 30$). Measurements of kinetoplast to nucleus distance (KN), kinetoplast to anterior end distance (KA), kinetoplast to posterior end distance (KP), and kinetoplast position (PK) were omitted because of the close association of the kinetoplast and nucleus.

Remarks:

This trypanosome has a broad mid-body and short tapering ends, with several granular vacuoles often visible (Figure 2.2.1 A-L). The cytoplasm stains a shade of light purple, fading in intensity until almost transparent towards the undulating membrane. When fixed and stained smears were examined under a microscope, the body was often curled in a U-shape, with the anterior and posterior ends sometimes touching. The nucleus and kinetoplast were observed to be closely associated and were positioned, on average, two thirds from the anterior body end. The nucleus was observed to stain pink and the kinetoplast a dark purple. A relatively large, almost transparent undulating membrane and long transparent flagellum were also notable.

Trypanosoma (Squamatrypanum) sp. 2N appears closest in morphology to *T. zonuri* Telford, 1995, but when compared with the three least variable characters of *T. zonuri* (BL, BW, and KA), according to Telford (1995b), *T. sp. 2N* is clearly a separate species. *Trypanosoma sp. 2N* is longer and broader ($35.40 \times 9.87 \mu\text{m}$) than *T. zonuri* ($29.6 \times 8.9 \mu\text{m}$). Although KA was not measured in the present study for this parasite, MA

CHAPTER 2.3

is presented as an analogous measurement due to the close association of the kinetoplast and nucleus of *T. sp. 2N*, for which it measures 23.4 μm versus a KA of 20.1 μm for *T. zonuri*. Both species have closely associated nuclei and kinetoplasts, with similar nucleus positions relative to the body (66.01 and 67.5%, respectively), but the nuclear index of *T. sp. 2N* (1.18) is more round compared to *T. zonuri* (1.3). The undulating membrane of *T. sp. 2N* (2.69 μm) appears larger than that of *T. zonuri* when compared to its illustration with the scale accounted for, however a measurement was not included in the original description for comparison.

The sequence of *T. sp. 2N* is well nested within the *Squamatrypanum* clade of the phylogeny, forming a monophyly with *Trypanosoma sp. 109* (LC471399) and *Trypanosoma sp. gecko* (AJ620548), and sister to *Trypanosoma varani* Wenyon, 1909 (AJ005279) and *T. cf. varani* (AB447493). While no morphological data was provided for its two closest relatives, it does share morphological characters with *T. varani* (AJ005279) and *T. cf. varani* (AB447493) (Sato *et al.*, 2009). The body shape of *T. varani* is similarly described as U-shaped by the original author (Wenyon, 1909). Although only basic measurements of *T. varani* were included in the original description, it can be deduced by using the scale in the illustration (Plate XIII, Figures 11–13 in Wenyon, 1909) that the nucleus was roughly 3.24–4.97 μm long and 3.18–3.67 μm wide. Despite being an approximate estimation, this range is more than double that of *T. sp. 2N* (1.2–2.16 \times 0.92–1.82 μm). *Trypanosoma cf. varani* has a similar body width (9.8 μm) to *T. sp. 2N* but is significantly longer (51.8 μm) with a shorter free flagellum (4.2 μm). A distance of 4.4 μm separates the kinetoplast and nucleus of *T. cf. varani*, unlike the close association observed for *T. sp. 2N*. Posterior to kinetoplast measurements of *T. varani* (15 μm) and *T. cf. varani* (16.4 μm) are greater than the MP distance (an analogous measurement) of *T. sp. 2N* (11.75 μm).

CHAPTER 2.3

Although closely related, the host species of *Trypanosoma* sp. 2N and *T. zonuri* are separated geographically by the arid corridor (Freitas *et al.*, 2018) and *Cordylus jonesii*, the host of *T.* sp. 2N, was shown by Greenbaum *et al.* (2012) to have a separate distribution from the Tanzanian species of *Cordylus* referred to in the description of Telford (1995b) as *C. cordylus sensu lato*, the host of *T. zonuri*. Therefore, due to the difference in host species, geography, morphology and with supporting molecular data, *Trypanosoma* sp. 2N is shown to be a distinct species of *Trypanosoma*, from a previously unreported host species.

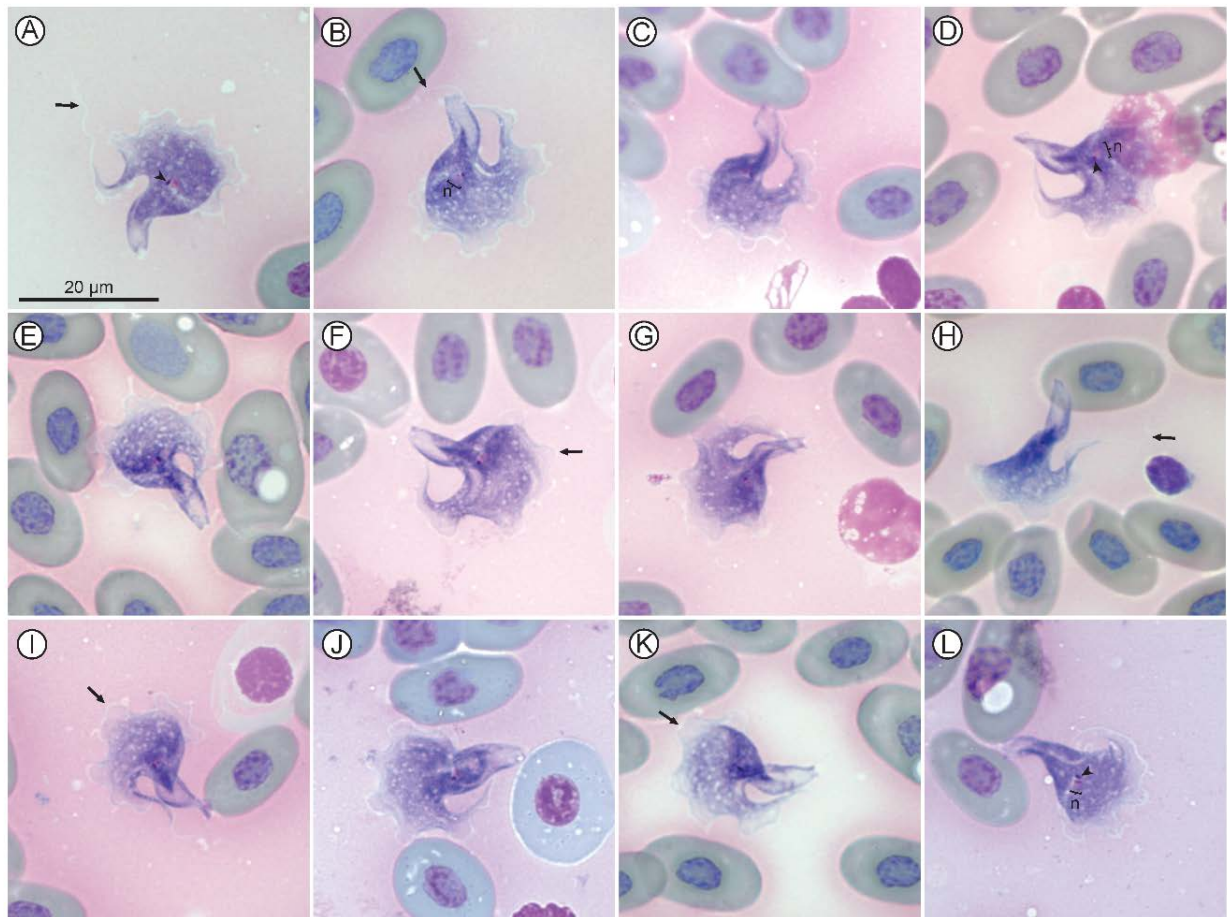


Figure 2.2.1: *Trypanosoma* sp. 2N plate. (A-L) Normal trypomastigote forms in the blood. Arrowheads show kinetoplast (A, D, and L); arrows show flagellum (A, B, and H) and undulating membranes (F, I, and K); nuclei are indicated by “n” (B, D, and L). Scale bar is 20 µm.

CHAPTER 2.3

Subgenus: *Trypanosoma* Gruby, 1843 emend. Votýpka and Kostygov, 2021

Description of *Trypanosoma* sp. 2T

Host: *Smaug depressus* FitzSimons, 1930 (Squamata: Cordylidae: Cordylinae)

Voucher material: Pending formal peer-review publication.

Representative DNA sequences: The sequence data specifically associated with *T.* sp. 2T (upon which the present biological description is based) have been submitted to GenBank and are as follows: Nuclear 18S rDNA (nu 18S) partial sequence OQ297739, OQ297740, OQ297741, OQ297742, OQ297743, OQ297744, OQ297745, OQ297746, and OQ297747.

ZooBank registration: Pending formal peer-review publication.

Locality: Soutpansberg mountain (23°01'58" S; 29°25'24" E), Lajuma research centre, Limpopo, South Africa.

Site of infection: Peripheral blood.

Vector: Unknown.

Stages in Vector: Unknown.

Description: Measurements in micrometres (μm). Range shown with mean \pm standard deviation in parentheses (Table 2.2.2). Body length 28.55–53.9 (42.63 ± 5.08) ($n = 39$) and body width 9.58–27.63 (16.71 ± 3.64) ($n = 38$). Nucleus length 9.56–20.54 (13.95 ± 2.68) ($n = 38$) and nucleus width 2.43–5.3 (3.69 ± 0.64) ($n = 38$). Undulating membrane width 2.35–5.65 (3.95 ± 0.86) ($n = 35$); number of undulations 6–10 (7.91 ± 0.95) ($n = 33$); kinetoplast length 0.59–1.05 (0.82 ± 0.12) ($n = 39$); and kinetoplast width 0.38–0.81 (0.57 ± 0.1) ($n = 39$). Mid-nucleus to anterior body end distance 16.81–31.24 (23.41 ± 3.16) ($n = 38$) and mid-nucleus to posterior body end distance 9.92–31.38 (20.31 ± 4) ($n = 38$). Free flagellum length 5.19–8.12 (7.18 ± 1.08) ($n = 8$). Mid-kinetoplast to anterior

CHAPTER 2.3

body end distance 24.41–36.83 (32.32 ± 2.69) (n = 38); mid-kinetoplast to posterior body end distance 2.79–24.62 (10.98 ± 4.12) (n = 38); and mid-kinetoplast to mid-nucleus distance 5.87–17.82 (10.7 ± 2.53) (n = 36). Body shape index 1.26–4.16 (2.68 ± 0.67) (n = 40) and nuclear index 2.29–6.77 (3.91 ± 1.09) (n = 38). Position of nucleus relative to body as a percent 39.73–72.19 (54.53 ± 7.58) (n = 38) and position of kinetoplast relative to body as a percent 53.47–94.55 (76.16 ± 9.03) (n = 39).

Remarks: A single trypomastigote morphotype was observed with a rounded, elongated body and a prominent undulating membrane (Figure 2.2.2 A-L). The cytoplasm stained a uniform dark blue/purple in colour, with fewer granular vacuoles in contrast to the lighter, uneven staining cytoplasm of *T. sp. 2N*. The undulating membrane (Fig. 2.2.2 C, K, & L arrows) stained a similar dark blue/purple to the cytoplasm, contrasting significantly to that of *T. sp. 2N*. A relatively long, elongated nucleus was present (Fig. 2.2.2 J), often positioned in the middle of the body, as is indicated by MA and MP distances being similar. A short, light pink-staining flagellum (Fig. 2.2.2 A & B arrows) was occasionally visible, compared to the long transparent flagellum of *T. sp. 2N*. Extremely low parasitaemia was evident, as trypanosomes were commonly not observed in blood smears during microscopic screening, despite the sample being known to be positively infected.

Trypanosoma sp. 2T is most similar morphologically to *T. cordyli* Telford, 1995, a trypanosome also described from cordylid lizard hosts, described from *Cordylus tropidosternum* (syn. *C. t. tropidosternum*) in Tanzania. The most consistent diagnostic morphological characteristics of *T. cordyli* are stated by Telford (1995b) to be the nucleus length, body width and kinetoplast to anterior body end distance. The nucleus of *T. sp. 2T* is longer, 9.56–20.54 μm ($13.95 \pm 2.68 \mu\text{m}$), than that of *T. cordyli*, 3–5 μm ($4.3 \pm 0.5 \mu\text{m}$). *Trypanosoma sp. 2T* is noticeably less broad than *T. cordyli*, 9.58–27.63 μm (16.71

CHAPTER 2.3

$\pm 3.64 \mu\text{m}$) and $19\text{--}31 \mu\text{m}$ ($24.6 \pm 3.3 \mu\text{m}$), respectively. The kinetoplast to anterior body end distance of *T. sp. 2T* is greater than that of *T. cordyli*, measuring $24.41\text{--}36.83 \mu\text{m}$ ($32.32 \pm 2.69 \mu\text{m}$) and $22\text{--}35 \mu\text{m}$ ($28.5 \pm 4.1 \mu\text{m}$), respectively. Furthermore, *T. sp. 2T* has a smaller, less prominent kinetoplast in contrast to that of *T. cordyli*, with a mean length of $0.82 \mu\text{m}$ and $1.5 \mu\text{m}$, respectively. Lastly, *T. sp. 2T* stained significantly darker blue than the pink colour exhibited by *T. cordyli* (see Plate 65 (B) i-l of Telford, 2009).

The host of *T. sp. 2T*, *Smaug depressus*, has a distribution restricted to the Soutpansberg mountain range and surrounding areas in Limpopo, South Africa, in addition to also being separated from host species of *T. cordyli*, *C. tropidosternum* by the arid corridor (Freitas *et al.*, 2018). Consequently, due to the morphological characteristic differences, different host species, and geographic distribution, *Trypanosoma sp. 2T* is a distinct species (note — ICZN disclaimer).

CHAPTER 2.3

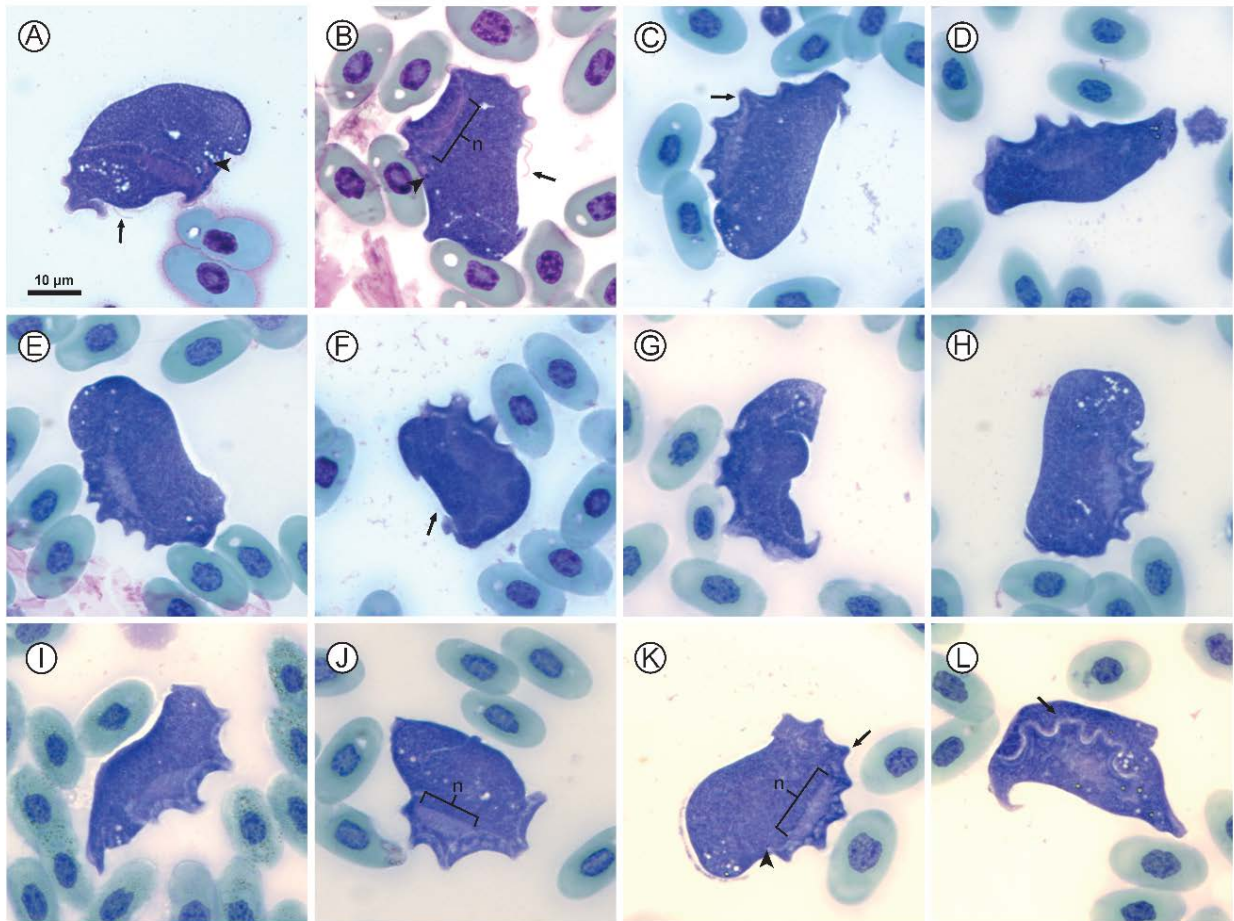


Figure 2.2.2: *Trypanosoma* sp. 2T plate. (A-L) Normal trypomastigote forms in the blood. Arrowheads show kinetoplast (A, B, and K); arrows show flagellum (A, B, and F) and undulating membranes (C, K, and L); nuclei are indicated by “n” (B, J, and K). Scale bar is 10 µm.

2.2.4.2. Molecular and phylogenetic analysis

An 18S rDNA sequence was obtained from one *C. jonesii* specimen, RE210312D1 (OQ297738) (1499 bp), for *Trypanosoma* sp. 2N (1499 bp) and from nine *S. depressus* specimens, RE210921A1 (OQ297739) (1436 bp), RE210921C1 (OQ297740) (1433 bp), RE220930A1 (OQ297741) (832 bp), RE221001A1 (OQ297742) (1410 bp), RE221001B2 (OQ297743) (1438 bp), RE221001B4 (OQ297744) (1441 bp), RE221002A2 (OQ297745) (1441 bp), RE221002B1 (OQ297746) (1445 bp), and RE221002C1 (OQ297746) (1443 bp) for *Trypanosoma* sp. 2T. Using a Geneious multiple sequence alignment of 1410 bp, a 100% identity match was observed for seven *T.* sp. 2T sequences, namely OQ297739, OQ297742, OQ297743, OQ297744, OQ297745, OQ297746, and OQ297746. Sequence OQ297741 was 100% identical for an alignment of 826 bp but was only half of the

CHAPTER 2.3

fragment length, as one of the nested PCR's was unsuccessful. There was a 0.14% intraspecific divergence between the sequences OQ297740 and OQ297739 (Table 2.2.3), which was due to OQ297740 differing by five base pairs, three of which were called as ambiguous nucleotide base pairs during editing of the chromatograph sequences due to a slightly lower quality sequence. Sequencing of *S. depressus* sample RE221002A1 was unsuccessful, although it was shown to have a positive trypanosome infection when screened molecularly with a nested PCR using trypanosome primers.

An nBLAST query of these sequences returned results showing a close relation (>99.67%) of *T. sp. 2N* to trypanosome sequences (Accession numbers LC471393 to LC471399) isolated from Italian sand flies, *Sergentomyia minuta*, (Phlebotominae) in the study of Abbate *et al.* (2020). As these sand fly sequences were identical, they were represented by the single sequence of *Trypanosoma sp. 109* (LC471399) in the phylogeny. It is important to note that the sequences of Abbate *et al.* (2020) were significantly shorter in length (834 – 917 bp) than the sequence of *T. sp. 2N* from this study (1499 bp), which could lead to a lower accuracy of the comparison. The second closest match was 99.13% with the sequence of *Trypanosoma sp. "gecko"* (AJ620548), isolated from a Senegalese *Tarentola annularis* specimen, a species of gecko native to northern Africa. An nBLAST query of the *T. sp. 2T* sequences returned several matches below 98% with unnamed anuran trypanosomes from South America and Europe, with the closest match being 98.05% with the sequence of *Trypanosoma sp. 858* (EU021228) isolated from the South American toad, *Rhinella icterica*.

The topologies of the Maximum Likelihood (ML) and Bayesian Inference (BI) phylogenies constructed using 18S rDNA trypanosome sequences were identical and were thus combined into a consensus phylogram in Figure 2.2.3. The phylogenetic relationships were consistent with described trypanosomatid phylogenetic relationships.

CHAPTER 2.3

Clades in the phylogram were well-supported, with the majority of bootstrap and nodal support values above 70% and 0.80, respectively.

The sequence of *Trypanosoma* sp. 2N is placed within the *Squamatrypanum* clade (subgenus *Squamatrypanum* Votýpka and Kostygov, 2021) in a monophyletic subclade closest to the European sandfly sequence, *Trypanosoma* sp. 109 and the West African gecko trypanosome sequence, *Trypanosoma* sp. “gecko”. Although, it should be taken into consideration that the sandfly sequence was significantly shorter in length and might, therefore, not necessarily represent an accurate relationship.

The ten sequences of *T.* sp. 2T isolated from the *Smaug depressus* specimens had an identical genotype and were thus represented by two of the sequences, OQ297739 and OQ297740. The sequences are placed in a new monophyletic subclade nested within the anuran trypanosome clade, clade Frog 2 (subgenus *Trypanosoma* Gruby, 1843 emend. Votýpka and Kostygov, 2021), closest to two unnamed anuran trypanosome species (MH424271 and MH424274) infecting Ukrainian *Pelophylax ridibundus* (Spodareva *et al.*, 2018).

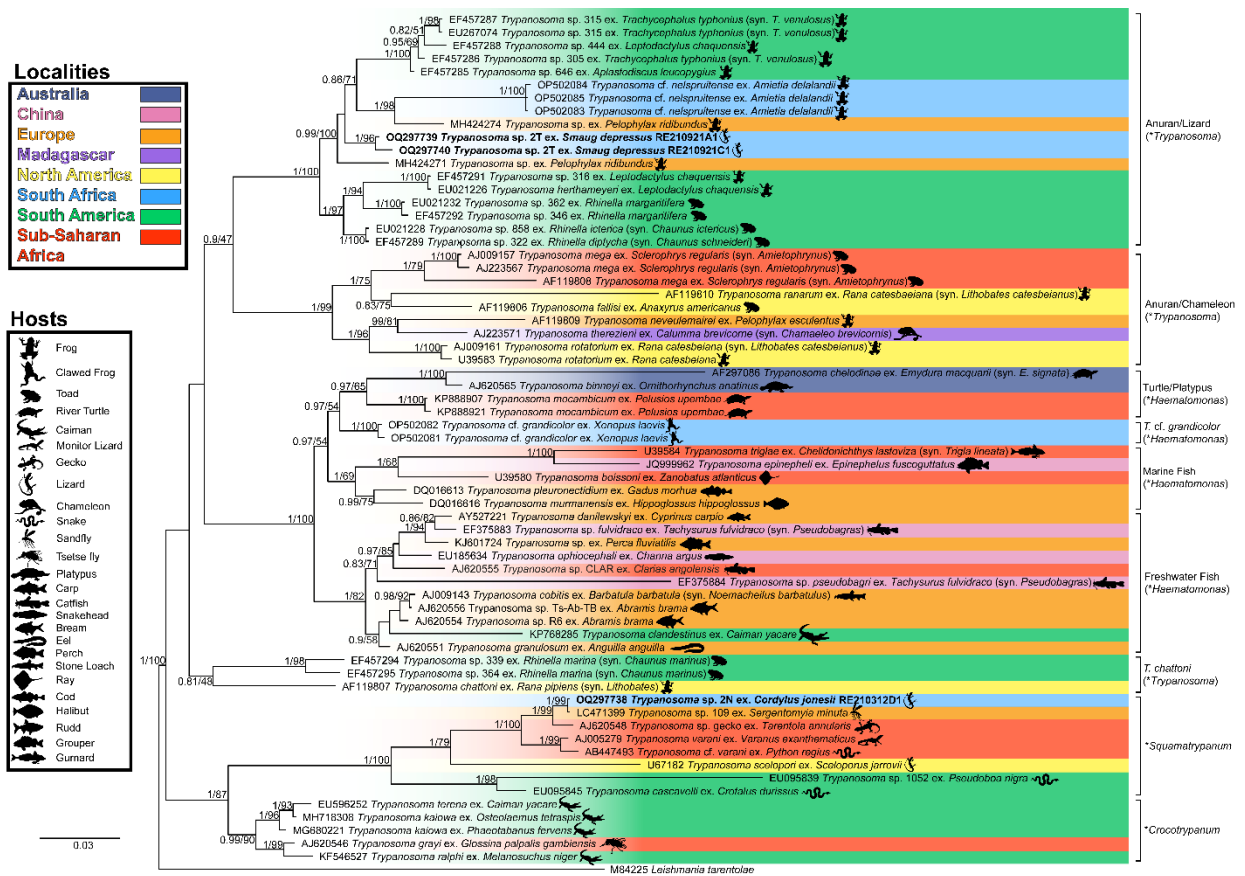


Figure 2.2.3: Consensus phylogram of the reptile trypanosome clade based on 18S rDNA sequences. Tree topologies of Maximum Likelihood (ML) and Bayesian Inference (BI) analyses were similar (represented on the BI tree). Nodal support values of BI posterior probability and ML bootstrap shown as BI/ML. Sequences from the present study are in bold. Subgenera are indicated by an asterisk (*). Scale shown is nucleotide substitutions per site.

2.2.5. Discussion

2.2.5.1. Morphological characterisation

Reptile trypanosomes are typically found as trypomastigote forms in the blood of their hosts and undergo different morphological transformation stages within the vector (Telford, 2009). Generally, only one trypomastigote form is observed in the squamate host, however, some species have been described as polymorphic, such as *T. martini* (syn. *T. mabuiae*), in spite of this not being definitively validated. Although it is difficult to distinguish species of *Trypanosoma* based on morphology alone, studies conducted by Telford (1995a, 1996, 2009) indicate comparative morphological analysis is a valid method of distinguishing saurian trypanosomes, despite their morphological variability.

CHAPTER 2.3

Among fourteen saurian trypanosome species, the body length and width were reported to be the most consistent measurements between species (Telford, 2009). Furthermore, additional morphological characteristics which aided in distinguishing species were differences in staining properties, the average position of the nucleus and kinetoplast relative to the body, the nuclear index, and body shape index (Telford, 2009). Differences in staining colour could potentially be explained by differing concentrations of lipid-compounds in the cytoplasm between species, as a result of the Giemsa stain being water-buffered. This was observed with the lighter-staining, vacuolated cytoplasm of *Trypanosoma* sp. 2N in contrast to the darker-staining, less vacuolated cytoplasm of *T.* sp. 2T.

During initial sampling, no trypomastigotes were observed during light microscopy screening of the blood smear slides of *Smaug depressus*, which were shown to be positive when screened with trypanosome primers using a nested PCR and gel electrophoresis. The absence of trypanosomes in the peripheral blood, despite a known positive infection, has been reported by other researchers previously. Telford (1995b) kept captive cordylid lizards known to be infected with trypanosomes over several years and periodically drew and screened their blood, noting on several occasions that no trypanosomes were present. He stated: "Parasites were often absent on [blood] slides taken at irregular intervals [over a 4-year period]". Viola *et al.* (2009) were also unsuccessful in detecting trypomastigotes of the South American snake trypanosome, *Trypanosoma serpentis*, in blood smear slides with light microscopy screening. It was hypothesised by Viola *et al.* (2009) that very low parasitaemia in infected hosts was the cause thereof. Ferreira *et al.* (2017) also noted the absence of trypomastigote forms in the blood smears slides of South American marsupials, *Monodelphis domestica*, infected with *Trypanosoma gennarii*. Lastly, Fermino *et al.* (2019) were unable to detect blood

CHAPTER 2.3

trypomastigotes of *T. kaiowa* in the blood smears of infected crocodylians, but were able to identify developmental forms in the invertebrate vectors with molecular confirmation.

Viola *et al.* (2009), Ferreira *et al.* (2017), and Fermino *et al.* (2019) utilised culturing methods to study the morphology of the aforementioned species of *Trypanosoma*, however, it has been shown that the morphology of cultivated trypanosomes can differ to the morphotypes observed in natural infections (Diamond, 1965). A wet-mount slide preparation technique was implemented in the present study as a method for more successful detection of trypanosomes when screening in the field, however, it was only as effective as the standard technique of screening stained blood smear slides. It appears that, as a result of the extremely low parasitaemia and, in spite of thorough microscopic screening of the blood smear slides, the infections are often not apparent. Ultimately, we recommend PCR screening using trypanosome-specific primers for trypanosomes.

2.2.5.2. *Molecular and phylogenetic analysis*

Although it is unexpected that *T. sp.* 2T clades with anuran trypanosomes, other lizard trypanosomes have been previously reported to clade in the anuran group as well — such as *T. therezieni*, isolated from a chameleon host (Haag *et al.*, 1998). Additionally, *Trypanosoma sp.* DNA was reported from geckoes in Thailand, which grouped with anuran trypanosomes in the phylogeny (Toontong *et al.*, 2022). It is unclear whether the findings reported by Toontong *et al.* (2022) were due to an incidental infection of geckos which fed upon sandflies infected with anuran trypanosomes; if it was a natural infection of a reptile trypanosome that merely clades with the anuran trypanosomes in the phylogeny; or if it is a species of trypanosome that infects both reptiles and anurans naturally. Perhaps, instead, these reptile trypanosomes clade with the anuran trypanosomes because of the lack of phylogenetic coverage due to the small amount of lizard/anuran sequences available or have split evolutionarily from a separate ancestral lineage to the other reptile trypanosomes.

CHAPTER 2.3

In the present study, the presence of trypanosome infections in nine *Smaug depressus* lizards from several localities suggests that it is unlikely to be an incidental infection of an amphibian trypanosome in reptile hosts, but rather a reptile trypanosome that clades with anuran trypanosomes or a trypanosome which is able to infect both classes of host species. The current evidence of three reptile trypanosomes being placed in separate anuran clades possibly indicates that there are multiple points of divergence in the ancestral lineage of reptile-infecting trypanosomes, with some clades having diverged more recently from a shared common ancestor with anurans. In contrast to crocodylian and varanid trypanosomes which appear to have diverged at an earlier point in the ancestral lineage. It is hypothesised that ancestral trypanosomatids were initially monoxenous parasites infecting insects (likely dipterans) and later became dixenous due to haematophagous invertebrate hosts (Spodareva *et al.*, 2018). Based on the phylogenetic evidence, Spodareva *et al.* (2018) suggest, that terrestrial trypanosomes originated from amphibian trypanosomes, as is shown by closely related infections in turtles, platypuses, fishes, and chameleon hosts. The lizard trypanosome in the present study, *T. sp. 2T*, and the trypanosomes infecting geckos reported by Toontong *et al.* (2022), which both clade within amphibian trypanosome groups, could potentially be evidence in support of this hypothesis.

2.2.6. Conclusion

Molecular and morphological evidence indicates that two distinct species were observed in two reptile host species during this study, *Cordylus jonesii* and *Smaug depressus*. Subsequently, two new species of *Trypanosoma* are presented in the present study with supporting morphological descriptions and molecular data. Molecular screening was shown to be more reliable than screening with light microscopy, due to the extremely low parasitaemia of these lizard trypanosome infections. Phylogenetic comparisons with

CHAPTER 2.3

other trypanosomes of a similar evolutionary history, suggest the possibility of a bloodsucking arthropod, such as a phlebotomine sandfly, as the vector, however, potential vectors for lizard trypanosomes need to be investigated in future studies.

2.2.7. Acknowledgements

The authors are grateful for aid from members of the African Amphibian Conservation Research Group and the Water Research Group for access to their facilities. We would also like to thank Ndumo Game Reserve, Tembe Elephant Park, Lajuma Research Centre, Vhembe Biosphere Reserve, and Goro Game Reserve, as well as Ezemvelo KZN Wildlife. This paper was submitted as part of a master's degree at the North-West University (Supervisor EC Netherlands and cosupervisor LH du Preez).

2.2.8. Author contributions

Authors BJ and ECN conceived and designed the study. BJ, ECN and JvA conducted data gathering and analyses thereof. BJ, ECN and JvA wrote the article.

2.2.9. Financial contributions

The financial assistance of the National Research Foundation (NRF) of South Africa, towards ECN, is hereby acknowledged. Opinions, findings and conclusions or recommendations expressed in any publication generated by an NRF supported study, is that of the author(s) alone and the NRF accepts no liability whatsoever in this regard (Grant UID 129669).

2.2.10. Conflicts of interest

The authors declare there are no conflicts of interest.

CHAPTER 2.3

2.2.11. Ethical standards

This study forms part of an approved NWU's AnimCare ethics committee project: Ecology, systematics, and evolutionary biology of ectotherm blood parasites (Ethics Number: NWU-00372-16-A5 and NWU-00427-21-A5; Ezemvelo research permit no. OP 594/2021).

CHAPTER 2.3 RESULTS



East African yellow-bellied mud turtle (*Pelusios castenoides castenoides*)



East African yellow-bellied mud turtle (*Pelusios castenoides castenoides*)

CHAPTER 2.3

Investigating the trypanosomes infecting pelomedusid (Pelomedusidae) freshwater turtles in Southern Africa with the supplementary description and molecular diagnosis of *Trypanosoma (Haematomonas) cf. neitzi* Dias, 1951 and *Trypanosoma (Haematomonas) cf. sheppardi* Dias, 1951, alongside the morphological and molecular characterisation of an undescribed species

Bernard J. Jordaan¹, Louis H. du Preez^{1,2}, and Edward C. Netherlands^{1,3}

¹ African Amphibian Conservation Research Group, Unit for Environmental Sciences and Management, North-West University, Potchefstroom, South Africa

² South African Institute for Aquatic Biodiversity, Somerset Street, Makhanda 6140, South Africa

³ Department of Zoology and Entomology, University of the Free State, PO Box 339, Bloemfontein, 9300, South Africa.

CHAPTER 2.3

2.3.1. Abstract

Species of *Trypanosoma* infecting reptiles are relatively poorly understood and understudied. The study of trypanosomes infecting turtles could lead to a greater understanding of the genus and its evolutionary history. A supplementary description is provided for two species of *Trypanosoma* infecting freshwater pelomedusid (Pelomedusidae) turtles, *T. (Haematomonas) cf. neitzi* and *T. (Haematomonas) cf. sheppardi*, with molecular data in the present study. Additionally, an undescribed species of *Trypanosoma* is characterised using morphological and molecular data. This study provides the first morphological descriptions and molecular data of South African turtle trypanosomes, setting a base for future research of the reptile trypanosomes of Africa.

2.3.2. Introduction

The genus *Trypanosoma* is a group of single-celled, obligate extracellular haemoparasites recognised by their characteristic flagellum and undulating membrane. These parasites have a significant socioeconomic impact and are well-known for causing African sleeping sickness and Chaga's disease in humans, which can be fatal (Hamilton *et al.*, 2004), as well as sleeping sickness in cattle and horses, known as nagana (Steverding, 2017). Species of *Trypanosoma* not infecting humans or livestock are relatively understudied and generally poorly understood, in addition the ancestral lineage of the first trypanosome vertebrate host is currently unknown (Spodareva *et al.*, 2018). Studying trypanosomes of vertebrate hosts which are both aquatic and terrestrial, such as amphibians or turtles, could be key in understanding the evolutionary link between the terrestrial and aquatic clades and the evolutionary history of the genus *Trypanosoma* and subsequently further our understanding of the pathogenic species (Hamilton *et al.*, 2004; Lukeš *et al.*, 2018; Spodareva *et al.*, 2018).

CHAPTER 2.3

Turtle (Order: Testudines) trypanosomes have a long historical record, being at the core of early trypanosome research in the 19th and early 20th centuries. In 1857, organisms with flagella and an undulating membrane were reported from the midgut of an ectoparasitic tortoise tick, *Amblyomma testudines* (syn. *Ixodes tustudinis*), but could not be linked to a vertebrate host (Leydig, 1857). Trypanosome-like flagellates infecting a turtle host were reported from a mud tortoise by Kunstler (1883) several years later. The first recognised turtle trypanosome, *Trypanosoma damoniae*, was reported infecting the host *Mauremys reevesii* (syn. *Damonia reevesii*) from turtles imported to Paris, France which were supposedly collected in Sri-Lanka (Ceylon), although the original authors believed them more likely to have originated from East Asia (Laveran and Mesnil, 1902). Among the first of any trypanosome developmental life cycle to be described, was that of *Trypanosoma vittate*, transmitted between a turtle host, *Lissemys punctata* (syn. *Emyda vittate*), and the leech vectors, *Glossiphonia* sp. and *Hirudinaria manillensis* (syn. *Limnatis granulosa*), from Sri-Lanka (Ceylon), South Asia (Robertson, 1908; Robertson, 1909).

In Africa, two unnamed trypanosome forms were reported from two “marsh tortoises” from Cape St. Mary, Gambia (formerly Senegambia) by Dutton and Todd (1903); Dutton *et al.* (1907) reported an unnamed trypanosome from an unidentified Gambian tortoise; Bouet (1909) described *Trypanosoma pontyi* infecting a freshwater turtle host, *Pelusios castaneus* (syn. *Sternotherus derbianus*), from Western Africa; Minchin (1910) reported trypanosomes from material of two unknown Ugandan tortoises, thought to be the same species. Furthermore, *Trypanosoma leroyi* was described infecting the terrestrial tortoise host, *Kinixys homeana* (syn. *Cinixys homeana*), from Bamako, Mali (Commes, 1919). The first trypanosomes in freshwater turtles from Southern Africa, *T. neitzi* and *T. sheppardi*, were described from the African hinged terrapin, *Pelusios sinuatus* Smith, 1938 (syn. *Pelusios sinuatus zuluensis*), from the

CHAPTER 2.3

Maputo River in Mozambique (Dias, 1951). Pienaar (1962) later reported a trypanosome from the same turtle host species from the Save River valley, Mozambique.

The present study aimed to screen for trypanosomes infecting several species of freshwater pelomedusid turtles, collected from various sites within the Maputo River basin in South Africa, using a combination of morphological and molecular techniques. These turtles were specifically targeted because they are the type hosts of the only three recognised species of Southern African turtle trypanosomes.

2.3.3. Methods

2.3.3.1. *Collection of research specimens*

Turtles were captured with an active sampling method by using baited net traps, placed in shallow water and checked frequently, at several sites in northern KwaZulu-Natal, South Africa (see Supplementary Table 2.3.1). Turtles were identified using Rhodin *et al.* (2021) and Branch (2012). After capture animals were examined for external parasites and blood was collected through femoral venipuncture. Two *Pelomedusa galeata* specimens collected in March 2020 were kept in captivity and blood was later collected in March 2021.

The standard methods of blood smear slide preparation were followed, where blood smears were made onto a clean microscope slide, air-dried, and fixed with absolute methanol (Netherlands *et al.*, 2015). Once dry, the slides were stained for approximately twenty minutes with a 10% solution of modified Giemsa (Sigma-Aldrich, Steinheim, Germany). After smear preparations were completed, excess blood was stored in sterile 2 ml screw cap cryovials.

CHAPTER 2.3

2.3.3.2. *Morphological characterisation*

Light microscopy was used to screen stained blood smear slides for trypanosomes. Images were taken at 1600× magnification using a Zeiss Axiocam 305 color in combination with a Zeiss AX10 microscope. ImageJ version 1.52a (Schneider *et al.*, 2012) was used to measure morphometric characters according to a system adapted from Telford (1995a), Ferreira (2010), and Jordaan *et al.* (Chapter 2.1 and 2.2). Measurements include body length (BL); body width (BW) (measured at point of maximum width, excluding the undulating membrane); nucleus length (NL); nucleus width (NW); undulating membrane width (UMW); number of undulations (NU); kinetoplast length (KL); kinetoplast width (KW); mid-nucleus to anterior body end distance (MA); mid nucleus to posterior body end distance (MP); free flagellum length (F); mid-kinetoplast to anterior body end distance (KA), mid-kinetoplast to posterior body end distance (KP), mid-kinetoplast to mid-nucleus distance (KN). Derived measurements were nuclear index, NL/NW (NI); and body shape index, BL/BW (BI), expressed as ratios. Nucleus position from the anterior end relative to body length, MA/BL (PN); and kinetoplast position from the anterior end relative to body length, KA/BL (PK), shown as a percentage.

2.3.3.3. *DNA extraction, amplification, and sequencing*

DNA extraction, amplification and sequencing followed the methods of Jordaan *et al.* (Chapter 2.2). DNA was extracted using a NucleoSpin® Tissue DNA, RNA and protein purification kit (Macharey-Nagel, Düren, Germany).

Seven turtle samples (see Supplementary Table 2.3.1) were screened molecularly for trypanosomes using a nested polymerase chain reaction (PCR) strategy adapted from McInnes *et al.* (2009) and Egan *et al.* (2020), following Jordaan *et al.* (unpublished data) whereby two overlapping fragments of the 18S rRNA gene were targeted for amplification using one primary and two secondary PCRs. The primary PCR was conducted with the

CHAPTER 2.3

forward primer SLF (5'-GCTTGTTTCAAGGACTTAGC-3') with reverse primer S762.2 (5'-GACTTTTGCTTCCTCTAATG-3'). The cycle conditions of the primary PCR included an initial denaturation step 95°C for 5 minutes, annealing step of 50°C for 2 minutes and extension step of 72°C for 4 minutes. This was followed by 35 cycles containing a denaturation step of 94°C for 30 seconds, annealing step of 60°C for 30 seconds and an extension step of 72°C for 2 minutes and 20 seconds. Lastly, a final denaturation step of 72°C for 7 minutes was performed. The two secondary PCRs were performed using two different primer sets, namely forward primer B (5'-CGAACAACTGCCCTATCAGC-3') with reverse primer I (5'-GACTACAATGGTCTCTAATC-3'); and forward primer S825 (5'-ACCGTTTCGGCTTTTGTGG-3') with reverse primer SLIR (5'-ACATTGTAGTGCGCGTGTC-3'). The conditions of both secondary PCRs consisted of an initial denaturation step of 95°C for 5 minutes, followed by 35 cycles of a denaturation step of 95°C for 30 seconds, annealing step of 57°C for 30 seconds and an extension step of 72°C for 1 minute. Thereafter, a final denaturation step of 72°C for 7 minutes was carried out.

The resultant amplicons were electrophoresed with a 1% agarose gel to determine if they were of the correct size (\pm 900 bp) and desired quality for sequencing. Samples showing clear bands of the correct size were sent to Inqaba Biotech to be sequenced with the chain-termination method in both directions. Poor quality samples were discarded.

2.3.3.4. *Phylogenetic analysis*

Chromatograph sequences (received from Inqaba Biotech) were edited and trimmed using Geneious R9 (Kearse et al., 2012). From the forward and reverse sequences of both B/I and S825/SLIR primer sets, a consensus sequence was created for each sample using the De Novo assembly method within Geneious R9 (Kearse et al., 2012).

CHAPTER 2.3

The percent similarity of the final sequences was calculated within Geneious R9. Final sequences were input into a standard nucleotide BLAST™ (McEntyre & Ostell, 2013) search of the NCBI database to determine the percent identity matches of the samples. Comparable 18S rDNA sequences from the NCBI GenBank database were identified using BLAST™ (McEntyre & Ostell, 2013) for the construction of a phylogenetic tree. Additionally, sequences from the phylogenetic trees by Bernal and Pinto (2016) and Jordaan *et al.* (Chapter 2.1) were retrieved from NCBI GenBank by accession number. The MUSCLE alignment method in Geneious R9 (Kearse *et al.*, 2012) with default settings was used to construct a multiple sequence alignment. Thereafter, the most appropriate nucleotide substitution model for the multiple sequence alignment was selected with an Akaike information criterion (AIC) calculation, using jModelTest (Darriba *et al.*, 2012; Guindon & Gascuel, 2003). The most suitable model was shown to be the general time-reversible (GTR) model (Tavaré 1986) with inverse (+I) and gamma (+G) distribution, with a proportion of invariable sites of 0.4010 and gamma shape of 0.4630. Maximum likelihood (ML) analysis with thorough bootstrap setting and 1000 bootstrap replicates were used to construct phylogenetic trees with RAxMLGUI 2.0 (Edler *et al.*, 2021). A Bayesian Inference (BI) analysis was conducted using the Markov Chain Monte Carlo (MCMC) algorithm with 10 000 000 generations, where every 100th generation was sampled, using the program MrBayes (Huelsenbeck & Ronquist, 2001; Ronquist & Huelsenbeck, 2003). The first 25% of trees were discarded as burn-in. A model-corrected pairwise distance (p-distance) matrix was calculated in PAUP* v.4.0a169 (Swofford, 2003) using the same multiple sequence alignment as the ML and BI analyses.

2.3.4. Results

Molecular PCR screening using trypanosome primers showed positive infections in all seven turtles (100%) from northern KwaZulu-Natal, South Africa (see Supplementary

CHAPTER 2.3

Table 2.3.1). Two *Pelomedusa galeata* from Lebombo (specimens RE210331A2 and RE210331A3); three *Pelusios castenoides* from Tembe Elephant Park (RE210313C1, RE210314A3, and RE210314A5); and two *Pelusios sinuatus* from Ndumo Game Reserve (RE210311A3 and RE210311B1).

Light microscopy screening of the blood smear slides confirmed the presence of trypomastigote forms in the peripheral blood of six of seven turtles. No trypanosomes could be detected in the blood slides of the *P. sinuatus* specimen RE210311B1. A single distinct morphotype was observed in each of the three host species, except for one *P. castenoides* specimen, RE2103314A3, which exhibited two morphotypes, a broad and a slender form. Leeches preliminarily identified as Glossiphoniidae were found feeding upon several of the turtles (Oosthuizen, 1991).

Table 2.3.1: Morphometric measurements of turtle trypanosomes Southern Africa. Species from present study shown in bold. Asterisk (*) indicates values calculated from original descriptions. Measurement range in μm , with mean \pm standard deviation shown in parentheses. Body length (BL), body width (BW), nucleus length (NL), Nucleus width (NW), mid-nucleus to anterior (MA), mid-nucleus to posterior (MP), undulating membrane width (UMW), number of undulations (NU), kinetoplast length (KL), kinetoplast width (KW), mid-kinetoplast to anterior body end distance (KA), mid-kinetoplast to posterior body end distance (KP), mid-kinetoplast to mid-nucleus distance (KN), length of free flagellum (F). Body shape index (BI), nuclear index (NI), nucleus position (PN), kinetoplast position (PK).

Species	Host species	BL	BW	NL	NW	MA	MP	UMW	NU	KL	KW	KA	KP	KN	F	BI	NI	PN (%)	PK (%)
<i>Trypanosoma sp. 1A</i> (present study)	<i>Pelomedusa galeata</i>	52.93–61.79 (56.91 \pm 2.85) n = 16	2.48–5.06 (3.89 \pm 0.81) n = 16	3.11–4.78 (3.75 \pm 0.42) n = 16	1.98–3.24 (2.59 \pm 0.36) n = 16	25.89–33.99 (31.34 \pm 2.45) n = 16	21.76–29.62 (25.66 \pm 2.22) n = 16	1.5–2.24 (1.94 \pm 0.22) n = 16	11–15 (13.47 \pm 1.25) n = 15	0.76–1.24 (0.99 \pm 0.13) n = 16	0.39–0.7 (0.55 \pm 0.08) n = 16	47.81–57.36 (53.24 \pm 2.51) n = 16	1.04–5.49 (3.61 \pm 1.33) n = 16	19.27–22.86 (21.63 \pm 0.95) n = 16	17.22–21.56 (19.62 \pm 1.3) n = 8	10.49–24.13 (15.31 \pm 3.7) n = 16	1.07–1.9 (1.46 \pm 0.2) n = 16	48.28–62.53 (55.11 \pm 3.83) n = 16	90.24–99.11 (93.59 \pm 2.39) n = 16
<i>Trypanosoma cf. neitzi</i> (present study)	<i>Pelusios castenoides</i>	43.66–53.06 (49.08 \pm 2.87) n = 19	4.47–8.95 (5.59 \pm 1.38) n = 19	3.18–4.96 (4.05 \pm 0.44) n = 19	2.12–4.21 (2.87 \pm 0.56) n = 19	20.55–31.94 (27.4 \pm 3.25) n = 19	18.24–25.14 (22.28 \pm 1.66) n = 19	1.12–2.53 (1.91 \pm 0.36) n = 19	9–14 (10.63 \pm 1.3) n = 19	0.76–1.08 (0.92 \pm 0.11) n = 19	0.32–0.67 (0.52 \pm 0.1) n = 19	39.79–48.88 (45.18 \pm 2.89) n = 19	2.35–6.71 (3.99 \pm 1.04) n = 19	15.53–20.27 (18.17 \pm 1.2) n = 19	10.42–17.09 (13.54 \pm 3.36) n = 3	5.49–11.48 (9.16 \pm 1.73) n = 19	1.05–1.73 (1.44 \pm 0.18) n = 19	46.78–64.89 (55.71 \pm 4.59) n = 19	85.01–98.48 (92.07 \pm 3.36) n = 19
<i>Trypanosoma cf. sheppardi</i> (present study)	<i>Pelusios sinuatus</i>	43.68–66.66 (56.84 \pm 6.4) n = 15	4.25–11.86 (7.3 \pm 2.33) n = 15	2.78–6.7 (4.91 \pm 1.06) n = 15	1.5–4.02 (3.04 \pm 0.76) n = 15	27.36–44.48 (35.7 \pm 4.55) n = 15	12.12–27.23 (22.81 \pm 3.96) n = 15	1.27–2.32 (1.83 \pm 0.25) n = 14	7–12 (9.47 \pm 1.41) n = 15	0.6–1.09 (0.94 \pm 0.13) n = 15	0.49–0.7 (0.59 \pm 0.07) n = 15	37.57–61.72 (50.81 \pm 6.44) n = 15	1.51–8.93 (6.28 \pm 1.9) n = 15	4.69–20.08 (16.85 \pm 4.02) n = 15	11.42–11.42 (11.42 \pm 0) n = 1	4.48–12.84 (8.44 \pm 2.35) n = 15	1.16–2.46 (1.66 \pm 0.36) n = 15	52.03–75.6 (62.96 \pm 5.79) n = 15	85.49–99.85 (89.31 \pm 4.06) n = 15
<i>Trypanosoma mocambicum</i> (Dvořáková et al., 2015)	<i>Pelusios rhodesianus</i> , <i>P. subniger</i> , and <i>P. upembae</i>	47.0–60.0 (52.3 \pm 3.3) n = 22	4.0–8.0 (5.4 \pm 0.9) n = 22	3.0–5.0 (3.8 \pm 0.7)	3.0–4.0 (3.1 \pm 0.4)	24.0–32.0 (27.3 \pm 2.3)	23–28 (25)*					40.0–54.0 (47.7 \pm 3.1)	3.0–5.0 (3.9 \pm 0.7)	15.0–25.0 (20.9 \pm 2.2)	13.0–17.0 (15.0 \pm 1.8) n = 4	6.9–13.0 (9.6 \pm 1.3)	1.0–1.7 (1.2 \pm 0.2)	51.06–53.33 (52.19)*	85–90 (91.2)*
<i>Trypanosoma mocambicum</i> (Pienaar, 1962)	<i>Pelusios sinuatus</i>	50–75	5–6											12–15	10–12.5*			"posterior to centre"	"very near posterior"
<i>Trypanosoma neitzi</i> (Dias, 1951)	<i>Pelusios sinuatus</i>	39.9–52.0	3.6–5.7	3.1–3.9	1.8–2.6	15.85–29.95*	22.45–23.65*	1–1.5	8	0.7–1.0		33.8–47.7*	0.7–1.0	19.5–19.7	2.6–5.7	9.9*	1.6*	39.72–57.59*	84.71–91.73*
<i>Trypanosoma sheppardi</i> (Dias, 1951)	<i>Pelusios sinuatus</i>	48.9–49.4	7.8–8.8	4.4–4.9	2.8–3.1	26.6–28.55*	20.2–22.95*	0.52–1.04		0.7–1.0		41.3–44.6	2.0–2.8	16.1–17.6	8.3–13.5	6*	1.6*	54.39–57.79*	84.45–90.28*

CHAPTER 2.3

2.3.4.1. *Diagnosis*

Phylum: Euglenozoa Cavalier-Smith, 1981

Class: Kinetoplastea Honigberg, 1963, emend. Vickerman, 1976

Subclass: Metakinetoplastina Vickerman, 2004

Order: Trypanosomatida Kent, 1880

Family: Trypanosomatidae Doflein, 1951

Genus: *Trypanosoma* Gruby, 1843

Subgenus: *Haematomonas* Mitrophanow, 1883 emend. Votýpka and Kostygov, 2021

Supplementary description of *Trypanosoma cf. neitzi* Dias, 1951

Synonym: *Trypanosoma mocambicum* Pienaar, 1962 emend. Dvořáková *et. Šíroky*, 2015

Type host: *Pelusios sinuatus* Smith, 1838 (Testudines: Pelomedusidae) (syns. *Pelusios sinuatus zuluensis* and *Pelusios sinuatus sinuatus*).

Other hosts: *Pelusios castenoides castenoides* Hewitt, 1931 (present study); *P. upembae* Broadley, 1981, *P. bechuanicus* Fitzsimons, 1932, *P. rhodesianus* Hewitt, 1927, and *P. subniger* Bonnaterre, 1789 (Dvořáková *et al.*, 2015).

Type material: No type material was designated by Dias (1951) in the original description of *T. neitzi*. Neohapantotype, blood smear KO-7-12 from the host *Pelusios upembae*, deposited by Dvořáková *et al.* (2015) in the collection of Department of Biology and Wildlife Diseases, University of Veterinary and Pharmaceutical Sciences Brno, Brno, Czech Republic.

Additional material: Pending formal peer-review publication.

Type locality: near Maputo River, Catuane region, Maputo, Mozambique (Dias, 1951).

Additional localities: Save River valley, Mozambique (Pienaar, 1962). Luena vicinity, Bukama region, Democratic Republic of the Congo; Catabola, Bié, Angola; Guija, Gaza,

CHAPTER 2.3

Mozambique; and Democratic Republic of the Congo (unspecified) (Dvořáková *et al.*, 2015).

Localities in this study: Zimambeni Pan (27°02'21" S, 32°28'54" E) and near Vukuzani Pan (27°00'23" S, 32°26'00" E), Tembe Elephant Park, KwaZulu-Natal, South Africa.

Site of infection: Peripheral blood.

Vector: Unknown.

Stages in vector: Unknown.

Representative DNA sequence: The sequence data specifically associated with *T. cf. neitzi* will be submitted to GenBank pending formal peer-review publication.

Description: Measurement range shown in μm (mean \pm standard deviation). Body length 43.66–53.06 (49.08 ± 2.87) ($n = 19$) and body width 4.47–8.95 (5.59 ± 1.38) ($n = 19$); with a body shape index of 5.49–11.48 (9.16 ± 1.73) ($n = 19$). Nucleus length 3.18–4.96 (4.05 ± 0.44) ($n = 19$) and nucleus width 2.12–4.21 (2.87 ± 0.56) ($n = 19$); with a nuclear index of 1.05–1.73 (1.44 ± 0.18) ($n = 19$). Undulating membrane width 1.12–2.53 (1.91 ± 0.36) ($n = 19$) and number of undulations 9–14 (10.63 ± 1.3) ($n = 19$). Kinetoplast length 0.76–1.08 (0.92 ± 0.11) ($n = 19$) and kinetoplast width 0.32–0.67 (0.52 ± 0.1) ($n = 19$). Mid-nucleus to anterior body end distance 20.55–31.94 (27.4 ± 3.25) ($n = 19$) and mid-nucleus to posterior body end distance 18.24–25.14 (22.28 ± 1.66) ($n = 19$). Kinetoplast to anterior body end distance 39.79–48.88 (45.18 ± 2.89) ($n = 19$) and kinetoplast to posterior body end distance 2.35–6.71 (3.99 ± 1.04) ($n = 19$). Kinetoplast to mid-nucleus distance 15.53–20.27 (18.17 ± 1.2) ($n = 19$). Free flagellum length 10.42–17.09 (13.54 ± 3.36) ($n = 3$). The nucleus and kinetoplast are positioned 46.78–64.89 (55.71 ± 4.59) ($n = 19$) and 85.01–98.48 (92.07 ± 3.36) ($n = 19$) from the anterior body end, respectively.

Remarks: A single broad morphotype (Figure 2.3.1 A-E) was detected with no dividing forms. A small number of slender trypomastigote forms (see Figure 2.3.1 F) were

CHAPTER 2.3

observed in a single host specimen, RE210314A3, alongside the normal broad trypomastigote forms but their morphometrics were not combined in the present study. The body of the normal broad form was relatively broad and elongate with striations occasionally visible (Figure 2.3.1 B, C, and E).

The normal broad forms of this parasite are closest morphologically to *Trypanosoma neitzi* Dias, 1951 and *T. mocambicum* Pienaar, 1962 (see Table 2.3.1). The trypanosome from the present study is described from the turtle, *Pelusios castenoides*, a sister species within the same genus as the type host of both *T. neitzi* Dias, 1951 and *T. mocambicum* Pienaar, 1962, *Pelusios sinuatus* (syn. *P. s. zuluensis* and *P. s. sinuatus*). As the species description of Pienaar (1962) did not designate any type material and the morphological data could be considered inadequate, a redescription was provided by Dvořáková *et al.* (2015). However, Pienaar (1962) discloses in a footnote of his thesis to only learning of the existence of Dias' (1951) work after the completion of his own report and personally states that *T. mocambicum* is likely synonymous with one of the species described by Dias (1951).

The average body dimensions of the broad forms in the present study 49.08 ± 2.87 by $5.59 \pm 1.38 \mu\text{m}$, are within the morphometric ranges of 39.9–52.0 by 3.6–5.7 μm , for the in the description of *T. neitzi* (see Dias, 1951). These dimensions also corresponded to the morphometrics in the redescription of *T. mocambicum*, 52.3 ± 3.3 by $5.4 \pm 0.9 \mu\text{m}$ (Dvořáková *et al.*, 2015), as well as the 'short' forms in the original description by Pienaar (1962), 50–55 by 5–6 μm . Although Dias (1951) employed a slightly different system of measuring the nucleus dimensions of *T. neitzi* compared to the authors of this study, where the nucleus was measured from the anterior to posterior, instead of the maximum length, the measurements are still comparable due to the rounded shape of the nucleus. In the present study, the nucleus of the broad form measured 4.05 ± 0.44 by $2.87 \pm 0.56 \mu\text{m}$, which was near the upper range described for *T. neitzi*, of 3.1–3.9 by 1.8–2.6 μm . A

CHAPTER 2.3

nucleus of similar size was present in the redescription of *T. mocambicum*, measuring 3.8 ± 0.7 by 3.1 ± 0.4 μm (Dvořáková *et al.*, 2015). Pienaar (1962) was unable to distinguish the nucleus size in the original description of *T. mocambicum*. The mid-nucleus to posterior end distances of this trypanosome and *T. neitzi* were consistent, measuring 22.28 ± 1.66 and $22.45\text{--}23.65$ μm , respectively. These distances were within the range described for *T. mocambicum*, $23\text{--}28$ (Dvořáková *et al.*, 2015). A slightly shorter kinetoplast to posterior end distance of $0.7\text{--}1.0$ μm was described for *T. neitzi*, in contrast to 3.99 ± 1.04 μm in the present study. This distance was close to that of *T. mocambicum* 3.9 ± 0.7 (Dvořáková *et al.*, 2015). A prominent undulating membrane and long flagellum are commonly described in the present study and for *T. neitzi* and *T. mocambicum*.

Furthermore, the trypanosome from the present study resembles the trypanosomes in the plates of Dias (1951), Pienaar (1962), and Dvořáková *et al.* (2015), although Pienaar (1962) does not indicate whether the specimens of *T. mocambicum* in his photo plates are large, intermediate, or short forms, and does not provide a scale of the image. As present study and the studies of Dias (1951), Pienaar (1962), and Dvořáková *et al.* (2015) used similar Romanowsky-Giemsa type stains, the reason for the darker, basophilic properties of Pienaar's (1962) description could be due to longer staining durations. However, the staining time is not specified by Pienaar (1962).

The small number of slender forms observed in the present study were smaller and narrower and their nucleus was positioned more towards the posterior than the normal broad forms'. The slender forms of a different species described by Dvořáková *et al.* (2015) have a broader posterior and taper towards the anterior, whereas the slender forms from the present study were more transversely symmetrical in shape. As these slender forms were not observed in any of the other hosts infected with the normal broad form in the present study, and because reptile trypanosomes generally only have a single

CHAPTER 2.3

trypomastigote form in the vertebrate host (Telford, 2009), they could subsequently not be classified as the same species and are suspected to be a mixed infection. However, further investigation is needed to determine whether they are indeed a separate species or just a different morphotype of the same species, as the number of slender forms found was too small for accurate morphometric comparisons.

The hosts of the trypanosome from the present study were collected from water pans in Tembe Elephant Park, northern KZN, South Africa, which are supplied by tributaries of the Maputo River. The type host of *T. neitzi* was collected by Dias (1951) near Catuane, Mozambique from the Maputo River, which borders South Africa and Mozambique. In the original description of *T. mocambicum*, the type host was collected in the Save River valley, Mozambique (Pienaar, 1962). Although Dvořáková *et al.* (2015) redesignated the type locality in the redescription of *T. mocambicum* as a locality in the Democratic Republic of the Congo, the *T. mocambicum* was additionally redescribed from the town Guija, near the Limpopo River in southern Mozambique. The aforementioned localities are all situated within the same river basin in southern Mozambique and north-eastern South Africa, and are geographically connected by a network of river systems supplied by tributaries of the Save River, Limpopo River, Komati River, and Mbuluzi River (Bullock and Hülsmann, 2015). African pelomedusid turtles are known to migrate great distances over land in addition to being proficient swimmers (Branch, 2012; Vamberger *et al.*, 2019; Price *et al.*, 2022). Thus, it is conceivable that their parasites would be spread throughout the river basin and surrounding areas, as infected individuals diligently travel within their habitat range, transmitting their accompanying parasites throughout their journey as they are fed upon by invertebrate vectors.

Due to the reasons above, *Trypanosoma neitzi* Dias, 1951 and *T. mocambicum* Pienaar, 1962 *emend.* Dvořáková *et. Šíroký*, are shown to be synonymous and the

CHAPTER 2.3

species name *Trypanosoma neitzi* Dias, 1951 takes priority according to the Principle of Priority in Article 23 of the ICZN code, as it is the oldest name first used to describe this organism. Thus, *Trypanosoma mocambicum* Pienaar, 1962 *emend.* Dvořáková *et. Šíroký* is designated as a junior synonym of *Trypanosoma neitzi* Dias, 1951 (note — ICZN disclaimer). Subsequently, the normal broad trypanosome from the present study is classified as *T. (Haematomonas) cf. neitzi*, as it conforms to the original descriptions of *T. neitzi* Dias, 1951 and *T. mocambicum* Pienaar, 1962, and redescription of *T. mocambicum* by Dvořáková *et al.* (2015). No type material was designated by Dias (1951) in the original description of *T. neitzi*.

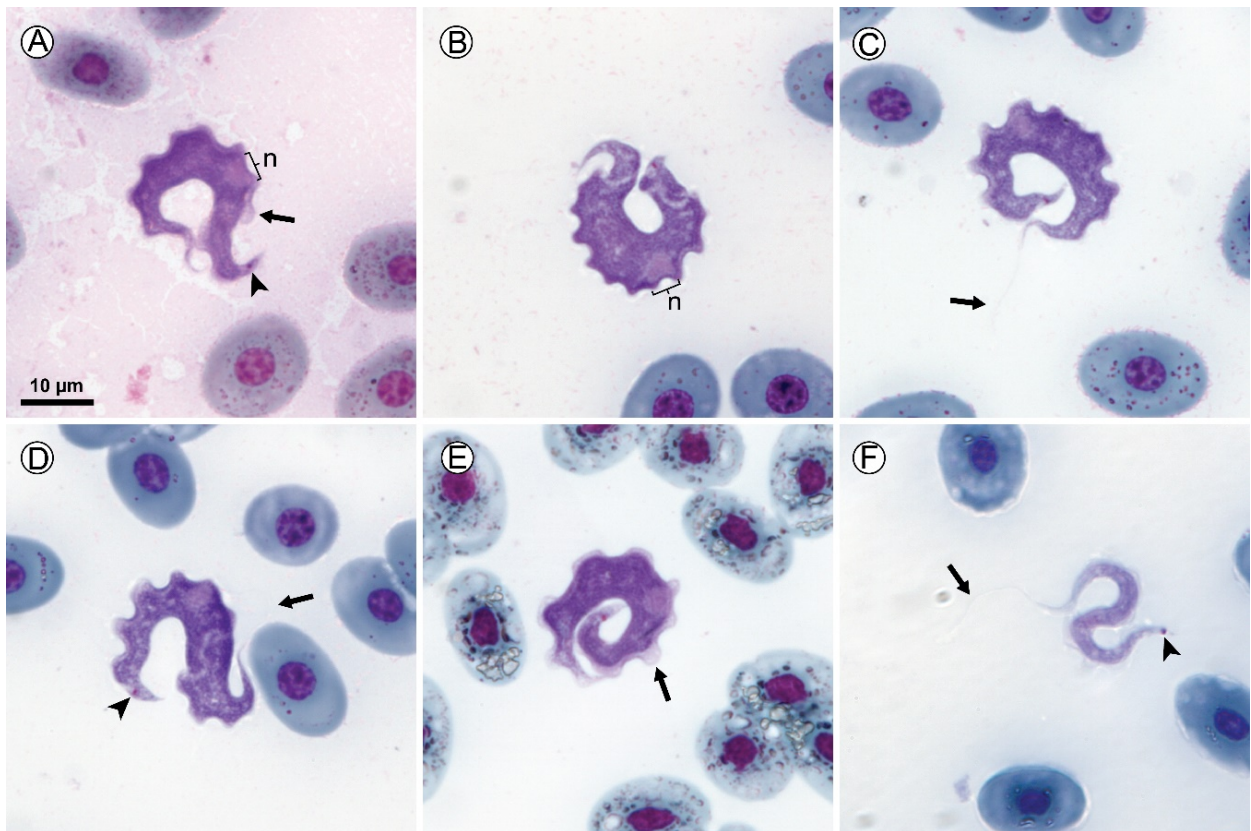


Figure 2.3.1: *Trypanosoma cf. neitzi* plate. Normal trypomastigote forms A-E. Slender *Trypanosoma* sp. form F. Scale shown is 10 µm. Arrowheads show kinetoplast (A, D, and F); arrows show flagellum (C and D) and undulating membrane (A and E); nuclei are indicated by “n” (A and B).

CHAPTER 2.3

Supplementary description of *Trypanosoma cf. sheppardi* Dias, 1951

Type host: *Pelusios sinuatus* Smith, 1838 (Testudines: Pelomedusidae) (syn. *Pelusios sinuatus zuluensis*).

Type material: No type material was designated by Dias (1951) in the original description of *T. sheppardi*.

Additional material: Pending formal peer-review publication.

Type locality: Maputo River, Catuane region, Maputo, Mozambique (Dias, 1951).

Localities in this study: Water pan 0.6 km south of the Maputo River (26°51'55" S, 32°09'59" E), Ndumo Game Reserve, KwaZulu-Natal, South Africa. Nyamiti Pan (26°54'00" S, 32°15'46" E), Ndumo Game Reserve, KwaZulu-Natal, South Africa.

Site of infection: Peripheral blood.

Vector: Unknown.

Stages in vector: Unknown.

Representative DNA sequence: The sequence data specifically associated with *T. cf. sheppardi* (upon which the present biological description is based) will be submitted to GenBank pending formal peer-review publication.

Description: Measurement range shown in μm (mean \pm standard deviation). Body length 43.68–66.66 (56.84 ± 6.4) ($n = 15$) and body width 4.25–11.86 (7.3 ± 2.33) ($n = 15$); with a body shape index of 4.48–12.84 (8.44 ± 2.35) ($n = 15$). Nucleus length 2.78–6.7 (4.91 ± 1.06) ($n = 15$) and nucleus width 1.5–4.02 (3.04 ± 0.76) ($n = 15$); with a nuclear index of 1.16–2.46 (1.66 ± 0.36) ($n = 15$). Undulating membrane width 1.27–2.32 (1.83 ± 0.25) ($n = 14$) and number of undulations 7–12 (9.47 ± 1.41) ($n = 15$). Kinetoplast length 0.6–1.09 (0.94 ± 0.13) ($n = 15$) and kinetoplast width 0.49–0.7 (0.59 ± 0.07) ($n = 15$). Mid-nucleus to anterior body end distance 27.36–44.48 (35.7 ± 4.55) ($n = 15$) and mid-nucleus to posterior body end distance 12.12–27.23 (22.81 ± 3.96) ($n = 15$). Kinetoplast to anterior

CHAPTER 2.3

body end distance 37.57–61.72 (50.81 ± 6.44) ($n = 15$) and kinetoplast to posterior body end distance 1.51–8.93 (6.28 ± 1.9) ($n = 15$). Kinetoplast to mid-nucleus distance 4.69–20.08 (16.85 ± 4.02) ($n = 15$). Free flagellum length 11.42–11.42 (11.42 ± 0) ($n = 1$). The nucleus and kinetoplast are positioned 52.03–75.6 (62.96 ± 5.79) % ($n = 15$) and 85.49–99.85 (89.31 ± 4.06) % ($n = 15$) from the anterior body end, respectively.

Remarks: This trypanosome had a broad body, thicker in the middle with tapering anterior and posterior ends (Figure 2.3.2 A-F). The cytoplasm uniformly stained a faint purple with few cytoplasmic vacuoles visible. The nucleus was round and stained light pink with a nucleolus occasionally visible. A relatively long flagellum was present but was often obscured. The morphology of this trypanosome was most similar to the description of *T. sheppardi* Dias, 1951.

The body dimensions of the trypanosome in the present study were more variable, but were within the measurement range described by Dias (1951) for *T. sheppardi*, measuring 43.68–66.66 by 4.25–11.86 μm , and 48.9–49.4 by 7.8–8.8 μm , respectively. Although, the average body length of 56.84 ± 6.4 μm for this trypanosome was slightly larger than the original description of *T. sheppardi*, the average width of 7.3 ± 2.33 μm was close to the lower range in the original description, and the body shape index was similar, measuring 1.66 ± 0.36 vs. 1.6 in the original description. The kinetoplast to nucleus distance of this trypanosome, 16.85 ± 4.02 μm , was within the range described for *T. sheppardi* of 16.1–17.6 μm . The mid-nucleus to posterior end distance of this parasite was within the range of *T. neitzi*, measuring 22.81 ± 3.96 μm and 22.45–23.65 μm , respectively. Dimension of the nucleus of this parasite were 4.91 ± 1.06 by 3.04 ± 0.76 μm , which are consistent with the range of *T. sheppardi*, 4.4–4.9 by 2.8–3.1 μm . The position of the kinetoplast from the anterior body end of this parasite corresponded to the position calculated for *T. sheppardi*, of 89.31 ± 4.06 % and 84.45–90.28 %, respectively.

CHAPTER 2.3

When compared to the morphometrics of another similar species, *T. cf. neitzi*, this species was proportionately broader, with a body shape index of 8.44 ± 2.35 vs. 9.16 ± 1.73 . The nucleus of *T. cf. neitzi* was positioned closer to the middle of the body compared to this trypanosome, $55.71 \pm 4.59\%$ vs. $62.96 \pm 5.79\%$ from the anterior, respectively.

The trypanosome in the present study was described from the same host species as the type host of *Trypanosoma sheppardi*, namely the serrated hinged terrapin, *Pelusios sinuatus* (syn. *P. s. zuluensis*). Furthermore, host specimens in the present study were collected within 10 km from the type locality and same river system, the Maputo River, originally described for *T. sheppardi*. Therefore, due to the aforementioned reasons, this species is described as *Trypanosoma (Haematomonas) cf. sheppardi* (note — ICZN disclaimer).

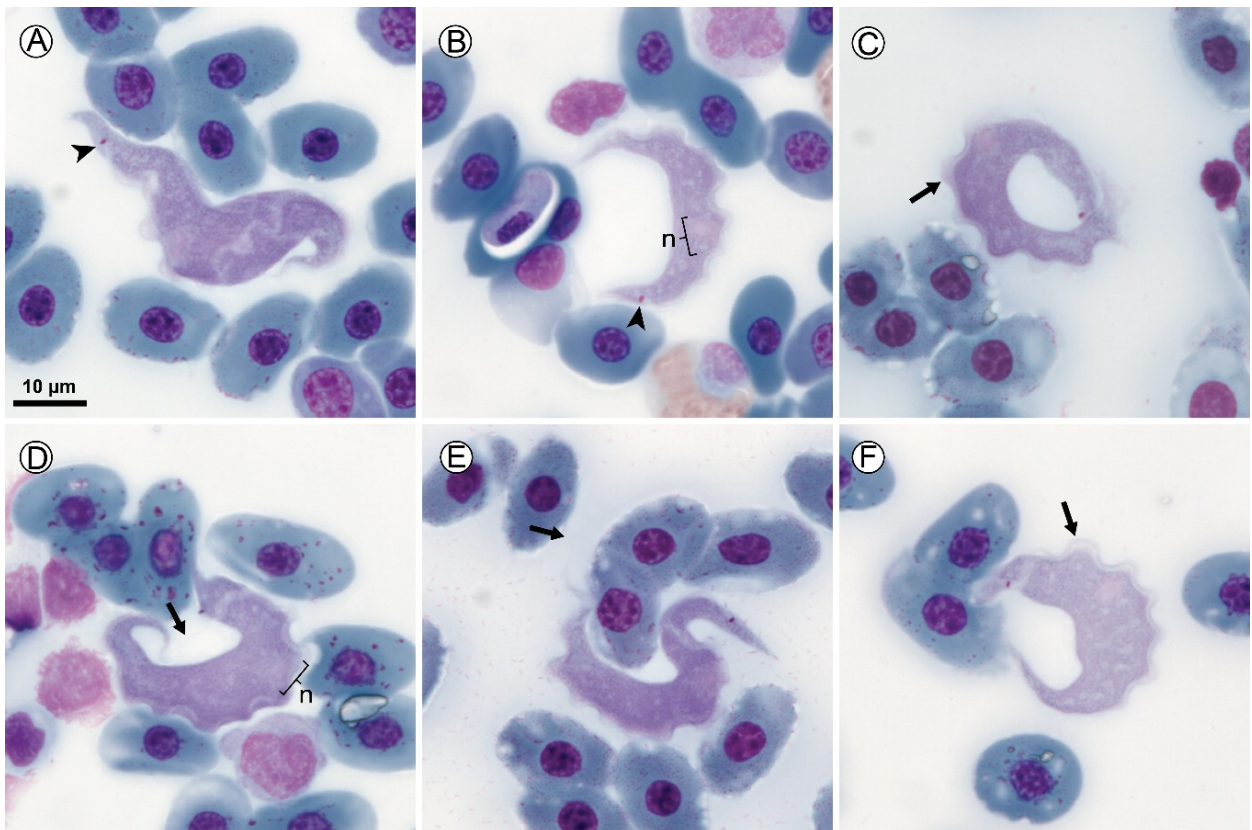


Figure 2.3.2: *Trypanosoma cf. sheppardi* plate. Normal trypomastigote forms A-F. Scale shown is 10 µm. Arrowheads show kinetoplast (A and B); arrows show flagellum (D and E) and undulating membrane (C and F); nuclei are indicated by “n” (B and D).

CHAPTER 2.3

Description of *Trypanosoma* sp. 1A

Host: *Pelomedusa galeata* Schoepff, 1792 (Testudines: Pelomedusidae)

Voucher material: Pending formal peer-review publication.

Representative DNA sequence: The sequence data specifically associated with *Trypanosoma* sp. 1A (upon which the present biological description is based) will be submitted to GenBank pending formal peer-review publication.

ZooBank registration: Pending formal peer-review publication.

Locality: Borrow pit near Mkhanyeni, eastern Lebombo Mountain foothills, (27°00'51" S; 32°08'29" E), KwaZulu-Natal province, South Africa.

Site of infection: Peripheral blood.

Vector: Unknown.

Stages in vector: Unknown.

Description: Measurements in micrometres (μm). Range shown with mean \pm standard deviation in parentheses. Body length 52.93–61.79 (56.91 ± 2.85) ($n = 16$) and body width 2.48–5.06 (3.89 ± 0.81) ($n = 16$); with a body shape index of 10.49–24.13 (15.31 ± 3.7) ($n = 16$). Nucleus length 3.11–4.78 (3.75 ± 0.42) ($n = 16$) and nucleus width 1.98–3.24 (2.59 ± 0.36) ($n = 16$); with a nuclear index of 1.07–1.9 (1.46 ± 0.2) ($n = 16$). Undulating membrane width 1.5–2.24 (1.94 ± 0.22) ($n = 16$) and number of undulations 11–15 (13.47 ± 1.25) ($n = 15$). Kinetoplast length 0.76–1.24 (0.99 ± 0.13) ($n = 16$) and kinetoplast width 0.39–0.7 (0.55 ± 0.08) ($n = 16$). Mid-nucleus to anterior body end distance 25.89–33.99 (31.34 ± 2.45) ($n = 16$) and mid-nucleus to posterior body end distance 21.76–29.62 (25.66 ± 2.22) ($n = 16$). Kinetoplast to anterior body end distance 47.81–57.36 (53.24 ± 2.51) ($n = 16$) and kinetoplast to posterior body end distance 1.04–5.49 (3.61 ± 1.33) ($n = 16$). Kinetoplast to mid-nucleus distance 19.27–22.86 (21.63 ± 0.95) ($n = 16$). Free flagellum length 17.22–21.56 (19.62 ± 1.3) ($n = 8$). The nucleus and

CHAPTER 2.3

kinetoplast are positioned 48.28–62.53 (55.11 ± 3.83) ($n = 16$) and 90.24–99.11 (93.59 ± 2.39) ($n = 16$) from the anterior body end, respectively.

Remarks: The body is long and slender with sharply tapering ends (Figure 2.3.3 A-F). A proportionately long undulating membrane and flagellum were present. This trypanosome was often observed to be curled or in the shape of an “S”, “§”, “W”, and “C”. The nucleus is oval and stains pink. The cytoplasm stained a uniform light purple and contained several granular vacuoles. The flagellum was often visible and varied between staining light pink or being almost transparent. The nucleus was oval and often almost as broad across as the body width, and positioned roughly in the middle of the body. The kinetoplast positioned close to anterior end. In addition, this species had a relatively high number of undulations.

The trypanosome from the present study appears most similar morphologically to the unnamed trypanosome described by Minchin (1910) from an African tortoise (see Plate 9, fig. 65). No measurements were provided in the description by Minchin (1910), but the kinetoplast of both species was positioned closely to the posterior body end. Nucleus of both is round, pink-staining and appears similarly positioned posterior to the centre of the body. A distinct undulating membrane is shown in the species of which extends the entire length of the body, similar to the trypanosome of the present study. The species in the present study and that described by Minchin (1910) possess a relatively long and distinct flagellum, which both stain pink. Despite these two species both being reported from Africa, they are separated by vast geographic distance and several mountain ranges, as the trypanosome described by Minchin (1910) was from an unspecified locality in Uganda, and the host specimens of the trypanosome from the present study were from South Africa. It is also not known specifically what tortoise host was infected with the species described by Minchin (1910).

CHAPTER 2.3

When compared with the other trypanosomes of the present study, this trypanosome was proportionately more slender, with a body shape index of 15.31 ± 3.7 in contrast to that of *T. cf. neitzi* and *T. cf. sheppardi*, measuring 9.16 ± 1.73 and 8.44 ± 2.35 , respectively. The body of this trypanosome was also narrower, measuring $3.89 \pm 0.81 \mu\text{m}$, when compared to with body width of *T. cf. neitzi* and *T. cf. sheppardi*, $5.59 \pm 1.38 \mu\text{m}$ and $7.3 \pm 2.33 \mu\text{m}$, respectively. The kinetoplast of this trypanosome was positioned further from the anterior body end, at $93.59 \pm 2.39 \%$, than *T. cf. neitzi* and *T. cf. sheppardi*, $93.59 \pm 2.39 \%$ and $89.31 \pm 4.06 \%$, respectively.

Accordingly, as this trypanosome did not match any currently described species of *Trypanosoma*, it is presented as an undescribed species, referred to in the present study as *Trypanosoma (Haematomonas) sp. 1A* (note — ICZN disclaimer).

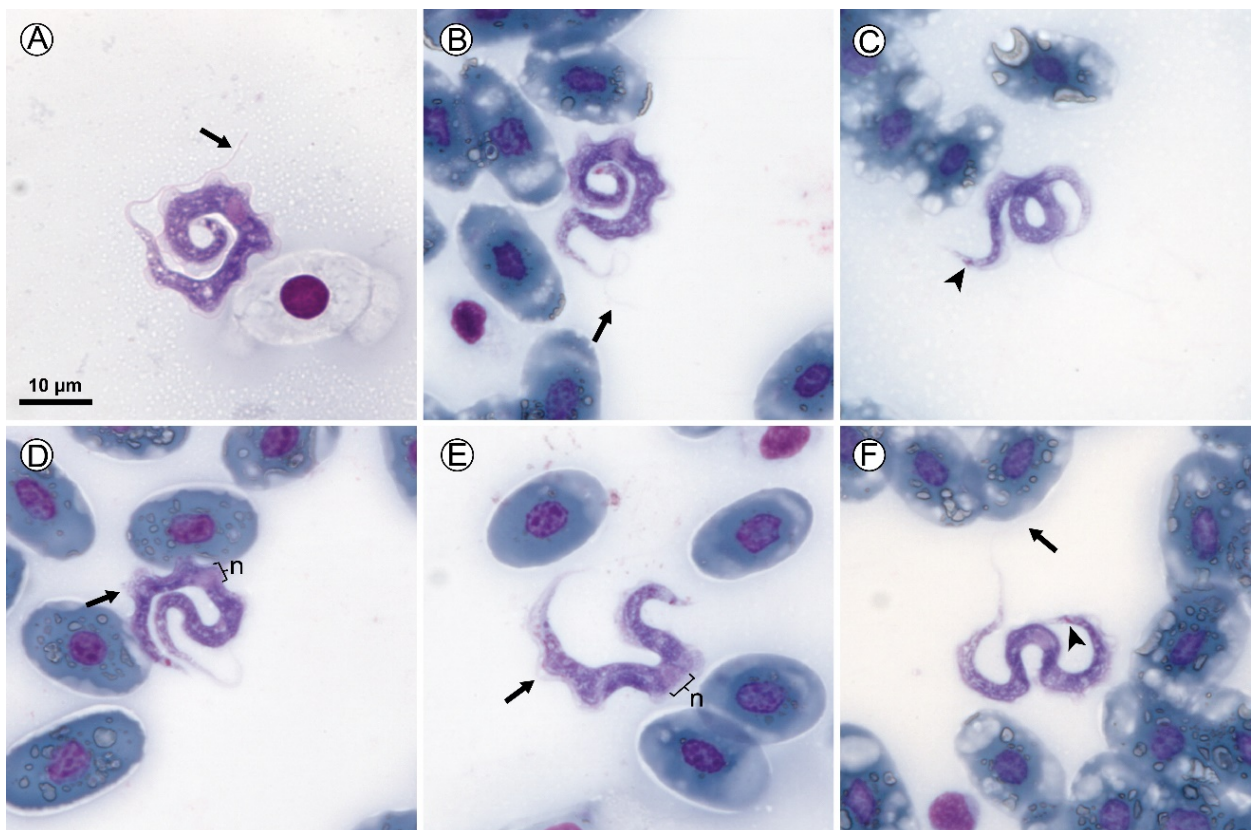


Figure 2.3.3: *Trypanosoma sp. 1A* plate. Normal trypomastigote forms A-F. Scale shown is $10 \mu\text{m}$. Arrowheads show kinetoplast (C and F); arrows show flagellum (A, B, and F) and undulating membrane (D and E); nuclei are indicated by “n” (D and E).

CHAPTER 2.3

2.3.4.2 *Molecular and phylogenetic analysis*

Sequences RE210313C1 (1453 bp), RE210314A3 (1454 bp), and RE210314A5 (1454 bp) isolated from the *Trypanosoma* sp. infecting *Pelusios castenoides*, described morphologically as *T. cf. neitzi*, were 100% identical (see Table 2.3.2), and were subsequently classified as genotype *Trypanosoma cf. neitzi*. Additionally, these sequences were 100% identical with those of *T. mocambicum* (KP888914 and KP888915) for an alignment cover of 872 bp. Thus, this trypanosome is identified as the same species as *T. mocambicum*. The sequences RE210311A3 (1454 bp) and RE210311B1 (1458 bp) isolated from an infection in the host species *Pelusios sinuatus* morphologically described as *T. cf. sheppardi* were 100% identical, and were classified as the genotype *Trypanosoma cf. sheppardi*. Sequences RE210331A2 (1455 bp) and RE210331A3 (1454 bp), isolated from *Pelomedusa galeata* trypanosome infections morphologically described as *Trypanosoma* sp. 1A were 100% identical, and were subsequently classified as genotype *Trypanosoma* sp. 1A. An nBLAST alignment revealed the closest match of *Trypanosoma cf. sheppardi* isolated from *Pelu. sinuatus* was 96.37% with the fish trypanosome, *T. ophiocephali* (EU185634). The closest nBLAST percent identity match of *Trypanosoma* sp. 1A isolated from *Pelo. galeata* was with *T. mocambicum* (KP888915), with a percent similarity of 97.94 % between the two sequences. However, the alignment of these two sequences was only 874 bp, as the sequence of *T. mocambicum* was much shorter than that of *Trypanosoma* sp. 1A isolated from *Pelo. galeata*, because *T. mocambicum* (KP888915) only had length of 897 bp.

The topologies of the BI and ML trees were identical, and were thus combined into a consensus phylogram, as seen in Figure 2.3.4. The clades were strongly supported with high nodal support values overall. However, weak values, specifically ML bootstraps, are shown for the resolution of the turtle, platypus, clawed frog, and marine fish trypanosome subclades within the *Haematomonas* clade but the topology corresponds

CHAPTER 2.3

with phylogenies in current literature (Dvořáková *et al.*, 2015; Bernal and Pinto, 2016; Spodareva *et al.*, 2018, Kostygov *et al.*, 2021).

All three genotypes from the present study, formed a monophyly with sequences of other trypanosomes also isolated from Southern African pelomedusid turtles that is well-nested within the freshwater turtle/platypus clade. Four distinct subclades were observed within this monophyly, namely *Trypanosoma* cf. *neitzi*, *T.* cf. *sheppardi*, and *Trypanosoma* sp. 1A, and *T. mocambicum*. Despite the sequence alignments having a 100% identity, *Trypanosoma* cf. *neitzi* and *T. mocambicum* were split into separate subclades within the same monophyly. This is likely a consequence of the sequences of *T. mocambicum* (KP888907 and KP888921) being approximately half the length of the *T.* cf. *neitzi* sequences from the present study. Sequences of *Trypanosoma* sp. 1A clade closest to the subclade of *T. mocambicum* but was clearly shown to be a separate genotype, which is supported by the morphological data. *Trypanosoma* cf. *sheppardi* was shown to also clade closely to the other pelomedusid turtle trypanosomes from Southern Africa but is distinctly a separate genotype, further supporting the morphological characterisation. The closest relative sister clades outside of this monophyly are of another species of *Trypanosoma* which infects pelomedusid turtles from Southern Africa, *Trypanosoma* sp. IC-2015a (KP888905 and KP888913); Australian freshwater turtle and platypus trypanosomes, *T. chelodinae* and *T. binneyi*; and the trypanosome of the fully aquatic clawed frog from South Africa, *Trypanosoma* cf. *grandicolor*, isolated from *Xenopus laevis* (see Chapter 2.1).

It is notable that all the 18S rDNA sequences currently available of turtle trypanosomes group together in the phylogeny (with the addition of the platypus trypanosome), albeit they only originate from two continents, Africa and Australia. This is possibly an indication of a common ancestral lineage which diverged with the breakup of the land mass connecting these continents. The common ancestor was potentially a fish

CHAPTER 2.3

trypanosome which was transmitted to other hosts by aquatic leeches, as suggested by Hamilton *et al.* (2004) and Dvořáková *et al.* (2015).

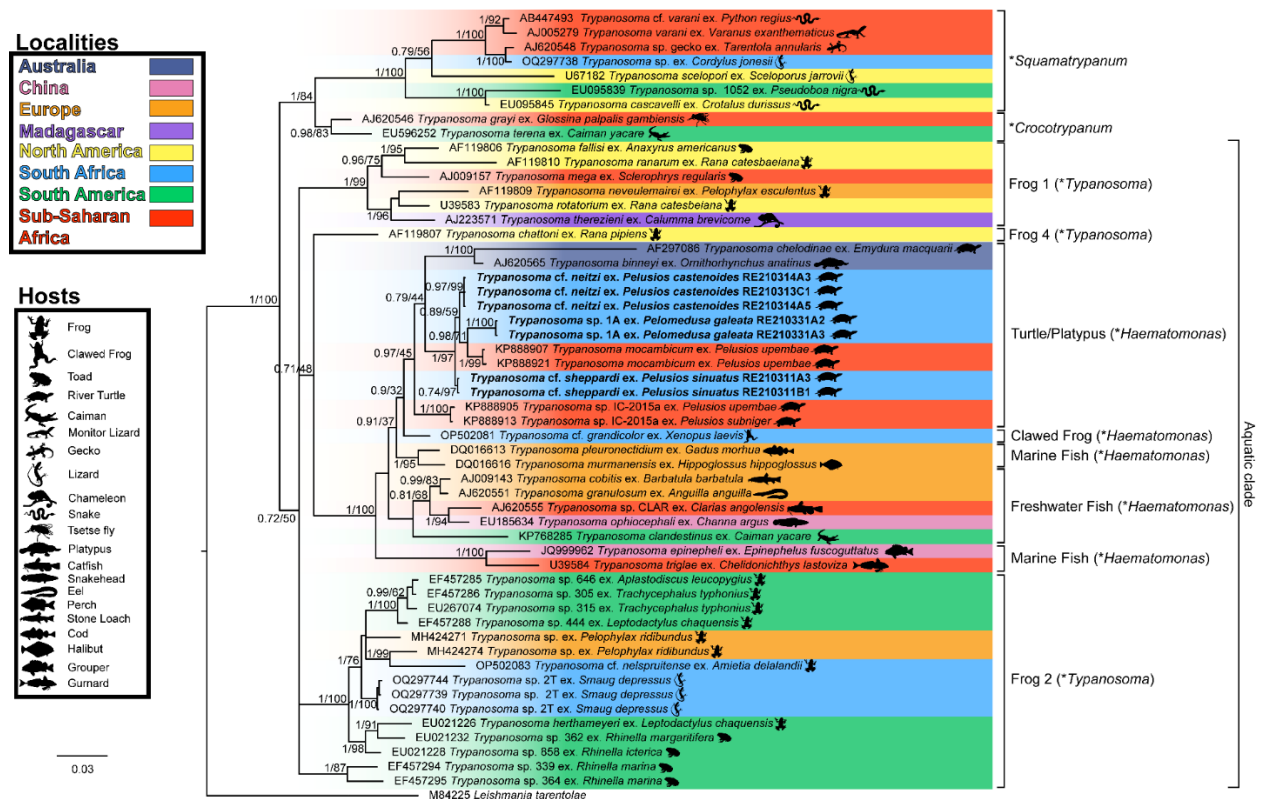


Figure 2.3.4: Consensus phylogram of the aquatic trypanosome clade based off the 18S rRNA gene. (Represented on BI tree). Nodal support values shown as posterior probability over bootstrap values. Values below 0.7 and 70, respectively, were omitted. Sequences from the present study are in bold. Subgenera are indicated by an asterisk (*). Scale shown is number of nucleotide substitutions per site.

2.3.5. Discussion

Using morphometrics alone to characterize species of reptile trypanosomes is possible, however, due to the morphological plasticity of trypanosomes, it can be unreliable (Telford, 2009). The morphometrics of the species from the present study showed some variation but were generally distinct and supported in the phylogeny. Molecular analyses showed that the short 18S rDNA sequences of approximately 900 bp appear robust enough for identification of *Trypanosoma* genotypes but might not be ideal for situations with closely related species of *Trypanosoma* or possible mixed infections,

CHAPTER 2.3

as seen in the present study and that of Dvořáková *et al.* (2015). Using a larger partial sequence of the 18S rRNA gene of approximately (1400-1500 bp) for molecular analyses, as with the present study, might prove more beneficial in providing a higher resolution of the phylogenetic relationships.

Low parasitaemia and absence of trypanosomes in the blood smear slides of turtle hosts which are known to be positively infected, as seen with several of the specimens in the present study, has been reported by several authors previously. Laveran and Mesnil (1902), when periodically screening two turtles naturally infected with *T. damoniae*, noted its scarcity. Dutton and Todd (1903) also report the absence of trypanosomes from peripheral blood from infected two marsh tortoises that were kept captive for three months and regularly screened. When these trypanosomes were observed, they were infrequently present with a low parasitaemia. Low parasitaemia is also reported by Dias (1951) in the original descriptions of *T. neitzi* and *T. sheppardi*. Freyre (2009) detected no trypomastigotes during microscopic screening of the Australian freshwater turtles, *Chelodina steindachneri*, but found a prevalence of 87.5% specimens to be positively infected by molecular screening. The preparation of thicker blood smear slides would possibly allow for greater sensitivity in detecting trypanosomes in samples with low parasitaemia for situations where molecular screening is not possible, as thinner blood smear slides were shown by Ohrt *et al.* (2008) to be less accurate in representing the parasite prevalence of Malaria in the blood, than thicker blood smears.

In future, increased sampling, larger size molecular sequence isolates, and using additional genetic barcodes, such as the gGAPDH gene or ITS regions, could be beneficial, could potentially be implemented to decipher closely related species. This is especially significant for when morphological characterisation is not available, due to low parasitaemia or mixed infections. Although, it is best to use both morphological and

CHAPTER 2.3

molecular methods in combination for taxonomic purposes, as suggested by other researchers, such as Valkiūnas *et al.* (2011) and Freyre (2009).

Minchin (1910), Dias (1951), Pienaar (1962), Freyre (2009), and Dvořáková *et al.* (2015) all report the regular occurrence of haemogregarine (*Haemogregarina* sp.) and trypanosome coinfections in the same host specimens. This was also true for the present study, where all except one of the host specimens examined exhibited haemogregarine and trypanosome coinfections. It is suggested by Dvořáková *et al.* (2015) that a possible reason for this common coinfection, is because of a shared aquatic leech vector between both parasites, as haemogregarines infecting African freshwater turtles are known to be transmitted by leech vectors. An indication possibly supporting the hypothesis of the African turtle trypanosomes being transmitted by leech vectors is shown in the phylogeny, where turtle trypanosomes are well-nested within the fish trypanosome clade, which have been shown to be transmitted by leech vectors (Hayes *et al.*, 2014). Leech vectors have successfully been demonstrated to be a mode of transmission for turtle trypanosomes outside of Africa, such as *Trypanosoma vittatae* in South Asia and *T. chrysemydis* in North America (Robertson, 1908; Robertson, 1909; Siddall and Dessler, 1992). Freyre (2009) implicated leeches as the vectors of trypanosomes infecting Australian turtles. Leeches were observed to be feeding upon the African pelomedusid turtle hosts by Dvořáková *et al.* (2015) and in the present study, and a leech vector for African turtle trypanosomes seems to be supported in the phylogeny as well. Ultimately, further investigation into the aquatic leeches which feed upon African pelomedusid turtles is needed.

Reptile trypanosomes are currently not known to replicate by division in the vertebrate host, instead replicating through asymmetrical binary fission in the invertebrate vector (Hamilton *et al.*, 2007; Telford, 2009; Magez *et al.*, 2021). Thus, the number of trypanosomes in the peripheral blood of the host would be expected to steadily decrease

CHAPTER 2.3

over time until reinfection occurs. It was hypothesised by Freyre (2009) that the commonly detected low parasitaemia of turtle trypanosomes was potentially due to a low survival rate of the aquatic leech vectors during dry seasons, resulting in lower rates of trypanosome infections and reinfections. The turtle specimens in the present study were all captured toward the end of the rain season in northern Kwazulu-Natal, yet samples with low parasitaemia were still common. It is also important to note that pelomedusid turtles are known to aestivate for long periods during dry seasons (Boycott and Bourquin, 2008; Branch, 2012; Petzold *et al.*, 2014; Vamberger *et al.*, 2019), and would accordingly not be exposed to potential leech vectors during this period. *Pelomedusa subrufa* from Namibia were found to remain burrowed underground for up to six years during periods of drought (Petzold *et al.*, 2014). Therefore, low parasitaemia of trypanosomes in these turtles would possibly be noted after recently emerging from the long period of inactivity while burrowed. It is not known if turtle trypanosome infections remain positive during these periods or how trypanosomes of other host species which aestivate or hibernate are affected. Perhaps trypanosomes are able to survive within the host during this period due to the lowered physiology and subsequently weakened immune system responses of the host. Very little is known about the relationship and effect reptile trypanosomes have on their hosts in general (Telford, 2009), and further research is required to gain a better understanding of this parasite group.

2.3.6. Acknowledgements

The authors are grateful for aid from members of the African Amphibian Conservation Research Group and the Water Research Group for access to their facilities. This paper was submitted as part of BJ Jordaan's master's degree at the North-West University (Supervisor EC Netherlands and cosupervisor LH du Preez).

CHAPTER 2.3

2.3.7. Author contributions

Authors BJ, ECN, and LdP conceived and designed the study. BJ, ECN, and LdP conducted data gathering and analyses thereof. BJ, ECN and LdP wrote the article.

2.3.8. Financial support

The financial assistance of the National Research Foundation (NRF) of South Africa, towards ECN, is hereby acknowledged. Opinions, findings and conclusions or recommendations expressed in any publication generated by an NRF supported study, is that of the author(s) alone and the NRF accepts no liability whatsoever in this regard (Grant UID 129669).

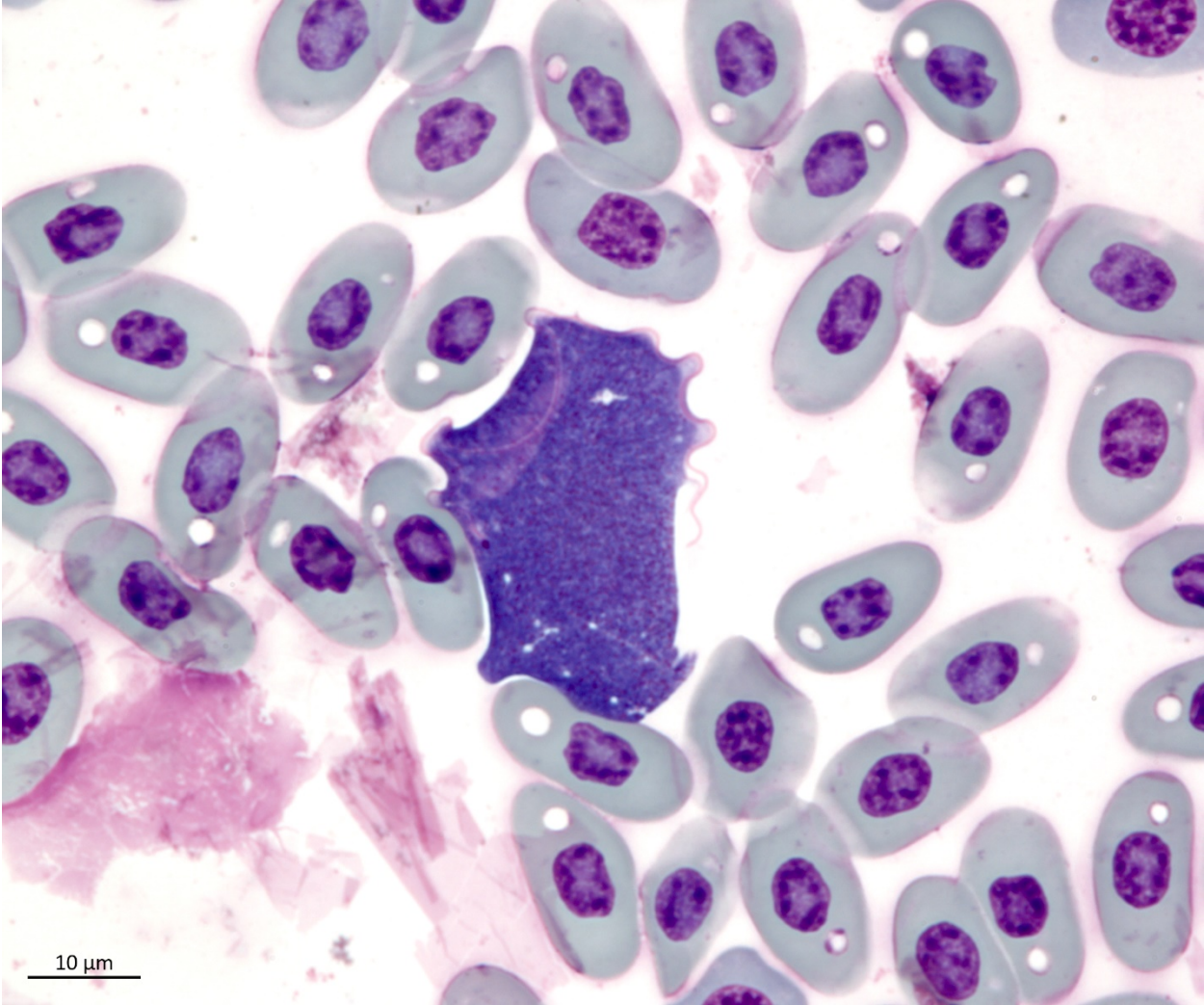
2.3.9. Conflicts of interest

The authors declare there are no conflicts of interest.

2.3.10. Ethical standards

This study forms part of an approved NWU's AnimCare ethics committee project: Ecology, systematics and evolutionary biology of ectotherm blood parasites (Ethics Number: NWU-00372-16-A5 and NWU-00427-21-A5; North West Department of Rural, Environmental and Agricultural Development (READ) research permit number: NW 7108/02/2019; Ezemvelo research permit no. OP 594/2021).

CHAPTER 3 GENERAL DISCUSSION



Trypanosoma sp. 2T ex. *Smaug depressus*

CHAPTER 3

Discussion

Due to the majority of reptile and amphibian trypanosome species being described before the introduction of molecular techniques in the 21st century, most species descriptions only contain morphological characteristics. Furthermore, many of these descriptions are severely lacking in information and most species have not been reported since their original descriptions (Telford, 2009; Bardsley and Harmsen, 1973). Common pleomorphism, lack of rigid structures, frequency of mixed infections, and low parasitaemia exacerbate the difficulty of identifying and distinguishing between trypanosome infections when using the traditional method of microscopic analysis (Freyre, 2009; D'Avila-Levy *et al.*, 2015; Hayes *et al.*, 2014; Shannon, 2016). Consequently, a reconstruction of the current *Trypanosoma* taxonomy with the verification and redescription of existing species using molecular data has been proposed (Valkiūnas *et al.*, 2011).

As was found in Chapter 2.1 of the present study, molecular analyses proved valuable alongside morphological characterisation for species identification, particularly when pleomorphism is observed (as seen with *Trypanosoma cf. nelspruitense*), which is common in anuran trypanosome infections (Diamond, 1965; Attias *et al.*, 2016; Spodareva *et al.*, 2018). However, conventional morphological and molecular analysis methods are limited in distinguishing species of mixed infections (Leal *et al.*, 2009; Spodareva *et al.*, 2018). This has been mitigated by other researchers with the inclusion of large enough sample sizes to obtain sufficient single-species infections, or with the use of culturing techniques (Diamond, 1965; Dvořáková *et al.*, 2015; Spodareva *et al.*, 2018; Fermino *et al.*, 2019). However, this is not always possible, due to low infection prevalence or mixed infections, and not all trypanosomes are able to be cultured (Diamond, 1965). Additionally, cultured trypanosomes' morphology is not necessarily representative of a natural infection (Diamond, 1965; Attias *et al.*, 2016).

CHAPTER 3

The findings of Chapter 2.2 in the present study revealed the frequent occurrence of infections with low parasitaemia and an absence of trypanosomes during microscopic screening, despite the confirmation of a positive infection. As has been suggested by other researchers, this indicates that the actual prevalence of trypanosome infections, and subsequently species diversity, is possibly much higher than previously thought (Freyre, 2009; Attias *et al.*, 2016). Furthermore, this study demonstrates the utility of molecular-based screening methods, to detect trypanosome infections much more accurately than the traditional method of light microscopy. This study also provides supporting evidence of the placement of several lizard trypanosomes within the anuran trypanosome clade of the phylogeny. Previously, these instances were thought to be incidental infections of anuran trypanosomes in lizards (Toontong *et al.*, 2022). Although, it is now shown to be more likely that these groups recently diverged from an ancestral lineage and is implicit of a host switching-resultant speciation due to a vector with loose specificity (Haag *et al.*, 1998). Subsequently, an inherent consequence of basing species descriptions solely off bloodstream trypomastigote forms, during the life cycle stage within the vertebrate host, is shown (Leal *et al.*, 2009).

The need for the revision and verification of currently recognised species, using modern techniques, is further emphasised with the results of Chapter 2.3. Furthermore, the flaw of traditional morphological species characterisation is apparent through the difficulty of distinguishing intraspecific polymorphism and interspecific variation (Leal *et al.*, 2009; Telford, 2009; Hayes *et al.*, 2014). A consequence of this is shown in the present study, where synonymous species, such as *T. neitzi* and *T. mocambicum*, result in a discordant taxonomy and resultantly ineffective communication of scientific information (Dias, 1951; Pienaar, 1962). This study sets a platform for future research of anuran, turtle, and other reptile trypanosomes in South Africa, by providing the first morphometric and molecular data of several South African anuran and reptile species of

CHAPTER 3

Trypanosoma. Thus, more effective species identification and comparisons in future studies is permitted. Subsequently, the results of the present study provide a basis for further work on the ecology of ectotherm trypanosomes, such as identifying complete life cycle stages, modes of transmission, host-vector relationships, and evolutionary history. A greater sampling effort in future studies, targeting both the trypanosomes' host and vector species, would be key in acquiring a sufficient quantity and diversity of species data for comparative analyses. Future improvements of existing analytical techniques of trypanosome diagnosis, DNA isolation, and more accurate methods of detection, would not only assist in deciphering mixed infections and identifying cryptic and polymorphic species, but could have complimentary benefits for research of pathogenic species of *Trypanosoma*, as well as other haemoparasites, such as malaria (Ohrt *et al.*, 2008).

As is indicated by the diverse species described in the present study from a relatively small number of hosts, there is great potential for further research on South African anuran and reptile trypanosomes. However, it is evident that much is still unknown about these organisms, particularly about the parasite-host relationship, and what effect trypanosome infections have on their respective host, if any. Thus, more attention should be dedicated to exploring the life cycles and modes of transmission of these marvellous parasites in future. Although, a robust taxonomic system is first required for effective research to expand upon our current understanding of the group, which this study has advanced the progression of.

REFERENCE LIST

REFERENCE LIST

- Abbate, J. M., Maia, C., Pereira, A., Arfuso, F., Gaglio, G., Rizzo, M., Caracappa, G., Marino, G., Pollmeier, M. and Giannetto, S.** (2020). Identification of trypanosomatids and blood feeding preferences of phlebotomine sand fly species common in Sicily, Southern Italy. *PloS One*, **15**, e0229536. doi: <https://doi.org/10.1371/journal.pone.0229536>.
- Attias, M., Sato, L. H., Ferreira, R. C., Takata, C. S. A., Campaner, M., Camargo, E. P., Teixeira, M. M. G. and de Souza, W.** (2016). Developmental and ultrastructural characterization and phylogenetic analysis of *Trypanosoma herthameyeri* n. sp. of Brazilian Leptodactilydae frogs. *Journal of Eukaryotic Microbiology*, **63**, 610-622. doi: <https://doi.org/10.1111/jeu.12310>.
- Bardsley, J. E. and Harmsen, R.** (1973). The trypanosomes of Anura. *Advances in Parasitology*, **11**, 1-73.
- Bernal, X. E. and Pinto, C. M.** (2016). Sexual differences in prevalence of a new species of trypanosome infecting Túngara frogs. *International Journal for Parasitology: Parasites and Wildlife*, **5**, 40-47. doi: <https://doi.org/10.1016/j.ijppaw.2016.01.005>.
- Bouet, G.** (1909). Sur quelques trypanosomes des vertébrés asang froid de l'Afrique Occidentale Française. *Comptes Rendus des Seances de la Société de Biologie et de ses Filiales*, **66**, 609-611.
- Boycott, R. and Bourquin, O.** (2008). *Pelomedusa subrufa* (Lacépède 1788), helmeted turtle, helmeted terrapin. *Conservation biology of freshwater turtles and tortoises: a compilation project of the IUCN/SSC tortoise and freshwater turtle specialist group. Chelonian Research Monographs*, 007.001-007.006.
- Branch, B.** (2012). *Tortoises, terrapins & turtles of Africa*. Cape Town, South Africa: Random House Struik.
- Bullock, A. and Hülsmann, S.** (2015). *Strategic opportunities for hydropower within the water-energy-food nexus in Mozambique*. Dresden, Germany: United Nations

REFERENCE LIST

- University Institute for Integrated Management of Material Fluxes and of Resources (UNU-FLORES). doi: 10.53325/MRGO5555.
- Castro, P. D. J., Pietzsch, M. and Pantchev, N.** (2019). Ectoparasites in captive reptiles. *The Veterinary Nurse*, **10**, 33-41. doi: 10.12968/vetn.2019.10.1.33.
- Commes, C.** (1919). Hémogrégarine et trypanosome d'un chelonian (*Cinixis homeana*). *Bulletin de la Société de Pathologie Exotique*, **12**, 14-16.
- Conradie, R., Cook, C. A., du Preez, L. H., Jordaan, A. and Netherlands, E. C.** (2017). Ultrastructural comparison of *Hepatozoon ixoxo* and *Hepatozoon theileri* (Adeleorina: Hepatozoidae), parasitising South African anurans. *Journal of Eukaryotic Microbiology*, **64**, 193-203. doi: <https://doi.org/10.1111/jeu.12351>.
- d'Avila-Levy, C. M., Boucinha, C., Kostygov, A., Santos, H. L. C., Morelli, K. A., Grybchuk-Ieremenko, A., Duval, L., Votýpka, J., Yurchenko, V. and Grellier, P.** (2015). Exploring the environmental diversity of kinetoplastid flagellates in the high-throughput DNA sequencing era. *Memórias do Instituto Oswaldo Cruz*, **110**, 956-965. doi: <https://doi.org/10.1590/0074-02760150253>.
- Darriba, D., Taboada, G. L., Doallo, R. and Posada, D.** (2012). jModelTest 2: more models, new heuristics and parallel computing. *Nature Methods*, **9**, 772-772. doi: 10.1038/nmeth.2109.
- Desser, S. S.** (2001). The blood parasites of anurans from Costa Rica with reflections on the taxonomy of their trypanosomes. *Journal of Parasitology*, **87**, 152-160. doi: 10.1645/0022-3395(2001)087[0152:Tbpoaf]2.0.Co;2.
- Diamond, L. S.** (1965). A study of the morphology, biology and taxonomy of the trypanosomes of Anura. *Wildlife Diseases*, **44**, 1-85.
- Dias, J. A. T. S.** (1951). Duas novas espécies de tripanossomas parasitas da tartaruga "*Pelusios sinuatus zuluensis*" Hewitt, 1927. *Moçambique Documentario Trimestral*, **68**, 97-113.

REFERENCE LIST

- Dutton, J. E. and Todd, J. L.** (1903). First report of the trypanosomiasis expedition to Senegambia (1902). *Liverpool School of Tropical Medicine and Medical Parasitology*, **11**.
- Dutton, J. E., Todd, J. L. and Tobey, E. N.** (1907). Concerning certain parasitic Protozoa observed in Africa: Being the eighth interim report of the expedition of the Liverpool School of Tropical Medicine to the Congo, 1903-5. *Annals of Tropical Medicine & Parasitology*, **1**, 286-371.
- Dvořáková, N., Čepička, I., Qablan, M. A., Gibson, W., Blažek, R. and Široký, P.** (2015). Phylogeny and morphological variability of trypanosomes from African pelomedusid turtles with redescription of *Trypanosoma mocambicum* Pienaar, 1962. *Protist*, **166**, 599-608. doi: <https://doi.org/10.1016/j.protis.2015.10.002>.
- Edler, D., Klein, J., Antonelli, A. and Silvestro, D.** (2021). raxmlGUI 2.0: A graphical interface and toolkit for phylogenetic analyses using RAxML. *Methods in Ecology and Evolution*, **12**, 373-377.
- Egan, S. L., Taylor, C. L., Austen, J. M., Banks, P. B., Ahlstrom, L. A., Ryan, U. M., Irwin, P. J. and Oskam, C. L.** (2020). Molecular identification of the *Trypanosoma (Herpetosoma) lewisi* clade in black rats (*Rattus rattus*) from Australia. *Parasitology Research*, **119**, 1691-1696. doi: [10.1007/s00436-020-06653-z](https://doi.org/10.1007/s00436-020-06653-z).
- Fantham, H. and Porter, A.** (1950). The endoparasites of certain South African snakes, together with some remarks on their structure and effects on their hosts. *Proceedings of the Zoological Society of London*, **120**, 599-647. doi: <https://doi.org/10.1111/j.1096-3642.1950.tb00665.x>.
- Fantham, H., Porter, A. and Richardson, L.** (1942). Some haematozoa observed in vertebrates in eastern Canada. *Parasitology*, **34**, 199-226.
- Fermino, B. R., Paiva, F., Viola, L. B., Rodrigues, C. M. F., Garcia, H. A., Campaner, M., Takata, C. S. A., Sheferaw, D., Kisakye, J. J., Kato, A., Jared, C. A. G. S.,**

REFERENCE LIST

- Teixeira, M. M. G. and Camargo, E. P.** (2019). Shared species of crocodylian trypanosomes carried by tabanid flies in Africa and South America, including the description of a new species from caimans, *Trypanosoma kaiowa* n. sp. *Parasites & Vectors*, **12**, 225. doi: 10.1186/s13071-019-3463-2.
- Ferreira, J. I. G. S., da Costa, A. P., Nunes, P. H., Ramirez, D., Fournier, G. F. R., Saraiva, D., Tonhosolo, R. and Marcili, A.** (2017). New *Trypanosoma* species, *Trypanosoma gennarii* sp. nov., from South American marsupial in Brazilian Cerrado. *Acta Tropica*, **176**, 249-255. doi: <https://doi.org/10.1016/j.actatropica.2017.08.018>.
- Ferreira, M. L.** (2010). Systematics and ecology of Australian and South African gnathiid isopods, with observations on blood-inhabiting Protozoa found in some of their host fishes. PhD thesis, University of Johannesburg.
- Ferreira, R. C., Campaner, M., Viola, L. B., Takata, C. S. A., Takeda, G. F. and Teixeira, M. M. G.** (2007). Morphological and molecular diversity and phylogenetic relationships among anuran trypanosomes from the Amazonia, Atlantic Forest and Pantanal biomes in Brazil. *Parasitology*, **134**, 1623-1638. doi: 10.1017/S0031182007003058.
- Freitas, E. S., Bauer, A. M., Siler, C. D., Broadley, D. G. and Jackman, T. R.** (2018). Phylogenetic and morphological investigation of the *Mochlus afer-sundevallii* species complex (Squamata: Scincidae) across the arid corridor of sub-Saharan Africa. *Molecular Phylogenetics and Evolution*, **127**, 280-287. doi: <https://doi.org/10.1016/j.ympev.2018.04.020>.
- Freyre, A. S.** (2009). *Trypanosoma* of Australian freshwater turtles: Occurrence and diversity. M.S. thesis, University of Nebraska at Omaha, Ann Arbor.
- Geospiza** (2006). *FinchTV*. Version 1.4.0. Available from www.geospiza.com/finchtv
- Gluge, G.** (1842). Ueber ein eigenthümliches Entozoon im Blute des Frosches. *Archives*

REFERENCE LIST

- für Anatomy, Physiology und Wissenschaft Medicale, Berlin*, 148.
- Grassi, B.** (1881). Ad alcuni protisti endoparassitici ed appartenenti alle classe dei Flagellata, Lobosi, Sporozoi e Ciliati. *Atti della Societa Italiana di Scienze Naturali*, **24**, 174-176.
- Greenbaum, E., Stanley, E. L., Kusamba, C., Moninga, W. M., Goldberg, S. R. and Bursey, C. R.** (2012). A new species of *Cordylus* (Squamata: Cordylidae) from the Marungu Plateau of south-eastern Democratic Republic of the Congo. *African Journal of Herpetology*, **61**, 14-39. doi: doi:10.1080/21564574.2012.666505.
- Gruby, D.** (1843). Recherches et observations sur une nouvelle espèce d'hématozoaire, *Trypanosoma sanguinis*. *Comptes Rendus Hebdomadaire Des Séances de l'Académie Des Sciences, Paris*, **17**, 1134-1136.
- Guindon, S. and Gascuel, O.** (2003). A simple, fast, and accurate algorithm to estimate large phylogenies by Maximum Likelihood. *Systematic Biology*, **52**, 696-704. doi: 10.1080/10635150390235520.
- Haag, J., O'HUigin, C. and Overath, P.** (1998). The molecular phylogeny of trypanosomes: evidence for an early divergence of the Salivaria. *Molecular and Biochemical Parasitology*, **91**, 37-49. doi: [https://doi.org/10.1016/S0166-6851\(97\)00185-0](https://doi.org/10.1016/S0166-6851(97)00185-0).
- Hall, T. A.** (1999). BioEdit: a user-friendly biological sequence alignment editor and analysis program for Windows 95/98/NT. *Nucleic Acids Symposium Series*, **41**, 95-98.
- Hamilton, P. B., Gibson, W. C. and Stevens, J. R.** (2007). Patterns of co-evolution between trypanosomes and their hosts deduced from ribosomal RNA and protein-coding gene phylogenies. *Molecular Phylogenetics and Evolution*, **44**, 15-25. doi: <https://doi.org/10.1016/j.ympev.2007.03.023>.
- Hamilton, P. B., Stevens, J. R., Gaunt, M. W., Gidley, J. and Gibson, W. C.** (2004).

REFERENCE LIST

- Trypanosomes are monophyletic: evidence from genes for glyceraldehyde phosphate dehydrogenase and small subunit ribosomal RNA. *International Journal for Parasitology*, **34**, 1393-1404. doi: <https://doi.org/10.1016/j.ijpara.2004.08.011>.
- Hayes, P. M., Lawton, S. P., Smit, N. J., Gibson, W. C. and Davies, A. J.** (2014). Morphological and molecular characterization of a marine fish trypanosome from South Africa, including its development in a leech vector. *Parasites & Vectors*, **7**, 1-11. doi: 10.1186/1756-3305-7-50.
- Headrick, D. R.** (2014). Sleeping Sickness Epidemics and Colonial Responses in East and Central Africa, 1900–1940. *PLOS Neglected Tropical Diseases*, **8**, e2772. doi: 10.1371/journal.pntd.0002772.
- Hoare, C. A.** (1929). Studies on *Trypanosoma grayi*. 2. Experimental transmission to the crocodile. *Transactions of the Royal Society of Tropical Medicine and Hygiene*, **23**.
- Hoare, C. A.** (1931). Studies on *Trypanosoma grayi*. III. Life-cycle in the tsetse-fly and in the crocodile. *Parasitology*, **23**, 449-484.
- Huelsenbeck, J. P. and Ronquist, F.** (2001). MRBAYES: Bayesian inference of phylogenetic trees. *Bioinformatics*, **17**, 754-755.
- Hughes, A. L. and Piontkivska, H.** (2003). Molecular phylogenetics of Trypanosomatidae: contrasting results from 18S rRNA and protein phylogenies. *Kinetoplastid Biology and Disease*, **2**, 1-10. doi: 10.1186/1475-9292-2-15.
- ICZN** (2012). *International code of zoological nomenclature*, 4th edn. London, UK: The International Trust for Zoological Nomenclature.
- IUCN** (2022). The IUCN Red List of Threatened Species. Version 2022-1. **2022**.
- Ivanic, H.** (1936). Structure du noyau au repos et sa division au début de la division multiple (Schizogonie) chez le *Trypanosoma rotatorium* Mayer. *Cellule*, **44**, 349-366.
- Kearse, M., Moir, R., Wilson, A., Stones-Havas, S., Cheung, M., Sturrock, S., Buxton,**

REFERENCE LIST

- S., Cooper, A., Markowitz, S., Duran, C., Thierer, T., Ashton, B., Meintjes, P. and Drummond, A.** (2012). Geneious Basic: An integrated and extendable desktop software platform for the organization and analysis of sequence data. *Bioinformatics*, **28**, 1647-1649. doi: 10.1093/bioinformatics/bts199.
- Kelly, S., Ivens, A., Manna, P. T., Gibson, W. and Field, M. C.** (2014). A draft genome for the African crocodylian trypanosome *Trypanosoma grayi*. *Scientific data*, **1**, 140024. doi: 10.1038/sdata.2014.24.
- Kostygov, A. Y., Karnkowska, A., Votýpka, J., Tashyreva, D., Maciszewski, K., Yurchenko, V. and Lukeš, J.** (2021). Euglenozoa: taxonomy, diversity and ecology, symbioses and viruses. *Open Biology* **11**, 200407. doi: 10.1098/rsob.200407.
- Kumar, S., Stecher, G., Li, M., Knyaz, C. and Tamura, K.** (2018). MEGA X: molecular evolutionary genetics analysis across computing platforms. *Molecular Biology and Evolution*, **35**, 1547. doi: 10.1093/molbev/msy096.
- Kunstler, M.** (1883). Recherches sur les infusoires parasites. Sur quinze protozoaires nouveaux. *Comptes Rendus Hebdomadaires des Seances de l'Academie des Sciences*, **97**, 755-757.
- Laveran, A.** (1904). Sur un nouveau Trypanosome d'une Grenouille. *Comptes Rendus Hebdomadaires Des Société de Biologie*, **56**, 158.
- Laveran, A. and Mesnil, F.** (1901). Sur la structure du trypanosome des grenouilles et sur l'extension du genre *Trypanosoma* Gruby. *Comptes Rendus de la Société de Biologie et Des Ses Filiales*, **53**, 678-680.
- Laveran, A. and Mesnil, F.** (1902). Sur quelques protozoaires parasites d'une tortue d'Asie (*Damonia reevesii*). *Comptes rendus hebdomadaires des séances de l'Académie des sciences Série III*, **135**, 609-614.
- Laveran, A. and Mesnil, F.** (1907). *Trypanosomes and trypanosomiasis*. Translated by

REFERENCE LIST

- Nabarro, D. London, UK: Baillière, Tindall and Cox.
- Leal, D. D. M., O'Dwyer, L. H., Ribeiro, V. C., Silva, R. J., Ferreira, V. L. and Rodrigues, R. B.** (2009). Hemoparasites of the genus *Trypanosoma* (Kinetoplastida: Trypanosomatidae) and hemogregarines in anurans of the São Paulo and Mato Grosso do Sul States-Brazil. *Anais da Academia Brasileira de Ciências*, **81**, 199-206. doi: 10.1590/S0001-37652009000200006.
- Leydig, F.** (1857). *Lehrbuch der Histologie des Menschen und der Thiere*. Frankfurt am Main, Germany: Meidinger Sohn & Comp.
- Lima, L., Silva, F. M. d., Neves, L., Attias, M., Takata, C. S. A., Campaner, M., de Souza, W., Hamilton, P. B. and Teixeira, M. M. G.** (2012). Evolutionary insights from bat trypanosomes: morphological, developmental and phylogenetic evidence of a new species, *Trypanosoma (Schizotrypanum) erneyi* sp. nov., in African bats closely related to *Trypanosoma (Schizotrypanum) cruzi* and allied species. *Protist*, **163**, 856-872. doi: <https://doi.org/10.1016/j.protis.2011.12.003>.
- Lovich, J. E., Ennen, J. R., Agha, M. and Gibbons, J. W.** (2018). Where have all the turtles gone, and why does it matter? *BioScience*, **68**, 771-781. doi: 10.1093/biosci/biy095.
- Lukeš, J., Butenko, A., Hashimi, H., Maslov, D. A., Votýpka, J. and Yurchenko, V.** (2018). Trypanosomatids are much more than just trypanosomes: Clues from the expanded family tree. *Trends in Parasitology*, **34**, 466-480. doi: 10.1016/j.pt.2018.03.002.
- Magez, S., Pinto Torres, J. E., Oh, S. and Radwanska, M.** (2021). Salivarian trypanosomes have adopted intricate host-pathogen interaction mechanisms that ensure survival in plain sight of the adaptive immune system. *Pathogens*, **10**. doi: 10.3390/pathogens10060679.
- Martin, D. S., Wright, A.-D. G., Barta, J. R. and Desser, S. S.** (2002). Phylogenetic

REFERENCE LIST

- position of the giant anuran trypanosomes *Trypanosoma chattoni*, *Trypanosoma fallisi*, *Trypanosoma mega*, *Trypanosoma neveulemairei*, and *Trypanosoma ranarum* inferred from 18S rRNA gene sequences. *Journal of Parasitology*, **88**, 566-571. doi: 10.1645/0022-3395(2002)088[0566:Ppotga]2.0.Co;2.
- Mayer, A. F. J. K.** (1843). *Spicilegium observationum anatomicarum de organo electrico in Raiis anelectricis et de haematozois*. Bonnae, Typis Caroli Georgii.
- McEntyre, J. and Ostell, J.** (2013). *The NCBI Handbook*, 2nd edn. Bethesda, MD: National Center for Biotechnology Information.
- McInnes, L. M., Gillett, A., Ryan, U. M., Austen, J., Campbell, R. S. F., Hanger, J. and Reid, S. A.** (2009). *Trypanosoma irwini* n. sp (Sarcomastigophora: Trypanosomatidae) from the koala (*Phascolarctos cinereus*). *Parasitology*, **136**, 875-885.
- Minchin, E.** (1910). Report on a collection of blood-parasites made by the sleeping sickness commission, 1908-1909. *Reports of the Sleeping Sickness Commission of the Royal Society*, **10**, 73-86.
- Netherlands, E., Cook, C., Smit, N. and Preez, L.** (2014). Redescription and molecular diagnosis of *Hepatozoon theileri* (Laveran, 1905) (Apicomplexa: Adeleorina: Hepatozoidae), infecting *Amietia queketti* (Anura: Pyxicephalidae). *Folia Parasitologica*, **61**, 293-300. doi: 10.14411/fp.2014.046.
- Netherlands, E. C.** (2019). Ecology, systematics and evolutionary biology of frog blood parasites in northern KwaZulu-Natal. PhD thesis, North-West University Potchefstroom Campus (South Africa).
- Netherlands, E. C., Cook, C. A., Kruger, D. J., du Preez, L. H. and Smit, N. J.** (2015). Biodiversity of frog haemoparasites from sub-tropical northern KwaZulu-Natal, South Africa. *International Journal for Parasitology: Parasites and Wildlife*, **4**, 135-141.

REFERENCE LIST

- Njagu, Z. W.** (1998). Role of the monitor lizard *Varanus niloticus laurenti* in the epidemiology of trypanosomiasis along the shores of lake victoria, Kenya. PhD thesis, Kenyatta University.
- Ohrt, C., O'Meara, W. P., Remich, S., McEvoy, P., Ogutu, B., Mtalib, R. and Odera, J. S.** (2008). Pilot assessment of the sensitivity of the malaria thin film. *Malaria Journal*, **7**, 22. doi: 10.1186/1475-2875-7-22.
- Oosthuizen, J.** (1991). An annotated check list of the leeches (Annelida: Hirudinea) of the Kruger National Park with a key to the species. *Koedoe*, **34**, 25-38.
- Petzold, A., Vargas-Ramirez, M., Kehlmaier, C., Vamberger, M., Branch, W. R., Du Preez, L., Hofmeyr, M. D., Meyer, L., Schleicher, A. and Široký, P.** (2014). A revision of African helmeted terrapins (Testudines: Pelomedusidae: *Pelomedusa*), with descriptions of six new species. *Zootaxa*, **3795**, 523–548-523–548. doi: <https://doi.org/10.11646/zootaxa.3795.5.2>.
- Pienaar, U. D. V.** (1962). *Haematology of some South African reptiles*. Johannesburg, Gauteng: Witwatersrand University Press, 186-290.
- Poinar Jr, G.** (2005). *Triatoma dominicana* sp. n. (Hemiptera: Reduviidae: Triatominae), and *Trypanosoma antiquus* sp. n. (Stercoraria: Trypanosomatidae), the first fossil evidence of a triatomine-trypanosomatid vector association. *Vector-Borne and Zoonotic Diseases*, **5**, 72-81. doi: 10.1089/vbz.2005.5.72.
- Poinar Jr, G. and Poinar, R.** (2004). *Paleoleishmania proterus* n. gen., n. sp., (Trypanosomatidae: Kinetoplastida) from Cretaceous Burmese amber. *Protist*, **155**, 305-310. doi: <https://doi.org/10.1078/1434461041844259>.
- Price, C., Burnett, M. J., O'Brien, G. and Downs, C. T.** (2022). Presence and temporal activities of serrated hinged terrapin *Pelusios sinuatus* and marsh terrapin *Pelomedusa galeata* in KwaZulu-Natal, South Africa, assessed using telemetry. *Tropical Conservation Science*, **15**, 19400829221074241.

REFERENCE LIST

- Ramos, B. and Urdaneta-Morales, S.** (1977). Hematophagous insects as vectors for frog trypanosomes. *Revista de Biología Tropical*, **25**, 209-217.
- Rhodin, A., Iverson, J., Bour, R., Fritz, U., Georges, A., Shaffer, H. and Dijk, P. P.** (2021). *Turtles of the World: Annotated Checklist and Atlas of Taxonomy, Synonymy, Distribution, and Conservation Status*, 9th edn. Arlington, Vermont, USA: Chelonian Research Foundation and Turtle Conservancy.
- Robertson, M.** (1908). A preliminary note on Haematozoa from some Ceylon reptiles. *Spolia Zeylanica*, **5**, 178-185.
- Robertson, M.** (1909). Studies on Ceylon hæmatozoa: no.1. The life cycle of *Trypanosoma vittatæ*. *Journal of Cell Science*, **s2-53**, 665-696. doi: 10.1242/jcs.s2-53.212.665.
- Ronquist, F. and Huelsenbeck, J. P.** (2003). MrBayes 3: Bayesian phylogenetic inference under mixed models. *Bioinformatics*, **19**, 1572-1574. doi: 10.1093/bioinformatics/btg180.
- Sato, H., Takano, A., Kawabata, H., Une, Y., Watanabe, H. and Mukhtar, M. M.** (2009). *Trypanosoma* cf. *varani* in an imported ball python (*Python reginus*) from Ghana. *Journal of Parasitology*, **95**, 1029-1033. doi: 10.1645/ge-1816.1.
- Schneider, C. A., Rasband, W. S. and Eliceiri, K. W.** (2012). NIH Image to ImageJ: 25 years of image analysis. *Nature Methods*, **9**, 671-675.
- Shannon, R. P.** (2016). Amphibian blood parasites and their potential vectors in the Great Plains of the United States. MSc thesis, Oklahoma State University, Stillwater, Oklahoma.
- Siddall, M. E. and Desser, S. S.** (1992). Alternative leech vectors for frog and turtle trypanosomes. *The Journal of Parasitology*, **78**, 562-563. doi: 10.2307/3283672.
- Spodareva, V. V., Grybchuk-Ieremenko, A., Losev, A., Votýpka, J., Lukeš, J., Yurchenko, V. and Kostygov, A. Y.** (2018). Diversity and evolution of anuran

REFERENCE LIST

- trypanosomes: insights from the study of European species. *Parasites & Vectors*, **11**, 1-12.
- Steverding, D.** (2008). The history of African trypanosomiasis. *Parasites & Vectors*, **1**, 3.
doi: 10.1186/1756-3305-1-3.
- Steverding, D.** (2017). Sleeping sickness and nagana disease caused by *Trypanosoma brucei*. In *Arthropod Borne Diseases* (ed. Marcondes, C. B.), pp. 277-297. Norwich, UK: Springer International Publishing, Cham.
https://doi.org/10.1007/978-3-319-13884-8_18
- Swofford, D. L.** (2003). *PAUP*. Phylogenetic analysis using parsimony (*and other methods)*. Version 4.0a169. Sunderland, MA: Sinauer Associates.
- Tavaré, S.** (1986). Some probabilistic and statistical problems in the analysis of DNA sequences. *Lectures on Mathematics in the Life Sciences*, **17**, 57-86.
- Telford, S. R.** (1995a). A review of trypanosomes of gekkonid lizards, including the description of five new species. *Systematic Parasitology*, **31**, 37-52.
- Telford, S. R.** (1995b). Two new trypanosome species from East African cordylid lizards. *Systematic Parasitology*, **31**, 61-65.
- Telford, S. R.** (1996). A review of the trypanosomes from lizards of the family Iguanidae (*sensu lato*), including the descriptions of five new species, and an evaluation of the effect of host difference upon taxonomic characters of saurian trypanosomes. *Systematic Parasitology*, **34**, 215-237.
- Telford, S. R.** (2009). *Hemoparasites of the Reptilia*. Boca Raton, FL: CRC Press.
- Toontong, P., Sunantaraporn, S., Tiawsirisup, S., Pongsakul, T., Boonserm, R., Phumee, A., Siriyasatien, P. and Preativatanyou, K.** (2022). First report of anuran *Trypanosoma* DNA in flat-tailed house geckos (Reptilia: Gekkonidae) collected from southern Thailand: No evidence as a reservoir for human trypanosomatids. *Pathogens*, **11**, 247.

REFERENCE LIST

- Valkiūnas, G., Iezhova, T. A., Carlson, J. S. and Sehgal, R. N.** (2011). Two new *Trypanosoma* species from African birds, with notes on the taxonomy of avian trypanosomes. *Journal of Parasitology*, **97**, 924-930. doi: 10.1645/GE-2796.1
- Vamberger, M., D'Anuniação, P., Hofmeyr, M. and Fritz, U.** (2019). Mind the gap - Is the distribution range of *Pelomedusa galeata* really disjunct in western South Africa? *Amphibian and Reptile Conservation*, **13**, 57-60.
- Vanhove, M. P. M., Kmentová, N., Luus-Powell, W. J., Netherlands, E. C., de Buron, I. and Barger, M. A.** (2022). Chapter 15 - A snapshot of parasites in tropical and subtropical freshwater wetlands: modest attention for major players. In *Fundamentals of Tropical Freshwater Wetlands* (eds. Dalu, T., and Wasserman, R. J.), pp. 417-485. Chennai, India: Elsevier.
- Viola, L. B., Attias, M., Takata, C. S. A., Campaner, M., De Souza, W., Camargo, E. P. and Teixeira, M. M. G.** (2009). Phylogenetic analyses based on small subunit rRNA and glycosomal glyceraldehyde-3-phosphate dehydrogenase genes and ultrastructural characterization of two snake trypanosomes: *Trypanosoma serpentis* n. sp. from *Pseudoboa nigra* and *Trypanosoma cascavelli* from *Crotalus durissus terrificus*. *Journal of Eukaryotic Microbiology*, **56**, 594-602. doi: <https://doi.org/10.1111/j.1550-7408.2009.00444.x>.
- Viola, L. B., Campaner, M., Takata, C. S., Ferreira, R. C., Rodrigues, A. C., Freitas, R. A. d., Duarte, M. R., Grego, K. F., Barrett, T. V. and Camargo, E. P.** (2008). Phylogeny of snake trypanosomes inferred by SSU rDNA sequences, their possible transmission by phlebotomines, and taxonomic appraisal by molecular, cross-infection and morphological analysis. *Parasitology*, **135**, 595-605.
- Walliker, D.** (1965). *Trypanosoma superciliosae* sp. nov. from the lizard *Uranoscodon superciliosa* L. *Parasitology*, **55**, 601-606. doi: 10.1017/S0031182000086194.

REFERENCE LIST

- Wenyon, C.** (1909). Report of travelling pathologist and protozoologist. In *Third Report Wellcome Research Laboratories at the Gordon Memorial College Khartoum* (ed. Balfour, A.), pp. 141-150. London, UK: Baillere, Tindall & Cox.
- Yazaki, E., Ishikawa, S. A., Kume, K., Kumagai, A., Kamaishi, T., Tanifuji, G., Hashimoto, T. and Inagaki, Y.** (2017). Global Kinetoplastea phylogeny inferred from a large-scale multigene alignment including parasitic species for better understanding transitions from a free-living to a parasitic lifestyle. *Genes & Genetic Systems*, **92**, 35-42. doi: 10.1266/ggs.16-00056.

APPENDIX

APPENDIX

Supplementary Table 2.2.1: Host sample data.

Host species	Field number	Locality	Coordinates	Sample date	Molecular screening for trypanosomes
<i>Smaug depressus</i>	RE201126B1	Soutpansberg, Lajuma Research Centre, Limpopo	23.03921° S, 29.44727° E	26/11/2020	
<i>Smaug depressus</i>	RE201126B2	Soutpansberg, Lajuma Research Centre, Limpopo	23.03921° S, 29.44727° E	26/11/2020	
<i>Smaug depressus</i>	RE210921A1	Soutpansberg, Lajuma Research Centre, Limpopo	23.03921° S, 29.44727° E	21/09/2021	Infected
<i>Smaug depressus</i>	RE210921C1	Soutpansberg, Lajuma Research Centre, Limpopo	23.03599° S, 29.42872° E	21/09/2021	Infected
<i>Smaug depressus</i>	RE210921C2	Soutpansberg, Lajuma Research Centre, Limpopo	23.03599° S, 29.42872° E	21/09/2021	
<i>Smaug depressus</i>	RE220930A1	Soutpansberg, Lajuma Research Centre, Limpopo	23°02.3593' S; 29°26.9504' E	30/09/2022	Infected
<i>Smaug depressus</i>	RE221001A1	Soutpansberg, Lajuma Research Centre, Limpopo	23°02.3593' S; 29°26.9504' E	01/10/2022	Infected
<i>Smaug depressus</i>	RE221001B1	Soutpansberg, Lajuma Research Centre, Limpopo	23°01.9960' S; 29°25.3967' E	01/10/2022	
<i>Smaug depressus</i>	RE221001B2	Soutpansberg, Lajuma Research Centre, Limpopo	23°01.9960' S; 29°25.3968' E	01/10/2022	Infected
<i>Smaug depressus</i>	RE221001B3	Soutpansberg, Lajuma Research Centre, Limpopo	23°01.9972' S; 29°25.3841' E	01/10/2022	
<i>Smaug depressus</i>	RE221001B4	Soutpansberg, Lajuma Research Centre, Limpopo	23°01.9754' S; 29°25.4142' E	01/10/2022	Infected
<i>Smaug depressus</i>	RE221002A1	Soutpansberg, Lajuma Research Centre, Limpopo	23°02.3638' S; 29°27.0269' E	02/10/2022	Infected
<i>Smaug depressus</i>	RE221002A2	Soutpansberg, Lajuma Research Centre, Limpopo	23°02.3666' S; 29°27.0647' E	02/10/2022	Infected
<i>Smaug depressus</i>	RE221002B1	Soutpansberg, Lajuma Research Centre, Limpopo	23°02.4714' S; 29°26.727' E	02/10/2022	Infected
<i>Smaug depressus</i>	RE221002C1	Soutpansberg, Lajuma Research Centre, Limpopo	23°02.3091' S; 29°27.1867' E	02/10/2022	Infected
<i>Cordylus jonesii</i>	RE210321B1	Ndumo Game Reserve, KZN	26.86745° S, 32.16901° E	12/03/2021	
<i>Cordylus jonesii</i>	RE210321D1	Ndumo Game Reserve, KZN	26.88668° S, 32.22807° E	12/03/2021	Infected
<i>Trachylepis striata</i>	RE210310C1	Ndumo Game Reserve, KZN	26.90709° S, 32.32000° E	10/03/2021	
<i>Varanus albigularis</i>	RE210312A1	Ndumo Game Reserve, KZN	26.88407° S, 32.21680° E	12/03/2021	
<i>Varanus albigularis</i>	RE210312C1	Ndumo Game Reserve, KZN	26.87401° S, 32.17762° E	12/03/2021	
<i>Naja subfulva</i>	RE210313A1	Tembe Elephant Park, KZN	27.04434° S, 32.42137° E	13/03/2021	
<i>Homopholis wahlbergii</i>	RE210313B1	Tembe Elephant Park, KZN	27.04434° S, 32.42137° E	13/03/2021	
<i>Nucras lalandii</i>	RE210314C1	Tembe Elephant Park, KZN	27.04434° S, 32.42137° E	14/03/2021	
<i>Acanthocercus atricollis atricollis</i>	RE210315A1	Sodwana Bay, KZN	27.48510° S, 32.65831° E	15/03/2021	
<i>Bradypodion setaroi</i>	RE210317A1	Richard's Bay, KZN	S28.76579° S; 32.05511° E	17/03/2021	
<i>Bradypodion setaroi</i>	RE210317A4	Richard's Bay, KZN	28.76579° S; 32.05511° E	17/03/2021	
<i>Chamaeleo dilepis</i>	RE210207C1	Vhembe Biosphere Reserve, Limpopo	22.85352° S, 29.57521° E	7/02/2021	
<i>Python natalensis</i>	RE210208D1	Vhembe Biosphere Reserve, Limpopo	22.81697° S, 29.46972° E	8/02/2021	
<i>Varanus albigularis</i>	RE210208C1	Vhembe Biosphere Reserve, Limpopo	22.85935° S, 29.60545° E	8/02/2021	
<i>Platysaurus intermedius intermedius</i>	RE210209B1	Goro Game Reserve, Limpopo	22.9587° S, 29.428° E	9/02/2021	
<i>Chondrodactylus turneri</i>	RE210209C1	Goro Game Reserve, Limpopo	22.9587° S, 29.428° E	9/02/2021	
<i>Chamaeleo dilepis</i>	RE210210A1	Goro Game Reserve, Limpopo	22.85611° S, 29.54766° E	10/02/2021	

APPENDIX

Supplementary Table 2.3.1: Host sample data. Pelomedusid turtles collected in KwaZulu-Natal, South Africa.

Field number	Host species	Locality	Date collected	Coordinates (decimal)	Coordinates (DMS)	Molecular screening
RE210311A3	<i>Pelusios sinuatus</i>	Water pan 600m south of Maputo River, Ndumo Game Reserve, KZN	11 March 2021	-26.86554; 32.16660	26°51'55"S; 32°09'59"E	Infected
RE210311B1	<i>Pelusios sinuatus</i>	Nyamiti Pan, Ndumo Game Reserve, KZN	11 March 2021	-26.90012; 32.26288	26°54'00"S; 32°15'46"E	Infected
RE210313C1	<i>Pelusios castenoides</i>	Zimambeni Pan, Tembe Elephant Park, KZN	13 March 2021	-27.03940; 32.48190	27°02'21"S; 32°28'54"E	Infected
RE210314A3	<i>Pelusios castenoides</i>	near Vukuzani Pan, Tembe Elephant Park, KZN	14 March 2021	-27.00653; 32.43343	27°00'23"S; 32°26'00"E	Infected
RE210314A5	<i>Pelusios castenoides</i>	near Vukuzani Pan, Tembe Elephant Park, KZN	14 March 2021	-27.00653; 32.43343	27°00'23"S; 32°26'00"E	Infected
RE210331A2	<i>Pelomedusa galeata</i>	Borrow pit near Mkhanyeni, eastern Lebombo Mountain foothills, KZN	8 March 2020	-27.01416; 32.14138	27°00'51"S; 32°08'29"E	Infected
RE210331A3	<i>Pelomedusa galeata</i>	Borrow pit near Mkhanyeni, eastern Lebombo Mountain foothills, KZN	8 March 2020	-27.01416; 32.14138	27°00'51"S; 32°08'29"E	Infected